Annual Report
Jahresbericht

2015

Walther–Meißner–Institut
für Tieftemperaturforschung

Bayerische Akademie der Wissenschaften

Contact:

Prof. Dr. Rudolf Gross
Walther–Meißner–Institut für Tieftemperaturforschung
Bayerische Akademie der Wissenschaften
and
Lehrstuhl für Technische Physik – E23
Technische Universität München

Address:

Walther–Meißner–Str. 8	Phone:	+49 – (0)89 289 14201
D - 85748 Garching	Fax:	+49 – (0)89 289 14206
GERMANY	e–mail:	Rudolf.Gross@wmi.badw.de
	www:	http://www.wmi.badw.de

Secretary's Office and Administration:

Emel Dönertas	Phone:	+49 – (0)89 289 14202
	Fax:	+49 – (0)89 289 14206
	e–mail:	Emel.Doenertas@wmi.badw.de
		Sekretariat@wmi.badw.de
Ludwig Ossiander	Phone:	+49 – (0)89 289 14205
	Fax:	+49 – (0)89 289 14206
	e–mail:	Ludwig.Ossiander@wmi.badw.de
		Verwaltung@wmi.badw.de

Preface

Dear colleagues, friends, partners, and alumni of the Walther-Meißner-Institute for Low Temperature Research (WMI) of the Bavarian Academy of Sciences and Humanities (BAdW)!

Our ***Annual Report 2015*** aims at providing an overview of our last year's teaching, research and public outreach activities as well as some statistical data about publications, completed and ongoing Ph.D., master and bachelor theses, cooperations, funding sources, and recent developments in infrastructure and experimental facilities. As every year, our Annual Report comes early to give you a timely piece of information. The WMI research program extends from fundamental studies in condensed matter and quantum physics, application oriented studies, and materials science to technological developments in low temperature, thin film and nano-technology. Our main research topics cover the fields of superconductivity and superfluidity, magnetism, ordering and emergent phenomena in correlated electron systems, spin electronics and spin caloritronics, as well as quantum information processing and quantum coherence in solid-state systems.

Our successful research in 2015 resulted in more than 35 ISI-listed publications (see page 77), new extramural funding (see page 89), the participation in many coordinated research projects and graduate schools on the European and national level (see page 89), as well as fruitful collaborations with international research institutions and industry (see page 96). The high international impact of our research work is documented by more than 1800 citations of WMI publications in 2015 and a large number of invited conference presentations, colloquium and and seminar talks (see page 99). In 2015, WMI also has organized two international conferences and has contributed to public outreach events (see page 92).

The highly successful ***Collaborative Research Center 631*** on Solid-State Based Quantum Information Processing ended in June 2015. Within the full twelve-year funding period WMI played a key role in CRC 631 and provided its spokesman. The CRC 631 not only produced a huge number of high-quality research results but also formed an effective platform for fostering young talents (cf. page 13) and the nucleus for new coordinated projects in the field of quantum science. The most important is the Excellence Cluster ***Nanosystems Initiative Munich (NIM)***, with its Research Area 1 focussing on quantum nanophysics. However, we should also mention the Marie Curie Initial Training Network ***Cavity and Circuit Quantum Electrodynamics – CCQED*** and the FP7 Collaborative Project ***Quantum Propagating Microwaves in Strongly Coupled Environments – PROMISCE***, as well as the International Ph.D. School of Excellence (IDK) entitled ***Exploring Quantum Matter (ExQM)*** within the ***Elite-Netzwerk Bayern***. ExQM is a joint program of TU Munich and LMU Munich in cooperation with WMI and the Max Planck Institute of Quantum Optics. It aims at designing quantum matter and understanding its complex behavior by large-scale simulation of correlated quantum systems in laboratory experiments.

WMI is also an active player in the ***Munich Quantum Center (MQC)***. The virtual center MQC was founded in 2014 to foster the Munich research activities in quantum science and technology and to provide a unique platform for the communication of advances achieved in our teams. We are particulary happy that already in 2015 a joint effort of MQC scientists succeeded in acquiring funding for the new International Max Planck Research School ***Quantum Science and Technology (QST)*** which starts in 2016. In general, the WMI research program is strongly dependent on third party funding. To this end, our participation in medium- and long-term coordinated research programs is mandatory. Beyond the quantum science related projects mentioned above (cf. page 17), these research projects include the ***Transregional Collaborative Research Center TRR 80*** "From Electronic Correlations to Functionality" (second funding period: 01/2014 – 12/2017), the ***Priority Program SPP 1458*** "High T_c Superconductivity in

Iron Pnictides" (second funding period: 04/2013 – 03/2016), the ***Priority Program SPP 1538*** "Spin Caloritronic Transport" (second funding period: 07/2014 – 06/2017), and the ***Priority Program SPP 1601*** "New Frontiers in Sensitivity for EPR Spectroscopy" (second funding period: 07/2015 – 06/2018).

Keeping the technological infrastructure on a state-of-the-art level is a key prerequisite for successful experimental research. In this context, we made considerable progress recently. First, supported by substantial funding of the Excellence Cluster NIM, we were able replace our electron beam writer. The new 100 kV nB5 Electron Beam Lithography System of NanoBeam Ltd., UK, with total cost exceeding 1 Mio. Euro, was taken into full operation early in 2015. Second, the Bavarian Ministry for Science and Arts granted up to 4.92 Mio. Euro to WMI for redevelopment measures regarding the technical infrastructure, safety requirements and energy efficiency. The planning stage of this building project is almost completed. An important part is the reconstruction of the entrance area, providing then direct access to the new WMI Quantum Laboratories in the basement of the WMI building. Moreover, it includes the replacement of all windows, the upgrade of the technical infrastructure for cooling water, air conditioning, liquid nitrogen and helium storage, as well as various safety measures.

In October 2015, the Bavarian Academy of Sciences and Humanities (BAdW) has passed new statutes and standing orders also affecting WMI. An important change is the clear separation between the managing bodies of the Academy Institutes and Projects which are responsible for the implementation of the research programs, and the corresponding supervisory bodies which provide external quality control. Accordingly, the former Commissions of BAdW have been abolished and replaced by the Institute and Project Committees on the one hand and the Institute and Project Advisory Boards on the other hand. To this end, the former Commission for Low Temperature Research has become the WMI Advisory Board (see page 125). The director of WMI is chairman of the WMI Committee and consultive member of the WMI Advisory Board.

Our success in research is only possible by the strong commitment of our scientific, technical and administrative staff. Together with our guests and the large number of talented and dedicated students they make our ambitious research possible by their hard work and persistence. In 2015, the total number of student helpers, bachelor, master and Ph.D. students was again exceeding the high value of 50. In total, 10 bachelor, 16 master/diploma, and 6 Ph.D. theses were completed in 2015, while 13 master and 18 Ph.D. students are still ongoing with their work (see page 85). In the same way, an important prerequisite of success in science is the continuous support by various funding agencies. In this context we gratefully acknowledge financial support from the BAdW, the DFG, the Bavarian Ministry for Science and Arts, the BMBF and the EU. A further key to our success in research is the recruitment of outstanding, scientifically independent group leaders with complementary research interests and technical expertise, a process which is supported and monitored by the scientific advisory board of WMI. We are strongly committed to support and promote young scientists in their career.

I hope that our Annual Report 2015 inspires your interest in WMI. I take this opportunity to thank all the colleagues, guests, students, postdocs and cooperating partners, who contributed to our research and teaching activities within the last year, and last but not least all our friends and sponsors for their interest, trust and continuous support.

R. Gross

Rudolf Gross

Garching, December 2015

Contents

The Walther–Meißner–Institute

General Information

The ***Walther-Meißner-Institute for Low Temperature Research (WMI)*** was originally operated by the Commission for Low Temperature Research of the ***Bavarian Academy of Sciences and Humanities (BAdW)***. Between 2013 and 2015, the Bavarian Academy of Sciences and Humanities with its more than 300 employees was reorganized. With the passing of the new statutes in October 2015, the 36 Commissions (Research Groups) of the Academy — they were originally set up in order to carry out long-term projects, which are too ambitious for the lifetime or capacity of any single researcher, or which require the collaboration of specialists in various disciplines — have been abolished. The research program of BAdW is now implemented in Academy Institutes (such as the Walther-Meißner-Institute or the Leibniz Supercomputing Center) and Academy Projects. The Academy Institutes and Projects are managed by the Institute and Project Committees and supervised by the Institute and Project Advisory Boards, respectively. In this way a clear separation between the managing bodies of the institutes/projects (responsible for the implementation of the research programs) and the corresponding supervisory bodies (responsible for the quality control) has been established. To this end, also the Commission for Low Temperature Research was dissolved and replaced by the WMI Committee and the WMI Advisory Board in 2015.

The historical roots of WMI go back to Walther Meißner. He founded the Commission for Low Temperature Research in 1946 when he was president of BAdW (1946 – 1950). The first research activities then were started in 1946 in the Herrsching barracks. After the retirement of Walther Meißner in 1952, Heinz Maier-Leibnitz, who followed Walther Meißner on the Chair for Technical Physics of the Technische Universität München, became the new head of the Commission for Low Temperature Research. In 1967, the commission moved to the Garching research campus after the construction of the new "Zentralinstitut für Tieftemperaturforschung (ZTTF)" was completed (director: Prof. Heinz Maier-Leibnitz, technical director: Prof. Franz Xaver Eder). Until 1972, the theory group of the Institute Laue Langevin was hosted at the ZTTF. In 1980, Prof. Dr. Klaus Andres became the new director of the ZTTF again associated with the Chair for Technical Physics (E23) at the Technische Universität München, followed by Prof. Dr. Rudolf Gross in 2000. In 1982, the ZTTF was renamed into Walther-Meißner-Institute for Low Temperature Research (WMI) on the occasion of Walther Meißner's 100. birthday.

Starting from 2000, the so far unused basement of the WMI building was made available for technical infrastructure (airconditioning, particulate airfilters, pure water system etc. for clean room) and additional laboratory space. Fortunately, in 2008 WMI succeeded in getting extra money from the state government within the so-called "Konjunkturpaket II". This money has been used to establish the new "WMI Quantum Science Laboratory" in the basement of the building, providing about 150 m^2 additional laboratory space particularly suited for low temperature facilities and ultra-sensitive studies on solid state quantum systems. The WMI Quantum Science Laboratory was fully operational early in 2011 and meanwhile hosts three new mK systems and sophisticated experimental techniques for the study of solid state based quantum systems and circuits.

As already mentioned, it is a long tradition that WMI hosts the Chair for Technical Physics (E 23) of the Technische Universität München (TUM) with the director of the WMI being a full professor at the Faculty of Physics of TUM. However, there are also close ties with the Ludwig-Maximilians-Universität (LMU). Between 2004 and 2010, WMI hosted a scanning probe division with the head of this division being a professor at the Ludwig-Maximilians-Universität (LMU). In this way a tight collaboration has been established between WMI and research groups of both Munich universities, joining technological and human resources in the fields of experimental and theoretical solid-state and condensed matter physics, low temperature techniques, materials science as well as thin film and nanotechnology. Noteworthy, the WMI supplies liquid helium to more than 25 research groups at both Munich universities and provides the technological basis for low temperature research.

Research Activities

The research activities of the Walther-Meißner-Institute are focused on low temperature condensed matter physics (see reports below). The research program is devoted to both **fundamental** and **applied research** and also addresses **materials science, thin film and nanotechnology** aspects. With respect to **basic research** the main focus of the WMI is on

- superconductivity and superfluidity,
- magnetism, spin transport, spin mechanics and spin caloritronics,
- quantum phenomena and quantum coherence in mesoscopic systems and solid state nanostructures,
- circuit quantum electrodynamics and circuit electro-nanomechanics,
- ordering and emergent phenomena in correlated electron systems,
- and the general properties of metallic systems at low and very low temperatures.

The WMI also conducts **applied research** in the fields of

- solid-state quantum information processing systems,
- superconducting and spintronic devices,
- oxide electronics,
- multi-functional and multiferroic materials,
- and the development of low and ultra-low temperature systems and techniques.

With respect to **materials science, thin film and nanotechnology** the research program is focused on

- the synthesis of superconducting and magnetic materials,
- the single crystal growth of oxide materials,
- the thin film technology of complex oxide heterostructures including multifunctional and multiferroic material systems,
- and the fabrication of superconducting, magnetic, and hybrid nanostructures.

The WMI also develops and operates systems and techniques for low and ultra–low temperature experiments. A successful development have been dry mK-systems that can be operated without liquid helium by using a pulse-tube refrigerator for precooling. In the early 2000s, these systems have been successfully commercialized by the company VeriCold Technologies GmbH at Ismaning, Germany, which was taken over by Oxford Instruments in 2007. As further typical examples we mention a nuclear demagnetization cryostat for temperature down to below 100 μK, or very flexible dilution refrigerator inserts for temperatures down to about 20 mK fitting into a 2 inch bore. These systems have been engineered and fabricated at WMI. Within the last years, several dilution refrigerators have been provided to other research groups for various low temperature experiments. WMI also operates a helium liquifier with an annual capacity of above 180.000 liters and supplies both Munich universities with liquid helium. To optimize the transfer of liquid helium into transport containers, WMI has developed a pumping system for liquid helium that is commercialized in collaboration with a company.

To a large extent the research activities of WMI are integrated into national and international research projects such as Clusters of Excellence, Collaborative Research Centers, Research

Units, or EU projects. The individual research groups of WMI offer a wide range of attractive research opportunities for bachelor and master students, Ph.D. students and postdoctoral fellows.

Experimental Facilities and Resources

The WMI is equipped with state of the art facilities for the preparation and characterization of superconducting and magnetic materials as well as for various low and ultra–low temperature experiments. The main experimental and technological resources of WMI are listed in the following.

Materials Preparation and Fabrication of Nanostructures

- Laser Molecular Beam Epitaxy (L-MBE) system for oxide heterostructures (equipped with in–situ RHEED, Omicron AFM/STM system, atomic oxygen/nitrogen source, infrared-laser heating system, metallization)
- molecular beam epitaxy (MBE) system for metals
- UHV magnetron sputtering systems for metals (e.g. Nb, Al, NiPd, ...)
- magnetron sputtering system for oxide heteroepitaxy (equipped with four sputtering guns and an oxygen ion gun)
- reactive ion etching (RIE) system, Plasmalab 80 Plus with ICP plasma source, Oxford Instruments Plasma Technology
- ion beam etching (IBE) system equipped with a LN_2 cooled sample holder
- polishing machine for substrate preparation
- ultrasonic bonding machine
- 50 m^2 class 1000 clean room facility
- optical lithography (Süss maskaligner MJB 3 and projection lithography)
- 100 kV nB5 Electron Beam Lithography System by NanoBeam Limited, UK, with 6 inch laser stage
- four-mirror image furnace for crystal growth

Characterization

- 2–circle x–ray diffractometer (Bruker D8 Advance, sample temperature up to 1 600°C)
- high resolution 4–circle x–ray diffractometer with Göbel mirror and Ge monochromator (Bruker D8 Discover)
- Philips XL 30 SFEG scanning electron microscope with EDX analysis
- UHV room temperature AFM/STM system
- two Raman spectroscopy systems (1.5 to 300 K, in-situ sample preparation)
- SQUID magnetometer (Quantum Design, 1.5 to 700 K, up to 7 T)
- several high field magnet systems (up to 17 T Tesla) with variable temperature inserts
- 7 T split coil magnet systems with optical access and variable temperature insert
- 3D vector magnet (2/2/6 Tesla) with variable temperature inserts
- experimental set–ups for the measurement of noise including low noise SQUID amplifiers and signal analyzers
- high-frequency network analyzers (up to 40 GHz) and various microwave components (sources, mixers, circulators, attenuators) for the determination of high frequency parameters
- ultra-sensitive microwave receiver for state tomography of quantum microwaves (dual path method with FPGA signal processing)

- high-frequency cryogenic probing station (up to 20 GHz, $T > 4$ K)
- magnetooptical Kerr effect (MOKE) system
- ferromagnetic resonance (FMR) system

Low temperature systems and techniques

- several ^{3}He/^{4}He dilution refrigerator inserts for temperatures down to 10 mK
- “dry” mK-cooler based on a dilution refrigerator with pulse-tube precooling and equipped with a large number of microwave lines and cold electronics (e.g. amplifiers, circulators, attenuators) for ultra-sensitive experiments on solid state quantum systems
- “dry” dilution refrigerator with a base temperature of about 10 mK equipped with a 3D vector magnet (1/1/6 Tesla)
- ultra–low temperature facility for temperatures down to below 100 µK based on a nuclear demagnetization cryostat
- experimental set–ups for the measurement of specific heat, magnetization, thermal expansion as well as electrical and thermal transport properties as a function of temperature, magnetic field and pressure

Joint Research Projects

IMPRS-QST

SPP 1601

SPP 1458

SPP 1538

The Cluster of Excellence "Nanosystems Initiative Munich – NIM"

Rudolf Gross, Frank Deppe, Sebastian T.B. Gönnenwein, Hans Hübl, Achim Marx[1]

The excellence cluster ***Nanosystems Initiative Munich (NIM)*** was established in 2006. After a successful first funding period (2006 – 2012), a second five-year funding period (2012 – 2017) was granted. NIM comprises internationally recognized expertise in all relevant research areas of nanosciences, ranging from quantum nanophysics to the creation and study of nanosystems for biophysics and the life sciences. WMI is a founding member of NIM and significantly contributes to the research areas on ***Quantum Nanophysics*** (RA I) and ***Hybrid Nanosystems*** (RA II) of NIM's five research areas. Research area I is coordinated by R. Gross of WMI. Several WMI scientists (Deppe, Gönnenwein, Gross, Hübl, Marx) actively contribute to the ambitious research program of NIM. Several WMI Ph.D. students are members of the NIM Graduate School.

The research activities and technical infrastructure of WMI strongly profit from NIM. Early in 2015, the new 100 kV nB5 Electron Beam Lithography System of NanoBeam Ltd., UK, which has been delivered in October 2014, was fully operable. NIM covered about 2/3 of the total cost of more than 1 Mio. Euro. With this powerful instrument WMI has significantly improved its technological capabilities for nanofabrication. It is also available to other research groups within NIM.

Apart from the support for big investments, a particular strength of NIM is to provide seed funding for new research directions and to help to establish new coordinated research efforts (cf. page 17). Also in 2015, WMI profitted from NIM seed funding projects which are evaluated by the NIM Scientific Advisory Board. In a competitive process WMI could acquire three seed funding projects on (i) *Coupling nano-mechanical strings to transmons in circuit QED environment - a new form of a quantum hybrid system* (Hübl, Deppe, Gross), (ii) *Quantum magnetism in superconducting quantum networks* (Deppe, Gross), and (iii) *Pure Spin Currents on the Nanoscale* (Gönnenwein, Hübl). The NIM seed funding projects are highly effective for implementing new ideas and performing preliminary work for future project applications.

Following the recommendation of the NIM Scientific Advisory Board, in 2015 NIM organized the first NIM Research Conference. The topic of this first conference within the NIM Research Conference series was "Resonator Quantum Electrodynamics". In general, the NIM Research Conferences aim at bringing together leading international experts to discuss and explore emerging new fields as well as to bridge different communities to share, pursue and diffuse the benefits of collaborations. The International NIM Conference ***Resonator Quantum Electrodynamics (Resonator QED 2015)*** was organized by Rudolf Gross (WMI) jointly with Jonathan Finley (WSI) and Gerhard Rempe (MPQ). Achim Marx and Frank Deppe of WMI were members of the local organisation team and many Ph.D students of WMI contributed to the success of the conference. It took place in the Literaturhaus at Munich from 03 – 07 August 2015 and consisted of tutorials and invited talks, as well as a small number of contributed talks and poster presentations. More details can be found on page 92 in the section on conferences, workshops and public outreach.

As in previous years, also in 2015 the WMI research activities strongly profited from NIM. Some of our recent results are presented in the subsequent reports. They range from the field of superconducting quantum circuits [1–10], hybrid quantum systems [11–14], electro-nanomechanical systems [15–19], to spin dynamics, spin caloritronics and the study of physics related to pure spin currents [20–30].

[1]This work is supported by the German Excellence Initiative via the Nanosystems Initiative Munich (NIM).

References

[1] R. D. Candia, K. G. Fedorov, L. Zhong, S. Felicetti, E. P. Menzel, M. Sanz, F. Deppe, A. Marx, R. Gross, and E. Solano, Europ. Phys. J. Quant. Technol. **2**, 25 (2015).

[2] A. Baust, E. Hoffmann, M. Haeberlein, M. J. Schwarz, P. Eder, E. P. Menzel, K. Fedorov, J. Goetz, F. Wulschner, E. Xie, L. Zhong, F. Quijandria, B. Peropadre, D. Zueco, J.-J. G. Ripoll, E. Solano, F. Deppe, A. Marx, and R. Gross, Phys. Rev. B **91**, 014515 (2015).

[3] A. Baust, E. Hoffmann, M. Haeberlein, M. J. Schwarz, P. Eder, E. P. Menzel, K. Fedorov, J. Goetz, F. Wulschner, E. Xie, L. Zhong, F. Quijandria, B. Peropadre, D. Zueco, J.-J. Garcia Ripoll, E. Solano, F. Deppe, A. Marx, and R. Gross (2014). `arXiv:1405.1969`.

[4] R. D. Candia, E. P. Menzel, L. Zhong, F. Deppe, A. Marx, R. Gross, and E. Solano, New Journal of Physics **16**, 015001 (2014).

[5] J. Goetz, F. Deppe, M. Haeberlein, F. Wulschner, C. W. Zollitsch, S. Meier, M. Fischer, P. Eder, E. Xie, K. G. Fedorov, E. P. Menzel, A. Marx, and R. Gross. Loss mechanisms in superconducting thin film microwave resonators. Accepted for publication in J. Appl. Phys., `arXiv:1510.05957` (2015).

[6] M. Haeberlein, F. Deppe, A. Kurcz, J. Goetz, A. Baust, P. Eder, K. G. Fedorov, M. Fischer, E. P. Menzel, M. J. Schwarz, F. Wulschner, E. Xie, L. Zhong, E. Solano, A. Marx, J.-J. García-Ripoll, and R. Gross. Spin-boson model with an engineered reservoir in circuit quantum electrodynamics. Submitted for publication, `arXiv:1506.09114` (2015).

[7] F. Wulschner, J. Goetz, F. R. Koessel, E. Hoffmann, A. Baust, P. Eder, M. Fischer, M. Haeberlein, M. J. Schwarz, M. Pernpeintner, E. Xie, L. Zhong, C. W. Zollitsch, B. Peropadre, J.-J. G. Ripoll, E. Solano, K. Fedorov, E. P. Menzel, F. Deppe, A. Marx, and R. Gross. Tunable coupling of transmission-line microwave resonators mediated by an rf SQUID. Submitted for publication, `arXiv:1508.06758` (2015).

[8] M. J. Schwarz. *Gradiometric tunable-gap flux qubits in a circuit QED architecture*. Ph.D. thesis, TU München (2015).

[9] A. Baust. *Tunable Coupling and Ultrastrong Interaction in Circuit Quantum Electrodynamics*. Ph.D. thesis, TU München (2015).

[10] L. Zhong. *Generation and Reconstruction of Propagating Quantum Microwaves*. Ph.D. thesis, TU München (2015).

[11] C. W. Zollitsch, K. Mueller, D. P. Franke, S. T. B. Goennenwein, M. S. Brandt, R. Gross, and H. Huebl, Appl. Phys. Lett. **107**, 142105 (2015).

[12] G. Reithmaier, M. Kaniber, F. Flassig, S. Lichtmannecker, K. Müller, A. Andrejew, J. Vuckovic, R. Gross, and J. Finley, Nano Letters **15**, 5208–5213 (2015).

[13] G. Reithmaier, F. Flassig, P. Hasch, S. Lichtmannecker, K. Müller, J. Vučković, R. Gross, M. Kaniber, and J. J. Finley, Applied Physics Letters **105**, – (2014).

[14] F. Hoehne, C. Huck, M. S. Brandt, and H. Huebl, Phys. Rev. B **89**, 161305 (2014).

[15] M. Abdi, M. Pernpeintner, R. Gross, H. Huebl, and M. J. Hartmann, Phys. Rev. Lett. **114**, 173602 (2015).

[16] Y. Cao, P. Yan, H. Huebl, S. T. B. Goennenwein, and G. E. W. Bauer, Phys. Rev. B **91**, 094423 (2015).

[17] M. Pernpeintner, T. Faust, F. Hocke, J. P. Kotthaus, E. M. Weig, H. Huebl, and R. Gross, Appl. Phys. Lett. **105**, 123106 (2014).

[18] F. Hocke, M. Pernpeintner, X. Zhou, A. Schliesser, T. J. Kippenberg, H. Huebl, and R. Gross, Applied Physics Letters **105**, – (2014).

[19] F. Hocke. *Microwave Circuit-electrodynamics in a Nanomechanical Hybrid System*. Dissertation, Technische Universität München (2013).

[20] S. T. B. Goennenwein, R. Schlitz, M. Pernpeintner, K. Ganzhorn, M. Althammer, R. Gross, and H. Huebl, Applied Physics Letters **107** (2015).

[21] P. Ross, M. Schreier, J. Lotze, H. Huebl, R. Gross, and S. T. B. Goennenwein, Journal of Applied Physics **118** (2015).

[22] M. Schreier, T. Chiba, A. Niedermayr, J. Lotze, H. Huebl, S. Geprägs, S. Takahashi, G. E. W. Bauer, R. Gross, and S. T. B. Goennenwein, Phys. Rev. B **92**, 144411 (2015).

[23] A. Kamra, S. von Hoesslin, N. Roschewsky, J. Lotze, M. Schreier, R. Gross, S. T. B. Goennenwein, and H. Huebl, Eur. Phys. J. B **88**, 224 (2015).

[24] S. Meyer, R. Schlitz, S. Geprägs, M. Opel, H. Huebl, R. Gross, and S. T. B. Goennenwein, Applied Physics Letters **106** (2015).

[25] M. Schreier, G. E. W. Bauer, V. I. Vasyuchka, J. Flipse, K. ichi Uchida, J. Lotze, V. Lauer, A. V. Chumak, A. A. Serga, S. Daimon, T. Kikkawa, E. Saitoh, B. J. van Wees, B. Hillebrands, R. Gross, and S. T. B. Goennenwein, Journal of Physics D: Applied Physics **48**, 025001 (2015).

[26] J. Lotze, H. Huebl, R. Gross, and S. T. B. Goennenwein, Phys. Rev. B **90**, 174419 (2014).

[27] A. Kamra, F. P. Witek, S. Meyer, H. Huebl, S. Geprägs, R. Gross, G. E. W. Bauer, and S. T. B. Goennenwein, Phys. Rev. B **90**, 214419 (2014).

[28] N. Roschewsky, M. Schreier, A. Kamra, F. Schade, K. Ganzhorn, S. Meyer, H. Huebl, S. Geprägs, R. Gross, and S. T. B. Goennenwein, Appl. Phys. Lett. **104**, 202410 (2014).

[29] J. Lotze. *Spin Pumping in Ferrimagnet/Normal Metal Bilayers*. Ph.D. thesis, TU München (2015).

[30] S. Meyer. *Spin Caloritronics in Ferromagnet/Normal Metal Hybrid Structures*. Ph.D. thesis, TU München (2015).

The Collaborative Research Center 631

Rudolf Gross, Frank Deppe, Hans Hübl, Achim Marx[1]

The third and final funding period of the highly successful ***Collaborative Research Center 631*** on "Solid State Quantum Information Processing" has ended in June 2015. The ***CRC 631*** was established in 2003 and extended for a second and a third four-year funding period in 2007 and 2011, respectively. Since the start of CRC 631 more than a decade ago, quantum information science has developed into a fascinating and one of the most rapidly growing fields of science and technology, joining scientists from physics, mathematics, computer and materials science, and engineering. WMI was one of the key players within CRC 631. It was involved in the projects on *Superconducting Quantum Circuits as Basic Elements for Quantum Information Processing* (A3: Gross, Hübl, Marx), on *Cavity Quantum Electrodynamics with Superconducting Devices* (A8: Gross, Marx, Deppe) and on *Fundamentals of Quantum Logic Gates in Silicon* (C3: Hübl). In addition, WMI has coordinated the CRC 631 since the beginning (spokesman: Rudolf Gross). Supported by CRC 631, solid state quantum systems for quantum computing/simulation/communication, quantum spin and nanomechanical systems, and the combination of different degrees of freedom in hybrid quantum systems have evolved into key research directions at WMI.

The ***CRC 631*** has been highly successful. It not only produced a huge number of high-quality research results but also provided a very effective platform for fostering the careers of young talents. More than 25 young scientists who worked as Ph.D. students and postdocs within CRC 631 have become professors at universities or leading scientists at non-university research institutions. Prominent examples are (without being complete) Markus Betz, Robert Blick, Dominique Bougeard, Hans Briegel, Karl Brunner, Frank Deppe, Stefan Dürr, Anna Fontcuberta i Moral, Geza Giedke, Michael Hartmann, Alexander Högele, Alexander Holleitner, Hans Hübl, Andreas Hüttel, Siegmund Kohler, Hubert Krenner, Axel Kuhn, Alfred Leitenstorfer, Stefan Ludwig, Jacek Majewski, Matteo Mariantoni, Florian Marquardt, Jens Sievert, Enrique Solano, Eva Weig, Werner Wegscheider, Frank Wilhelm, Artur Zrenner, and David Zueco.

A further important impact of ***CRC 631*** is the fact that it was forming the nucleus for new coordinated projects in the field of quantum science and technology (cf. page 17). This includes the Excellence Cluster ***Nanosystems Initiative Munich (NIM)***, with its Research Area 1 focussing on quantum nanophysics. Also, the Marie Curie Initial Training Network ***Cavity and Circuit Quantum Electrodynamics – CCQED*** and the FP7 Collaborative Project ***Quantum Propagating Microwaves in Strongly Coupled Environments – PROMISCE*** would not have been possible without the preliminary work done within CRC 631. Moreover, the CRC 631 was paving the way for graduate schools such as the the international and interdisciplinary Ph.D. Program of Excellence entitled ***Quantum Computing, Control and Communication (QCCC)*** (2007–2013) and the International Ph.D. School of Excellence (IDK) entitled ***Exploring Quantum Matter (ExQM)*** within the ***Elite-Netzwerk Bayern*** which started in 2014. Finally, the scientists involved in CRC 631 are meanwhile active players in the ***Munich Quantum Center (MQC)***. MQC was founded as a virtual center in 2014 to foster the Munich research activities in quantum science and technology and to provide a unique platform for the communication of advances achieved in our teams. A first success of the joint effort of MQC scientists is the acquisition of funding for the new International Max Planck Research School ***Quantum Science and Technology (QST)*** which starts in 2016.

[1]This work is supported by the German Research Foundation through SFB 631.

The research work within CRC 631 has been very active until the end of the funding period. Several Ph.D. thesis [1–3], which have been at least partly supported by CRC 631, have been completed in 2015. The recent scientific and technological achievements of WMI related to CRC 631 are summarized in the following reports:

- Deppe *et al.*, *Displacement of propagating squeezed microwave states*, see page 29 and Ref. [4].
- Fedorov *et al.*, *Spin-boson model in circuit QED*, see page 31 and [5].
- Goetz *et al.*, *Time domain characterization of a transmon qubit*, see page 47.
- Goetz *et al.*, *Loss mechanisms in superconducting thin film microwave resonators*, see page 49 and Ref. [6].
- Pernpeintner *et al.*, *Nanomechanics Probes Magnetoelastics*, see page 45 and Refs. [7, 8].
- Xie *et al.*, *Construction of a new ^{3}He-^{4}He dilution refrigerator*, see page 57.

The WMI team closely collaborated with the theory groups at the Universidad del País Vasco - Euskal Herriko Unibertsitatea in Bilbao (Enrique Solano) [4, 5, 9–11], the University of Augsburg (Peter Hänggi, Achim Wixforth), the Heriot-Watt University in Edinburgh (Michael Hartmann) [7], and the Instituto de Física Fundamental at Madrid (Juan García-Ripoll) [5, 9–11]. In addition, there was fruitful scientific exchange with the experimental groups at the NTT Basic Research Laboratories (Semba), the Nanoelectronics Research Laboratories at NEC Corporation, Japan (Tsai, Yamamoto), the University of Tokyo (Nakamura), and the Walter Schottky Institute (Finley) [12–14].

References

[1] M. J. Schwarz. *Gradiometric tunable-gap flux qubits in a circuit QED architecture*. Ph.D. thesis, TU München (2015).

[2] A. Baust. *Tunable Coupling and Ultrastrong Interaction in Circuit Quantum Electrodynamics*. Ph.D. thesis, TU München (2015).

[3] L. Zhong. *Generation and Reconstruction of Propagating Quantum Microwaves*. Ph.D. thesis, TU München (2015).

[4] R. D. Candia, K. G. Fedorov, L. Zhong, S. Felicetti, E. P. Menzel, M. Sanz, F. Deppe, A. Marx, R. Gross, and E. Solano, Europ. Phys. J. Quant. Technol. **2**, 25 (2015).

[5] M. Haeberlein, F. Deppe, A. Kurcz, J. Goetz, A. Baust, P. Eder, K. G. Fedorov, M. Fischer, E. P. Menzel, M. J. Schwarz, F. Wulschner, E. Xie, L. Zhong, E. Solano, A. Marx, J.-J. García-Ripoll, and R. Gross. Spin-boson model with an engineered reservoir in circuit quantum electrodynamics. Submitted for publication, arXiv:1506.09114 (2015).

[6] J. Goetz, F. Deppe, M. Haeberlein, F. Wulschner, C. W. Zollitsch, S. Meier, M. Fischer, P. Eder, E. Xie, K. G. Fedorov, E. P. Menzel, A. Marx, and R. Gross. Loss mechanisms in superconducting thin film microwave resonators. Accepted for publication in J. Appl. Phys., arXiv:1510.05957 (2015).

[7] M. Abdi, M. Pernpeintner, R. Gross, H. Huebl, and M. J. Hartmann, Phys. Rev. Lett. **114**, 173602 (2015).

[8] C. W. Zollitsch, K. Mueller, D. P. Franke, S. T. B. Goennenwein, M. S. Brandt, R. Gross, and H. Huebl, Appl. Phys. Lett. **107**, 142105 (2015).

[9] A. Baust, E. Hoffmann, M. Haeberlein, M. J. Schwarz, P. Eder, E. P. Menzel, K. Fedorov, J. Goetz, F. Wulschner, E. Xie, L. Zhong, F. Quijandria, B. Peropadre, D. Zueco, J.-J. G. Ripoll, E. Solano, F. Deppe, A. Marx, and R. Gross, Phys. Rev. B **91**, 014515 (2015).

[10] A. Baust, E. Hoffmann, M. Haeberlein, M. J. Schwarz, P. Eder, J. Goetz, F. Wulschner, E. Xie, L. Zhong, F. Quijandria, D. Zueco, J.-J. G. Ripoll, L. Garcia-Alvarez, G. Romero, E. Solano, K. G. Fedorov, E. P. Menzel, F. Deppe, A. Marx, and R. Gross. Ultrastrong coupling in two-resonator circuit QED. Submitted for publication, arXiv:1412.7372 (2014).

[11] F. Wulschner, J. Goetz, F. R. Koessel, E. Hoffmann, A. Baust, P. Eder, M. Fischer, M. Haeberlein, M. J. Schwarz, M. Pernpeintner, E. Xie, L. Zhong, C. W. Zollitsch, B. Peropadre, J.-J. G. Ripoll, E. Solano, K. Fedorov, E. P. Menzel, F. Deppe, A. Marx, and R. Gross. Tunable coupling of transmission-line microwave resonators mediated by an rf SQUID. Submitted for publication, arXiv:1508.06758 (2015).

[12] G. Reithmaier, M. Kaniber, F. Flassig, S. Lichtmannecker, K. Müller, A. Andrejew, J. Vuckovic, R. Gross, and J. Finley, Nano Letters **15**, 5208–5213 (2015).

[13] G. Reithmaier, F. Flassig, P. Hasch, S. Lichtmannecker, K. Müller, J. Vučković, R. Gross, M. Kaniber, and J. J. Finley, Applied Physics Letters **105**, – (2014).

[14] G. Reithmaier, J. Senf, S. Lichtmannecker, T. Reichert, F. Flassig, A. Voss, R. Gross, and J. J. Finley, Journal of Applied Physics **113**, 143507 (2013).

The EU project "Quantum Propagating Microwaves in Strongly Coupled Environments – PROMISCE"

Frank Deppe, Kirill Fedorov, E. P. Menzel, Achim Marx, Rudolf Gross

The aim of the FP7 project ***PROMISCE*** is to provide the foundations propagating quantum microwave technologies based on superconducting quantum circuits, and to demonstrate its potential for scalable quantum information and communication technology applications. The project consists of two highly innovative and interdisciplinary scientific components. The first one, propagating quantum microwave photonics, is directed towards the generation, control and detection of quantum microwave beams and photons. The second component, propagating quantum microwave interactions, focuses on the exploration of novel techniques to engineer strong and controlled interactions between propagating microwave photons.

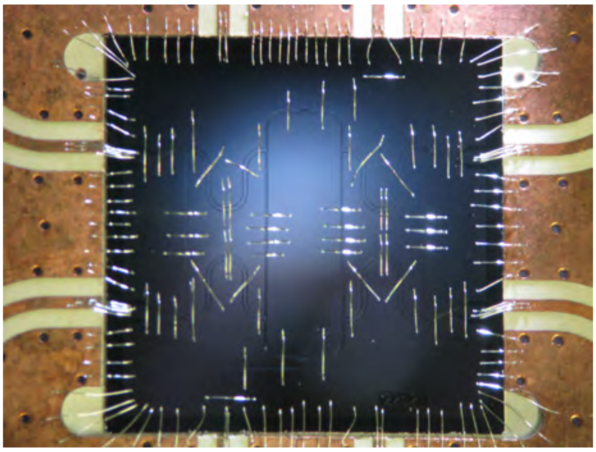

Figure 1: Optical micrograph of a superconducting microwave beam splitter with on-chip wirebonds used to contact isolated ground planes. The device is required for the realization of dual-rail encoded qubits based on propagating quantum microwaves.

PROMISCE started in April 2012 with a compact consortium of five European institutions working on superconducting quantum circuits: Chalmers University of Technology (Gothenburg, Sweden), University of the Basque Courtry (Bilbao, Spain), the Institute of Fundamental Physics (Madrid, Spain), and the WMI. PROMISCE has successfully ended in September 2015. Its scientific output has been summarized in 81 articles with more than 7 citations per paper on average, which is comparable to Physical Review Letters. Dissemination activities included support to the organization of 4 conferences, popular talks & articles, and media presence. At WMI, PROMISCE funded one postdoc and one Ph.D. position for three years and provided a substantial contribution the equipment required to carry out the desired experiments.

On the path towards the ultimate vision of quantum information processing with propagating microwave photons, which is still an active research focus at WMI, important insights have been gained within PROMISCE:

- On-chip superconducting microwave beam splitters (see Fig. 1) and interferometers were successfully realized [1, 2].
- Tunable coupling between superconducting resonators [3–6] and control over the coherent dynamics of superconducting qubits was achieved (see report of J. Goetz on page 47).
- Broadband quantitative experimental understanding of the environmental structure presented by open transmission line structures to superconducting qubits was achieved [7].
- First experiments on a transmon qubit inside an on-chip interferometer have triggered important theory progress towards a CPHASE gate with propagating microwaves.

References

[1] E. P. Menzel, M. Fischer, C. Schneider, F. Deppe, A. Marx, and R. Gross, WMI Ann. Rep. **2014**, 53–54 (2014).
[2] C. Schneider. *On-chip Superconducting Microwave Beam Splitter*. Master thesis, TU München (2015).
[3] A. Baust, E. Hoffmann, M. Haeberlein, M. J. Schwarz, P. Eder, E. P. Menzel, K. Fedorov, J. Goetz, F. Wulschner, E. Xie, L. Zhong, F. Quijandria, B. Peropadre, D. Zueco, J.-J. G. Ripoll, E. Solano, F. Deppe, A. Marx, and R. Gross, Phys. Rev. B **91**, 014515 (2015).
[4] A. Baust, E. Hoffmann, M. Haeberlein, M. J. Schwarz, P. Eder, J. Goetz, F. Wulschner, E. Xie, L. Zhong, F. Quijandria, D. Zueco, J.-J. G. Ripoll, L. Garcia-Alvarez, G. Romero, E. Solano, K. G. Fedorov, E. P. Menzel, F. Deppe, A. Marx, and R. Gross. Ultrastrong coupling in two-resonator circuit QED. Submitted for publication, `arXiv:1412.7372` (2014).
[5] A. Baust. *Tunable Coupling and Ultrastrong Interaction in Circuit Quantum Electrodynamics*. Ph.D. thesis, TU München (2015).
[6] F. Wulschner, J. Goetz, F. R. Koessel, E. Hoffmann, A. Baust, P. Eder, M. Fischer, M. Haeberlein, M. J. Schwarz, M. Pernpeintner, E. Xie, L. Zhong, C. W. Zollitsch, B. Peropadre, J.-J. G. Ripoll, E. Solano, K. Fedorov, E. P. Menzel, F. Deppe, A. Marx, and R. Gross. Tunable coupling of transmission-line microwave resonators mediated by an rf SQUID. Submitted for publication, `arXiv:1508.06758` (2015).
[7] M. Haeberlein, F. Deppe, A. Kurcz, J. Goetz, A. Baust, P. Eder, K. G. Fedorov, M. Fischer, E. P. Menzel, M. J. Schwarz, F. Wulschner, E. Xie, L. Zhong, E. Solano, A. Marx, J.-J. García-Ripoll, and R. Gross. Spin-boson model with an engineered reservoir in circuit quantum electrodynamics. Submitted for publication, `arXiv:1506.09114` (2015).

New Coordinated Projects on Quantum Science and Technology

Rudolf Gross, Frank Deppe, Kirill Fedorov, Hans Hübl, Achim Marx

With the end of the ***Collaborative Research Center 631*** on "Solid State Quantum Information Processing" in June 2015 and the European Projects ***Cavity and Circuit Quantum Electrodynamics – CCQED*** and ***Quantum Propagating Microwaves in Strongly Coupled Environments – PROMISCE*** in 2014 and 2015, respectively, it is mandatory for WMI to acquire new medium- and long-term projects in the field of quantum science and technology. To this end, WMI is participating in two European consortia submitting funding proposals early in 2016. Besides the application of new European projects, WMI contributed to setting up new Munich based graduate schools on quantum science and technology.

With respect to the implementation of coordinated research projects and graduate schools the ***Munich Quantum Center (MQC)*** is very useful. The same is true for the improvement of the outside visibility of the Munich research activities in the field of quantum science and technology. Since decades, the Munich area is hosting a large number of institutions and researchers playing a leading role in the study of quantum physics. Based on this long tradition and vivid atmosphere, the virtual center MQC was founded in 2014. MQC gathers more than 20 research groups belonging to different institutions, including the Ludwig-Maximilians University of Munich (LMU), the Technical University of Munich (TUM), the Max Planck Institute of Quantum Optics (MPQ) and the Walther-Meißner-Institute (WMI). MQC aims at providing a unique platform to communicate advances and developments achieved in our teams. It thus reflects and stresses the coherence and common points and directions existing behind our research activity.

The MQC member institutions cover a large variety of topics ranging from mathematical foundations, quantum information, computational methods, quantum nanosystems, quantum optics, and quantum many-body physics to superconducting devices. In MQC, mathematicians and theoretical and experimental physicists analyze physical systems exhibiting intriguing quantum mechanical properties. They also design new methods for leveraging and controlling such systems, thus paving the way for the development of quantum technologies.

Within the last two years, the coordinated effort of MQC scientists already succeeded in setting up two new graduate schools on quantum science and technology:

(i) Ph.D. School of Excellence "Exploring Quantum Matter (ExQM)"

In order to unite the unique competences in quantum physics in Munich and extend them into an international excellence network of doctoral training centres with partners at the Austrian Academy of Sciences in Vienna and Innsbruck, at ETH Zurich, ICFO Barcelona, Imperial College London, Caltech, and Harvard, the International Ph.D. School of Excellence (IDK) entitled ***Exploring Quantum Matter (ExQM)*** was founded within the Elite-Netzwerk Bayern in 2014. The participating institutions are the Technical University of Munich (TUM), the Ludwig-Maximilians University of Munich (LMU), the Max Planck Institute of Quantum Optics (MPQ), and the Walther-Meißner-Institute of BAdW. The research topics of ExQM include (i) quantum simulation of many-body systems, (ii) quantum phase transitions, (iii) open quantum systems, (iv) cavity an circuit QED, and (v) numerical and tensor methods. The training of Ph.D. students is supported by the development of new-media tools tailored to research requirements (e.g. visualization, outreach, interaction with partners).

A particular focus of WMI within ExQM is ***Scalable networks of solid-state quantum circuits***, which are becoming increasingly attractive for quantum simulations. For example, networks of nonlinear superconducting transmission line resonators or optical nanocavities can be used as scalable quantum simulators for the Bose-Hubbard Hamiltonian. The resonators are made nonlinear by a controllable coupling to superconducting or semiconductor quantum bits, thereby forming harmonic oscillators with tunable Kerr nonlinearity. Networks of these entities would be particularly well suited for accessing the strongly correlated regime and for investigating quantum many-body dynamics of interacting particles under the influence of driving and dissipation. Solid state quantum circuits with multiple drives are another attracting system (e.g. superconducting quantum bits strongly coupled to a resonator field mode and subjected to multiple classical drives can be used for quantum simulations of relativistic quantum physics such as the dynamics of the Dirac equation).

(ii) International Max Planck Research School on Quantum Science and Technology

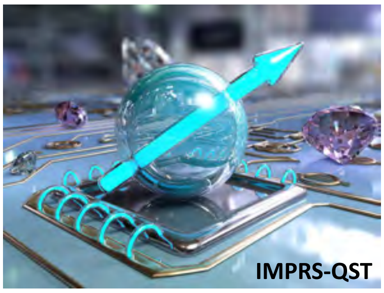

We are particulary happy that in a joint effort of MQC scientists we succeeded in acquiring funding for the new International Max Planck Research School (IMPRS) ***Quantum Science and Technology (QST)*** starting from 2016. The spokesman of the IMPRS is Ignacio Cirac of MPQ.

It is believed that quantum science is about to provide novel technologies enabled by new avenues, e.g., in information science, many-body systems, metrology, sensing, communication and material science. The quantum competences concentrated in Munich are unique in Europe and are on a par with leading centres worldwide. Thus, the IMPRS on Quantum Science and Technology provides the opportunity of a common research and teaching platform to unite the competences of leading research groups in Munich in an interdisciplinary, professional and coherent manner. The IMPRS will exploit the synergies between MPQ, WMI and the Munich universities of excellence LMU and TUM. The latter include the Walter Schottky Institute (WSI) and the Center for Nanoscience and Nanomaterials (CNN) of TUM as well as the Center for NanoScience (CeNS) of LMU.

With over twenty experimental and theoretical research groups, Munich is one of the leading research centers in the field of QST. This multidisciplinary and thriving field spans the entire spectrum of experimental and theoretical physics, mathematics, computer science and material science, and it promises extraordinary applications in the entire range, reaching from communication and processing of information, to sensor and metrological device design, the understanding of quantum many-body systems, as well as quantum phases and material science. At the same time, it has its roots in fundamental science, as it investigates and exploits the phenomena based on the fundamental principles of quantum mechanics. The unique combination and quality of activities in the Munich area places it in a particularly strong position to reach the very forefront of research on QST worldwide. The IMPRS Ph.D. students will therefore profit from an exceptionally broad, yet focussed, international training at the highest level that will combine theoretical, experimental and communication skills in a vibrant field pertinent to new technologies.

Basic Research

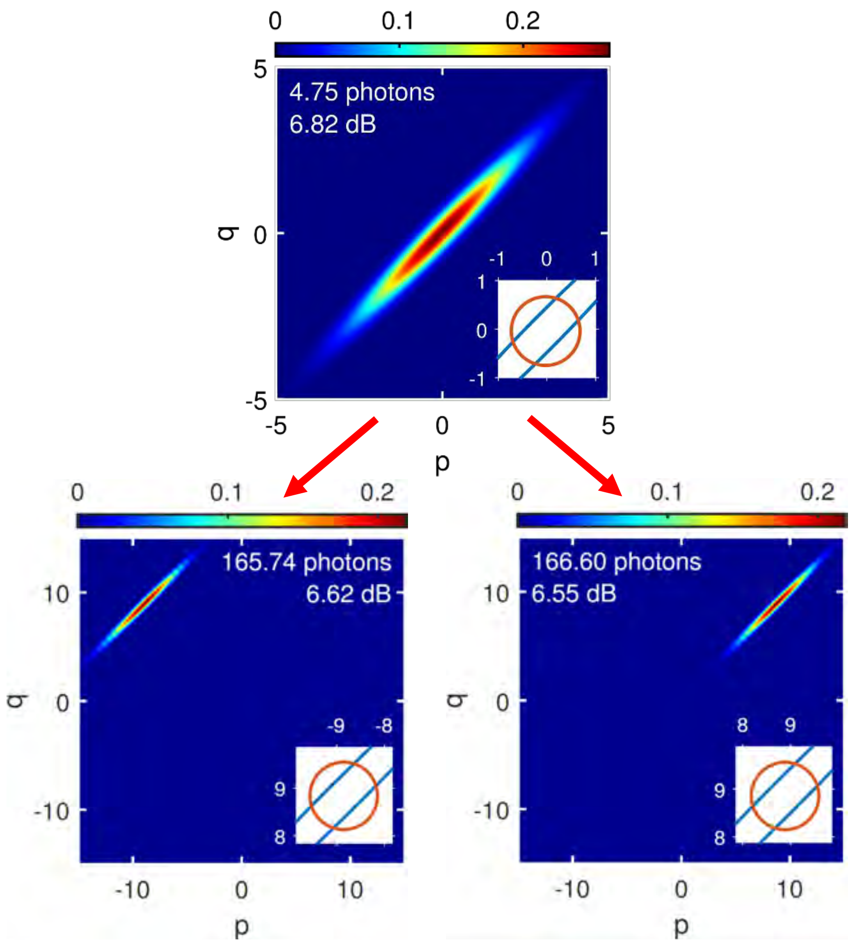

Wigner functions of a squeezed vacuum state with squeezing angle 45° (top figure) and displaced squeezed vacuum states with displacement angles 45° and 135° (bottom figures). The dimensionless variables p and q span the phase space. The bottom figures show that stable squeezing is preserved up to a displacement by 160photons. The insets show $1/e$ contour lines for the ideal vacuum (red), and the experimental squeezed states (blue).

Dissipation in phenomenological theories of superconductivity

Dietrich Einzel

Introduction

In this contribution I review various phenomenological descriptions of superconductivity, which are based on the notion of a macroscopic wave function, suitable for describing neutral and charged fermionic pair condensates. The first is the dynamic Schrödinger description, which is quantum–mechanical and dissipationless in origin and from which the celebrated London's theory emerges as the quasiclassical (or WKB) limit. The second is the stationary Ginzburg–Landau theory, which is also purely quantum–mechanical and dissipationless in origin, and includes in addition aspects of the phase transition from the normal to the superconducting or superfluid ground state. Finally, I review a new approach to introduce dissipation (characterized by a phenomenological relaxation time τ) into the description of superconductivity, proposed by A. A. Barybin [1] (hereafter referred to as AAB), which has the following virtues:

- It connects correctly the Schrödinger (slow relaxation, $\tau \to \infty$) with the stationary Ginzburg–Landau description (fast relaxation, $\tau \to 0$).
- In contrast to traditional treatments of the time–dependent Ginzburg–Landau equations [2], the AAB–description leads to the correct hydrodynamic equations for the motion of neutral and charged pair condensates.
- The dissipation effects can be related to the phenomenon of *intrinsic relaxation*, related to the transport coefficient of *second viscosity* ζ_3, which was investigated by the author in context with superfluid ^{3}He [3]

In what follows, I consider pair condensates of mass $m_s = 2m$ and charge $q_s = 2q$, which quite generally describe neutral ($q = 0$) or charged ($q = e$) fermion pairs. The quantum–mechanical properties of such condensates are described in terms of a macroscopic wave function

$$\Psi(\mathbf{r}, t) = a(\mathbf{r}, t)\mathrm{e}^{iS(\mathbf{r},t)/\hbar} \quad ; \quad S(\mathbf{r}, t) = \hbar\varphi(\mathbf{r}, t) \tag{1}$$

Here the amplitude a is related to a superfluid density n^s, the BCS result for which reads [4]

$$2a^2 = n^s = n\left\{1 - \int_0^\infty dt/\cosh^2\sqrt{t^2 + \left(\frac{\Delta(T)}{2k_B T}\right)^2}\right\} \tag{2}$$

This relation is seen to connect the order parameter Ψ of the phenomenological description with the energy gap $\Delta(T)$, which acts as the order parameter of the microscopic description. The scalar action field $S = \hbar\varphi$ represents the broken gauge or $U(1)$ symmetry associated with the superconducting or superfluid phase transition. In terms of the quasi–bosonic pair field Ψ, the phenomenological theories of superconductivity ("Ψ *theories*") can now be classified into Schrödinger and stationary as well as time–dependent Ginzburg–Landau descriptions, respectively.

Schrödinger description

The dissipationless dynamics of a pair condensate may be described by an application of the standard Schrödinger equation to the macroscopic wave function Ψ:

$$\left(i\hbar\frac{\partial}{\partial t} - \hat{\mathcal{H}}\right)\Psi = 0 \quad ; \quad \hat{\mathcal{H}} = \frac{1}{2m_s}\left(-i\hbar\boldsymbol{\nabla} - \frac{q_s}{c}\mathbf{A}\right)^2 + u_s \quad ; \quad u_s = q_s\Phi + 2\mu \tag{3}$$

Here $\hat{\mathcal{H}}$ can be referred to as the Hamiltonian of the Schrödinger description, in which Φ and $\mathbf{A}$ represent the electromagnetic scalar and vector potential, respectively. Moreover, u_s denotes the electrochemical potential, with μ being the ordinary chemical potential, absent from the Schrödinger equation for one Bose particle.

Stationary Ginzburg–Landau description

In the vicinity of the transition temperature T_c, the properties of a pair condensate, exposed to stationary external fields $\mathbf{B} = \boldsymbol{\nabla} \times \mathbf{A}$, are described by the celebrated Ginzburg–Landau equation [5]:

$$\hat{\mathcal{G}}\Psi = 0 \;\; ; \;\; \hat{\mathcal{G}} = \frac{1}{2m_s}\left(-i\hbar\boldsymbol{\nabla} - \frac{q_s}{c}\mathbf{A}\right)^2 - |\alpha| + \beta|\Psi|^2 \tag{4}$$

Here $\hat{\mathcal{G}}$ can be referred to as the Ginzburg–Landau differential operator, in which $\alpha = -|\alpha|$ and β are the well–known coefficients of an expansion of the free energy with respect to the order parameter Ψ [5].

Time–dependent Ginzburg–Landau (TDGL) description

The relaxational dynamics of pair condensates can finally be described by an extension of the Schrödinger equation to include a phenomenological relaxation term $\propto \tau^{-1}$ as follows [1]

$$\left(i\hbar\frac{\partial}{\partial t} - \hat{\mathcal{H}}\right)\Psi = \frac{i\hbar}{\tau}\hat{\mathcal{R}}\Psi \;\; ; \;\; \hat{\mathcal{R}} = -\frac{\hat{\mathcal{G}}}{|\alpha|} \tag{5}$$

The traditional time–dependent Ginzburg–Landau theory is seen to emerge from Eq. (5), if one replaces $\hat{\mathcal{H}} \to u_s$. There are two limits arising from Eq. (5), which can be easily identified with the Schrödinger description ($\tau \to \infty$) and the stationary Ginzburg–Landau description ($\tau \to 0$). Eqs. (3–5), though being fairly compact, are physically not particularly transparent. The physical content of these equations becomes visible after a decomposition of Ψ according to Eq. (1), which may be referred to as a Madelung–Feynman representation of the pair field [6, 7].

The Madelung–Feynman representation of the TDGL equations

Inserting (1) into the general TDGL equation (5), we arrive at the following two results:
(i) for the left hand side we get

$$\begin{aligned}
\left(i\hbar\frac{\partial}{\partial t} - \hat{\mathcal{H}}\right)\Psi &= -\left\{\dot{S} + 2H_S\right\}\Psi + \frac{i\hbar}{2n^s}\left\{\dot{n}^s + \boldsymbol{\nabla}\cdot\mathbf{j}^s\right\}\Psi \\
H_S &= q\Phi + \mu + \mu_{\mathrm{qm}} + \frac{m}{2}\mathbf{v}^{s2} \\
\mathbf{j}^s &= n^s\mathbf{v}^s \;\; ; \;\; \mathbf{v}^s = \frac{1}{m_s}\left(\boldsymbol{\nabla}S - \frac{q_s}{c}\mathbf{A}\right) \\
\mu_{\mathrm{qm}} &= -\frac{1}{2}\frac{\hbar^2\boldsymbol{\nabla}^2 a}{2m_s a}
\end{aligned} \tag{6}$$

Here $\mathbf{j}^s = n^s\mathbf{v}^s$ represents the *supercurrent density* and μ_{qm} is referred to as the *quantum–mechanical or Bohm potential* in the literature.

(ii) for the right hand side we obtain

$$\begin{aligned} \hat{\mathcal{R}}\Psi &= -\left\{ R + \xi^2 \frac{m_s}{i\hbar} \frac{\nabla \cdot \mathbf{j}^s}{n^s} \right\} \\ R &= \xi^2 \frac{8m}{\hbar^2} \left(\frac{m}{2} \mathbf{v}^{s2} + \mu_{qm} \right) + f^2 - 1 \\ \xi &= \frac{\hbar^2}{2m_s|\alpha|} \\ f &= \frac{a}{a_0} \; ; \; a_0^2 = \frac{|\alpha|}{\beta} \end{aligned} \tag{7}$$

Here ξ is referred to as the *Ginzburg–Landau coherence length* in the literature and f represents the order parameter of the TDGL theory normalized to its equilibrium value $a_0 = |\alpha|/\beta$. As a next step, we may now separate the real and the imaginary part of the TDGL equation. The *imaginary part* can be interpreted as a *continuity equation* with dissipation:

$$\dot{n}^s + \nabla \cdot \mathbf{j}^s = -\frac{2R}{\tau} n^s \tag{8}$$

The *real part* can be interpreted as a *Hamilton–Jacobi* or *Josephson equation* with dissipation:

$$-\frac{1}{2}\dot{S} = H_S + \mu_{diss} \; ; \; \mu_{diss} = -\xi^2 \frac{m}{\tau} \frac{\nabla \cdot \mathbf{j}^s}{n^s} \tag{9}$$

From the Josephson equation one may readily derive a superfluid acceleration equation (or Euler equation with dissipation, *different* from the Navier–Stokes equation):

$$\frac{d\mathbf{v}^s}{dt} = \frac{\partial \mathbf{v}^s}{\partial t} + \underline{(\mathbf{v}^s \cdot \nabla)\mathbf{v}^s} = \frac{q}{m}\left(\mathbf{E} + \underline{\frac{1}{c}\mathbf{v}^s \times \mathbf{B}} \right) - \frac{1}{m} \nabla \left(\mu + \mu_{diss} + \underline{\mu_{qm}} \right) \tag{10}$$

Note that the underlined terms in Eq. (10) are missing from the traditional TDGL treatment, which amounts to replacing $\hat{\mathcal{H}} \to u_s$. This clearly characterizes the deficiencies of the traditional TDGL description. It turns out that a physical interpretation of μ_{diss} is possible in terms of a *second viscosity* ζ_3 when applied to superfluid ^{3}He–B ($q = 0$), as the author has found in his doctoral thesis [3]

$$\frac{d\mathbf{v}^s}{dt} = -\frac{1}{m} \nabla \left\{ \mu - m\zeta_3 \nabla \cdot n^s(\mathbf{v}^s - \mathbf{v}^n) - \zeta_1 \nabla \cdot \mathbf{v}^n \right\} \equiv -\frac{1}{m} \nabla \left\{ \mu + \mu_{diss} \right\} \tag{11}$$

An identification of μ_{diss} in the limit $\mathbf{v}^n \to 0$ (in metals the normal fluid velocity $\mathbf{v}^n$ can be thought as pinned by the lattice) is now possible:

$$\mu_{diss} = -m \underbrace{\frac{\xi^2}{n^s \tau}}_{=\zeta_3} \nabla \cdot (n^s \mathbf{v}^s) = -m\zeta_3 \nabla \cdot (n^s \mathbf{v}^s) \tag{12}$$

One may now identify μ_{diss} as the coefficient of *second viscosity* ζ_3:

$$\zeta_3 = \frac{\xi^2}{n^s \tau} \tag{13}$$

We could therefore show, that the dissipation parameter μ_{diss}, which occurs in the TDGL theory, is related to the phenomenon of *intrinsic relaxation* of the order parameter, which sets in whenever there arises a mutual disequilibrium between normal ($n^n = n - n^s$) and superfluid (n^s) components at a constant total density $n = n^n + n^s$. Note that ζ_3 diverges in the limit $T \to T_c$ since there is a number conservation law in the normal state.

Eqs. (8–10) manifest the central result of this contribution. In the absence of dissipation (i.e. in the limit of slow relaxation, $\tau \to \infty$) these equations can easily be interpreted as (i) a quasi–conservation law for the superfluid density (from (8)) and (ii) a Josephson or equivalently Hamilton–Jacobi equation for the action field S (from (9)). It is worth noting, that the phenomenological dynamic London's theory of superconductivity emerges from Eqs. (8–10) in the quasiclassical limit ($\mu_{qm} \to 0$), in spirit of the WKB approximation of quantum mechanics [8–10]. In the opposite limit of fast relaxation ($\tau \to 0$) one is left with the traditional stationary Ginzburg–Landau theory ($\hat{\mathcal{G}}\Psi = 0$), which has to be amended by Ampere's law $\boldsymbol{\nabla} \times \mathbf{B} = 4\pi \mathbf{j}^s/c$. The latter describes screening effects of the supercurrent density $\mathbf{j}^s$ on the magnetic induction $\mathbf{B}$ inside the superconductor, that represent one important aspect leading to the Meissner–Ochsenfeld effect.

Summary and conclusion

In summary, I have formulated a version of the phenomenological theory of superconductivity and (fermionic) superfluidity, which elegantly unifies earlier approaches as different as the London's and the Ginzburg–Landau theory. The introduction of dissipation effects into this phenomenological description, being pioneered in Ref. [1] by a very smart extension of the traditional time–dependent Ginzburg–Landau theory, has eventually led me to the physical interpretation of the dissipation effects in terms of the well–studied phenomenon of intrinsic relaxation of the order parameter n^s. This interpretation is new and has, at least to my knowledge, never been formulated in previous work on the subject. The traditional TDGL theory could be shown to have deficiencies with respect to the explicit form of the superfluid acceleration or the Euler equation (c.f. underlined terms in Eq. (10)), which could be successfully corrected within the approach of Ref. [1].

References

[1] A. A. Barybin, Adv. Cond. Mat. Phys. **2011**, 1–10 (2011).
[2] A. Schmid, Phys. Kond. Materie **5**, 302–317 (1966).
[3] P. K. Wölfle, and D. Einzel, J. Low Temp. Phys. **32**, 39–56 (1978).
[4] J. Bardeen, L. N. Cooper, and J. R. Schrieffer, Phys. Rev. **108**, 1175–1204 (1957).
[5] V. L. Ginzburg, and L. D. Landau, Zh. Eksp. Teor. Fiz. **20**, 1064–1082 (1950).
[6] E. Madelung, Z. Phys. **40**, 322–326 (1926).
[7] R. P. Feynman, R. B. Leighton, and M. Sands (eds.) *The Feynman Lectures on Physics. Vol 3: Quantum Mechanics* (Addison–Wesley, Reading, Mass., USA, 1965).
[8] G. Wentzel, Z. Phys. **38**, 518–529 (1926).
[9] H. A. Kramers, Z. Phys. **39**, 828–840 (1926).
[10] L. Brillouin, Comptes Rendus de l'Academie des Siences **183**, 24–26 (1926).

Spin-driven nematicity in $Ba(Fe_{1-x}Co_x)_2As_2$

R. Hackl, T. Böhm, F. Kretzschmar, A. Baum, N. Chelwani, D. Jost [1]
U. Karahasanović, J. Schmalian [2]
S. Caprara, M. Grilli, C. Di Castro [3]
J.-H. Chu, I. R. Fisher [4,5]

The origin of phase transitions is among the challenging issues in condensed matter physics. For example, it took almost 100 years to find a description of the second order transition between a vapor and a liquid at the critical point or of magnetic ordering [1–3]. The BCS theory of superconductivity was presented only 46 years after the discovery of the phenomenon [4]. There is still no agreement on the interaction driving the Verwey transition [5–7]. Similarly, the magneto-structural transition in the iron pnictides and chalcogenides is controversial. Kontani and colleagues suggested that orbital ordering drives the magneto-structural transition in a fashion similar to that in the manganites [8] whereas Fernandes *et al.* argue that magnetism is the leading instability [9]. The subject becomes particularly interesting since the related fluctuations are suspected to be relevant for Cooper pairing [10].

For deeper insight we studied $Ba(Fe_{1-x}Co_x)_2As_2$ in the doping range $0 \leq x \leq 0.085$ by polarized Raman scattering. In $Ba(Fe_{1-x}Co_x)_2As_2$ the structural and the magnetic phase transition occur at distinct temperatures, T_s and T_{SDW}, respectively for $x > 0$. Between T_s and T_{SDW} the material exhibits nematic order where the C_4 rotational symmetry is broken while the O(3) symmetry is still preserved implying the absence of magnetic order. Given that critical fluctuations can be observed one would expect the fluctuations to disappear at the related phase transition temperature where the correlation length diverges. In contrast, the fluctuations of the amplitude of the order parameter (Higgs mode) appear above and below the transition. The plan is therefore to first identify the type of fluctuations and then to study and analyze their dependence on temperature and photon polarizations [11].

Since we are dealing with small temperature differences close to the heating by the laser the local temperature should be determined as precise as possible. We are in the fortunate situation that the sample offers internal thermometers since twin boundaries appear at the tetragonal to orthorhombic transition at T_s and some phonons sense the transition into the magnetic spin density wave (SDW) phase at T_{SDW}. The observation of the twin boundaries allows us to determine the laser heating and T_s with an accuracy of ± 0.1 K. The detailed studies also demonstrate that the crystals are (at least locally) very homogeneous in terms of Co substitution. As usual, there is no free lunch. The twin boundaries effectively getter the residual gas leading to a stronger elastic scattering close to the laser line that necessitates corrections. The phonon anomalies develop more continuously and T_{SDW} can be determined only to within ± 1 K, which is still significantly smaller than $T_s - T_{\mathrm{SDW}}$ at all doping levels studied.

[1] The project is funded by the German Research Foundation (DFG) via the Priority Program SPP 1458 (Grant-No. HA 2071/7-2) and partially via the Transregional Collaborative Research Center TRR 80. Additional support came from the Bavarian Californian Technology Center (BaCaTeC, project no. A5 [2012-2]).

[2] Institute for Theoretical Condensed Matter Physics (TKM), Karlsruhe Institute of Technology (KIT), 76128 Karlsruhe, Germany. Financial support from the German Research Foundation (DFG) via the Priority Program SPP 1458 (Grant-No. SCHM 1035/5) and the Helmholtz Association through the Helmholtz post-doctoral grant PD-075 'Unconventional order and superconductivity in pnictides' is gratefully acknowledged.

[3] Department of Physics, University of Rome "Sapienza", 00185 Roma, Italy

[4] Stanford Institute for Materials and Energy Sciences, SLAC National Accelerator Laboratory, 2575 Sand Hill Road, Menlo Park, CA 94025, USA. Work in the Stanford Institute for Materials and Energy Sciences (SIMES) at Stanford and SLAC was supported by the US Department of Energy, Office of Basic Energy Sciences, Division of Materials Sciences and Engineering, under Contract No. DE-AC02-76SF00515.

[5] Geballe Laboratory for Advanced Materials & Dept. of Applied Physics, Stanford University, CA 94305, USA.

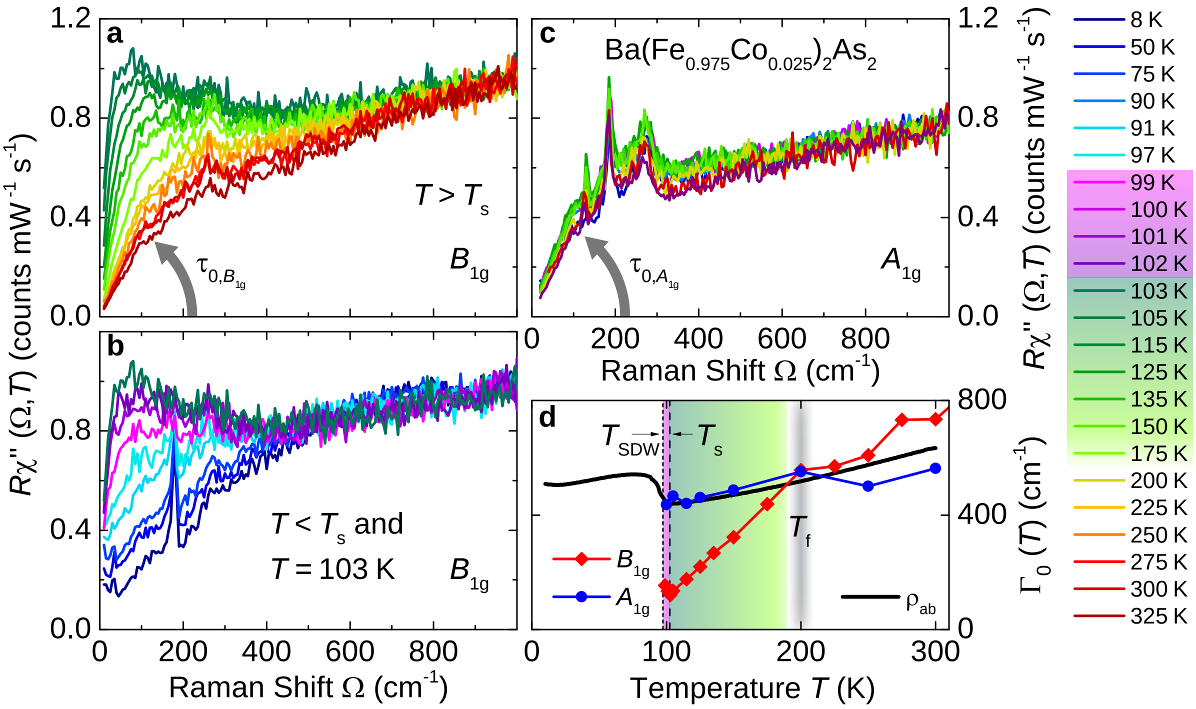

Figure 1: Raman response $R\chi''(\Omega, T)$ (raw data after division by the Bose-Einstein factor) of $Ba(Fe_{0.975}Co_{0.025})_2As_2$ in **a** B_{1g} above and **b** below T_s and **c** A_{1g} symmetry at temperatures as indicated. The initial slopes shown in **a** and **c** as grey arrows are proportional to the static two-particle lifetime in symmetry $\mu = A_{1g},\ B_{1g}$. **d** Raman relaxation rates $\Gamma_{0,\mu}(T)$ in A_{1g} (blue circles) and B_{1g} (red diamonds) symmetry as a function of temperature. The fluctuation range $T_s < T < T_f$ and the nematic phase $T_{\mathrm{SDW}} < T < T_s$ are indicated in green and magenta, respectively. The resistivity of the sample [17] (black line) is converted into a scattering rate via the Drude formula.

In Fig. 1 **a**, **b**, and **c** we show the Raman response $R\chi''(\Omega, T)$, with R an experimental constant, of $Ba(Fe_{1-x}Co_x)_2As_2$ at $x = 0.025$ for various temperatures in A_{1g} and B_{1g} symmetry with respect to the 1 Fe cell. Results for other doping levels x are shown in Ref. [11]. The spectra comprise a superposition of several types of excitations including narrow phonon lines and slowly varying continua arising from electron-hole (e-h) pairs; hence the continuum reflects the dynamical two-particle behaviour. The A_{1g} and B_{1g} spectra predominantly weigh out contributions from the central hole bands and the electron bands, respectively [12]. The symmetry-dependent initial slope $\tau_{0,\mu}(T)$ ($\mu = A_{1g}, B_{1g}, B_{2g}$) [see Fig. 1 **a** and **c**] can be compared to transport data. $[\tau_{0,\mu}(T)]^{-1}$ corresponds to the static transport relaxation rate $\Gamma_{0,\mu}(T)$ of the conduction electrons. The memory function method facilitates the quantitative determination of the dynamic relaxation $\Gamma(\Omega, T)$ in absolute energy units [13]. The static limit can be obtained by extrapolation, $\Gamma_{0,\mu}(T) = \Gamma_\mu(\Omega \to 0, T)$ and is shown in Fig. 1 **d**. Above approximately 200 K $\Gamma_{0,\mu}(T)$ varies slowly and similarly in both symmetries. The more rapid decrease of $\Gamma_{0,B1g}(T)$ below 200 K is accompanied by a strong intensity gain in the range 20–200 cm^{-1} [see Fig. 1 **a**] as observed before in similar samples [14–16]. The intensity gain indicates that there is an additional contribution superposed on the e-h continuum which arises from fluctuations. Therefore, the kink in $\Gamma_{0,B1g}(T)$ is labeled T_f and marks the crossover temperature below which nematic fluctuations can be observed by Raman scattering. The kink allows us to separate the two regimes of the low-energy response above and below T_f as being dominated by carrier excitations and fluctuations, respectively.

If we assume that the e-h continuum at low energies varies in a similar way as the resistivity the response from fluctuations can be separated out. We approximate the continuum at T_f by an analytic function which is then determined for each temperature according to the variation of the resistivity and the A_{1g} spectra and subtracted from all spectra at lower temperatures.

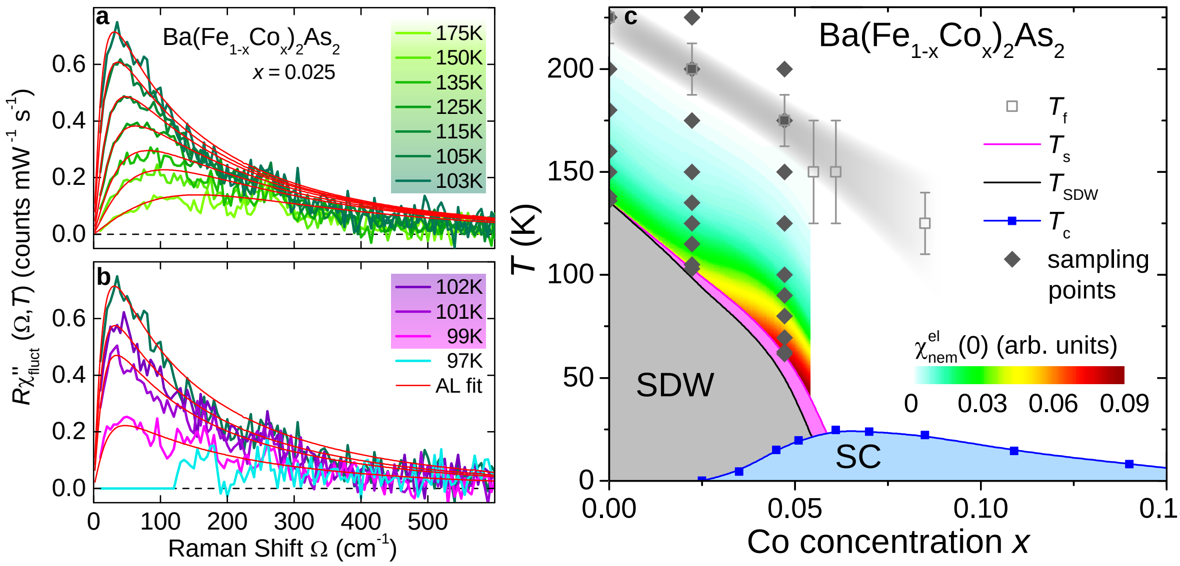

Figure 2: Fluctuations in $Ba(Fe_{1-x}Co_x)_2As_2$. **a** and **b** Fluctuation contribution to the Raman response of $Ba(Fe_{0.975}Co_{0.025})_2As_2$ **a** above $T_s = 102.8\,K$ and **b** between T_s and $T_{SDW} = 98\,K$. The red lines are theoretical predictions on the basis of Aslamazov-Larkin diagrams [18] describing the exchange of a pair of fluctuations. **c** Phase diagram of $Ba(Fe_{1-x}Co_x)_2As_2$ as derived from the initial slope of the fluctuation response. The full lines limiting the nematic phase (magenta) and the blue squares representing the transition temperature T_c of superconducting samples were derived in Ref. [17]. Grey diamonds represent doping and temperature positions of the current Raman data. The coloured field between T_s and T_f represents the initial slope of the spectra [those for $x = 0.025$ are shown in **a**] according to the colour scale on the right. The nematic susceptibility $\chi^{el}_{nem}(0)$ is proportional to the initial slope.

The results of the subtraction procedure are shown in Fig. 2 **a** and **b**. The response increases rapidly towards T_s without, however, diverging, and the maximum moves to lower energies.

The fluctuations do not disappear directly below T_s [Fig. 2 **b**] as one would expect if long-ranged order would be established. Rather, the intensity decreases continuously and the maximum stays approximately pinned implying that the correlation length does not change substantially between the two transitions at $T_s = 102.8 \pm 0.1\,K$ and $T_{SDW} = 98 \pm 1\,K$. The persistence of the fluctuations down to T_{SDW} argues for their magnetic origin.

We compare the data to the theoretical model for thermally driven spin fluctuations associated with the striped magnetic phase with ordering vectors along $\mathbf{Q}_x = (\pi, 0)$ or $\mathbf{Q}_y = (0, \pi)$ [19]. In leading order two noninteracting fluctuations carrying momenta $\mathbf{Q}$ and $-\mathbf{Q}$ are exchanged and entail $\mathbf{Q}$-dependent selection rules that were derived along with the spectral response by Caprara and coworkers [18]. For the ordering vectors $(\pi, 0)$ and $(0, \pi)$ the resulting selection rules explain the enhancement of the signal in B_{1g} symmetry and its absence in the A_{1g} and B_{2g} channels. The B_{1g} selection rules can also be explained if charge fluctuations between the electron bands are assumed to be at the origin of the response [15]. Then, however, the fluctuations are expected to disappear at T_s rather than T_{SDW} in contrast to our experimental observations.

For describing the fluctuations in the nematic phase it is important to include interactions between the fluctuations [20, 21]. In addition, since a structural transition precedes the SDW the lattice has to be taken into account [22]. This combination allows a consistent description of the response in terms of critical spin fluctuation at least at moderate doping levels [11].

The Raman response was also studied for various other doping levels in the range $0 \leq x \leq 0.085$. Up to 6.1% Co substitution fluctuations were observed. In contrast to other publications [15] we were not able to clearly identify and isolate the response of fluctuations at 8.5% although the kink in the B_{1g} relaxation rate, used to define T_f, is clearly observed. The results up to 5.1% are unambiguous and are represented as a color scale on the phase diagram in Fig. 2 **c**. Our phase diagram compares rather well to that derived from the elastic constant m_{66} [23]. In addition, we show T_f up to $x = 0.085$. The fluctuations can be observed over a temperature range of approximately 70–100 K. This is more than in most of the other experiments on unstrained samples and comparable to what is found in the cuprates [24, 25].

In summary, using Raman scattering we find clear indications of critical fluctuations related to the magneto-structural phase transition in $Ba(Fe_{1-x}Co_x)_2As_2$. The cross-section is large enough so as to allow us to isolate the response and to compare the spectra to theoretical predictions. The temperature dependence, the selection rules, and the spectral shape support a magnetic origin of the fluctuations [21]. Hence we find experimental support for magnetism to be the leading instability [11]. Since the fluctuations appear to survive longer than the ordered magnetic phase an interrelation with superconductivity is in fact possible [10]. However, there is still a long way to go to possibly analyze their contribution to Cooper pairing.

References

[1] C. Di Castro, and G. Jona-Lasinio, Phys. Lett. **A** **29**, 322 – 323 (1969).
[2] K. G. Wilson, Phys. Rev. B **4**, 3174–3183 (1971).
[3] K. G. Wilson, Phys. Rev. B **4**, 3184–3205 (1971).
[4] J. Bardeen, L. N. Cooper, and J. R. Schrieffer, Phys. Rev. **108**, 1175 (1957).
[5] N. F. Mott. *Metal-Insulator Transitions* (Taylor and Francis, London, 1990).
[6] M. Imada, A. Fujimori, and Y. Tokura, Rev. Mod. Phys. **70**, 1039–1263 (1998).
[7] F. Walz, J. Phys.: Condens. Matter **14**, R285.
[8] H. Kontani, T. Saito, and S. Onari, Phys. Rev. B **84**, 024528 (2011).
[9] R. M. Fernandes, A. V. Chubukov, J. Knolle, I. Eremin, and J. Schmalian, Phys. Rev. B **85**, 024534 (2012).
[10] E. Fradkin, S. A. Kivelson, and J. M. Tranquada, Rev. Mod. Phys. **87**, 457–482 (2015).
[11] F. Kretzschmar, T. Böhm, U. Karahasanović, B. Muschler, A. Baum, D. Jost, J. Schmalian, S. Caprara, M. Grilli, C. Di Castro, J. G. Analytis, J.-H. Chu, I. R. Fisher, and R. Hackl, ArXiv e-prints (2015). Accepted for publication in Nature Physics, `arXiv:1507.06116 [cond-mat.str-el]`.
[12] I. I. Mazin, T. P. Devereaux, J. G. Analytis, J.-H. Chu, I. R. Fisher, B. Muschler, and R. Hackl, Phys. Rev. B **82**, 180502 (2010).
[13] M. Opel, R. Nemetschek, C. Hoffmann, R. Philipp, P. F. Müller, R. Hackl, I. Tüttő, A. Erb, B. Revaz, E. Walker, H. Berger, and L. Forró, Phys. Rev. B **61**, 9752–9774 (2000).
[14] K.-Y. Choi, P. Lemmens, I. Eremin, G. Zwicknagl, H. Berger, G. L. Sun, D. L. Sun, and C. T. Lin, J. Phys.: Condens. Matter **22**, 115802 (2010).
[15] Y. Gallais, R. M. Fernandes, I. Paul, L. Chauvière, Y.-X. Yang, M.-A. Méasson, M. Cazayous, A. Sacuto, D. Colson, and A. Forget, Phys. Rev. Lett. **111**, 267001 (2013).
[16] V. K. Thorsmølle, M. Khodas, Z. P. Yin, C. Zhang, S. V. Carr, P. Dai, and G. Blumberg, ArXiv e-prints (2014). `arXiv:1410.6456 [cond-mat.supr-con]`.
[17] J.-H. Chu, J. G. Analytis, C. Kucharczyk, and I. R. Fisher, Phys. Rev. B **79**, 014506 (2009).
[18] S. Caprara, C. Di Castro, M. Grilli, and D. Suppa, Phys. Rev. Lett. **95**, 117004 (2005).
[19] D. S. Inosov, J. T. Park, P. Bourges, D. L. Sun, Y. Sidis, A. Schneidewind, K. Hradil, D. Haug, C. T. Lin, B. Keimer, and V. Hinkov, Nat. Phys. **6**, 178 (2010).
[20] M. Khodas, and A. Levchenko, Phys. Rev. B **91**, 235119 (2015).
[21] U. Karahasanovic, F. Kretzschmar, T. Böhm, R. Hackl, I. Paul, Y. Gallais, and J. Schmalian, Phys. Rev. B **92**, 075134 (2015).
[22] H. Kontani, and Y. Yamakawa, Phys. Rev. Lett. **113**, 047001 (2014).
[23] H.-H. Kuo, J.-H. Chu, S. A. Kivelson, and I. R. Fisher, ArXiv e-prints (2015). `arXiv:1503.00402 [cond-mat.supr-con]`.
[24] B. Muschler, W. Prestel, L. Tassini, R. Hackl, M. Lambacher, A. Erb, S. Komiya, Y. Ando, D. Peets, W. Hardy, R. Liang, and D. Bonn, Eur. Phys. J. Special Topics **188**, 131 (2010).
[25] S. Caprara, M. Colonna, C. Di Castro, R. Hackl, B. Muschler, L. Tassini, and M. Grilli, Phys. Rev. B **91**, 205115 (2015).

Spin-boson model in circuit QED

F. Deppe, M. Haeberlein, J. Goetz, A. Baust, P. Eder, K. Fedorov, M. Fischer, E. P. Menzel, F. Wulschner, E. Xie, L. Zhong, A. Marx, R. Gross [1]
E. Solano, [2] *A. Kurcz, J. J. García-Ripoll* [3]

Quantum impurity models consist of a small, finite-dimensional quantum system, interacting with a larger system, a bath or environment. If the focus is set on the impurity, such as in the spin-boson model [1], these models constitute canonical examples of open quantum systems, providing an insight into the validity of the Markovian approximation and in a variety of phase transitions such as the localization at large coupling strengths. However, the focus may also shift from the impurity to the environment, whose transport properties can be dramatically affected by small impurities. Superconducting circuits are ideal systems for the study of quantum impurity models and their dynamical properties. First, superconducting qubits are broadband tunable devices which allow both strong and, potentially, ultrastrong spin-boson coupling [2]. Finally, state-of-the-art superconducting circuit technology allows for engineering of various kinds of photonic/bosonic environments: linear, nonlinear or even quantum. Here [3], we report on an experimental characterization of the spin-boson model using a superconducting quantum two-level system (qubit) embedded into a broadband engineered environment, which is realized by a microwave transmission line. The latter is the dominant reservoir allowing for a quantitative comparison between a straightforward microscopic model and the experimental results. Exploiting the exceptionally strong qubit-line coupling, we use a single qubit in a resonance fluorescence experiment as a powerful probe of the bosonic bath.

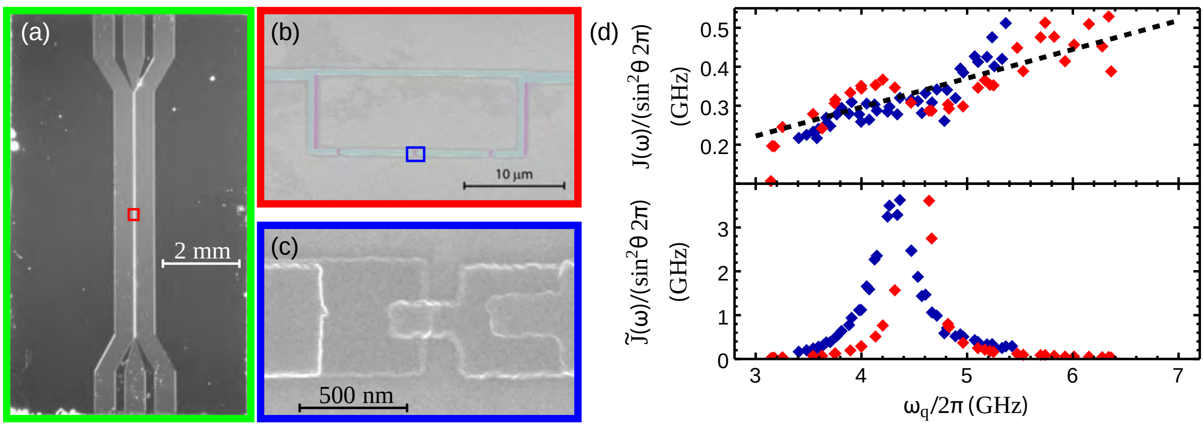

Figure 1: (a) Photograph of the sample chip. The bright structure is the transmission line. Dark grey: Substrate surface. (b) Zoom-in onto the red rectangle in (a) showing the qubit loop (optical microscopy image). (c) Zoom-in onto the blue rectangle in (b) showing one of the Josephson junctions (scanning electron microscopy image). (d) Top: Ohmic spectral function $J(\omega)$ of the bare transmission line. Blue (red) dots correspond to impedance mismatches of $103\,\Omega$ ($61\,\Omega$) at the reflection points. The dashed black line indicates $g/\omega \simeq 15\,\%$. Bottom: Peaked spectral functions $\tilde{J}(\omega)$ of the total environment including the reflectors.

Optical and SEM micrographs of our sample chip are shown in Figs. 1(a)-(c). The two-level system in our experiment is a superconducting flux qubit [4] built from a superconducting aluminum ring which is interrupted by three Al/AlO_x/Al-Josephson junctions. The engineered environment is realized by a 10 mm long on-chip superconducting aluminum coplanar waveguide transmission line with a characteristic impedance $Z_0 = 50\,\Omega$. In the framework of

[1] The authors acknowledge support from the German Research Foundation through SFB 631 and FE 1564/1-1, the EU project PROMISCE, the doctorate program ExQM of the Elite Network of Bavaria, and the German Excellence Initiative via the 'Nanosystem Initiative Munich' (NIM).
[2] University of the Basque Country UPV/EHU and IKERBASQUE Basque Foundation for Science, Spain
[3] Instituto de Física Fundamental IFF-CSIC, Spain

the spin-boson model, the interaction between flux qubit and reservoir is characterized by the spectral function $J(\omega)$. From our data, we are able to extract information on two scenarios. First, as shown in the top panel of Fig. 1(d), we recover the signature of the bare transmission line with a bath contribution to $J(\omega) \propto \omega$. Here, $J(\omega)|_{\omega=\omega_q} = \Gamma_1(\omega_q)$ is the spontaneous emission rate of the qubit into a quasi-one dimensional open space. From an independent experiment, we expect that the slope of the ohmic line should correspond to a scaled qubit-line coupling strength $g/\omega \simeq 15\,\%$. Figure 1(d) confirms that this is indeed the case. Second, the actual environment also contains the signature of two weak reflectors caused by the connection of our on-chip transmission line with external cabling. As shown in the bottom panel of Fig. 1(d), the spectral function $\tilde{J}(\omega)$ including the reflectors forms a broad peak centered just above 4 GHz. By thermal cycling, we move from a situation where $\tilde{J}(\omega)$ represents an enhanced spontaneous emission to the onset of the strong coupling regime where the spontaneous emission picture breaks down.

In summary, we experimentally implement the spin-boson model with an engineered reservoir using superconducting circuits. Our work constitutes an important step towards the quantum simulation of impurity models with superconducting circuits. In particular, the implementation of more complex scatterer configurations in the spirit of quantum metamaterials or band engineering in photonic crystals will allow for creation and experimental studies of highly non-ohmic environments.

References

[1] A. J. Leggett, S. Chakravarty, A. T. Dorsey, M. P. A. Fisher, A. Garg, and W. Zwerger, Rev. Mod. Phys. **59**, 1 (1987).

[2] T. Niemczyk, F. Deppe, H. Huebl, E. P. Menzel, F. Hocke, M. J. Schwarz, J. J. García-Ripoll, D. Zueco, T. Hümmer, E. Solano, A. Marx, and R. Gross, Nature Physics **6**, 772–776 (2010).

[3] M. Haeberlein, F. Deppe, A. Kurcz, J. Goetz, A. Baust, P. Eder, K. G. Fedorov, M. Fischer, E. P. Menzel, M. J. Schwarz, F. Wulschner, E. Xie, L. Zhong, E. Solano, A. Marx, J.-J. García-Ripoll, and R. Gross. Spin-boson model with an engineered reservoir in circuit quantum electrodynamics. Submitted for publication, `arXiv:1506.09114` (2015).

[4] T. Niemczyk, F. Deppe, M. Mariantoni, E. Menzel, E. Hoffmann, G. Wild, L. Eggenstein, A. Marx, and R. Gross, Supercond. Sci. Technol. **22**, 034009 (2009).

Displacement of propagating squeezed microwave states

K.G. Fedorov, S. Pogorzalek, P. Eder, M. Fischer, J. Goetz, F. Wulschner, E. Xie, F. Deppe, A. Marx, R. Gross [1]

One of the cornerstones of quantum communication is the paradigm of quantum teleportation which allows one to faithfully transmit an unknown quantum state between two spatially separated parties using a quantum resource and a classical communication channel. Fundamental operations needed to implement the quantum teleportation protocol include two-mode squeezed state generators, quadrature measurements, and a conditional displacement operator. While there are experimental advances for the first two operations, the controlled displacement of propagating quantum microwaves has not yet been demonstrated. Note that displacement belongs to the universal set of quantum gates required for quantum information processing with continuous variables [1]. Moreover, from a more fundamental point of view, displacement allows to study very general limits of quantum entanglement and coherence.

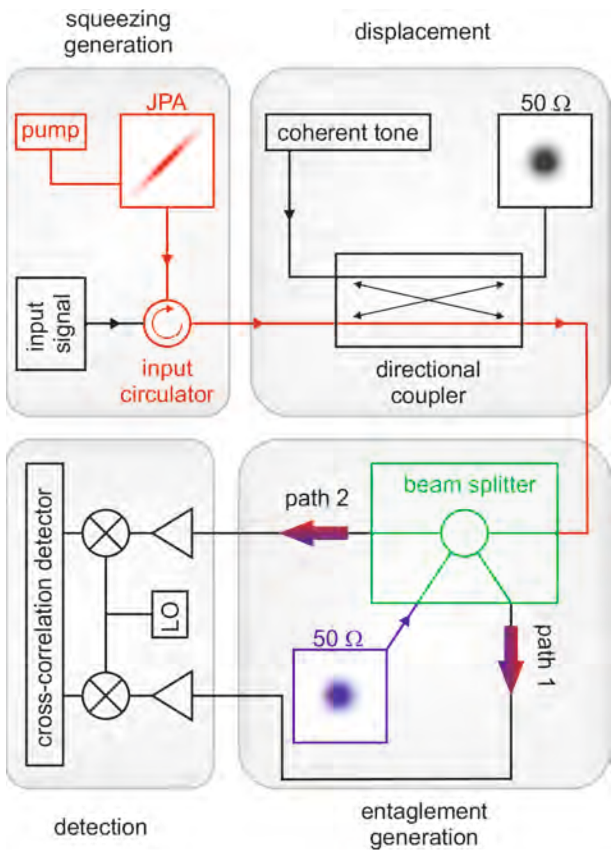

Figure 1: Schematic layout for the displacement of propagating squeezed microwave states.

Figure 1 shows a schematic layout of our experimental setup. We use a flux-driven Josephson parametric amplifier (JPA) for generation of squeezed microwave states. The JPA consists of a $\lambda/4$ coplanar resonator shunted by a dc-SQUID. The strong pump tone allows to modulate the Josephson inductance of the dc-SQUID at twice the JPA frequency $f_{\text{pump}} = 2f_{\text{JPA}}$, thus, fulfilling the condition for parametric amplification and squeezing an input microwave state [2, 3]. The JPA is placed in a magnetically shielded sample holder inside a custom-made dry dilution refrigerator. During all experiments the JPA temperature was stabilized at 50 mK.

The task of the JPA is to perform a squeezing operation on an incident vacuum state $\hat{S}(\xi)|0\rangle$, where $\hat{S}(\xi) = \exp(\frac{1}{2}\xi^*\hat{a}^2 - \frac{1}{2}\xi(\hat{a}^\dagger)^2)$, and $\xi = re^{i\phi}$ is the complex squeezing amplitude. Here, the phase ϕ determines the squeezed quadrature direction in phase space, while the squeezing factor r parameterizes the amount of squeezing. For implementation of a displacement operation $\hat{D}(\alpha) = \exp(\alpha\hat{a}^\dagger - \alpha^*\hat{a})$ on propagating squeezed states, we use a cryogenic directional coupler. The complex displacement amplitude α is controlled via a strong coherent signal incident to the coupling port of the directional coupler (see Fig. 1).

In order to reconstruct the displaced squeezed states, we apply a dual-path reconstruction scheme [2, 4]. It consists in splitting our signal into two paths with a hybrid ring, then amplifying the signal with a chain of cryogenic and room temperature rf-amplifiers and, finally,

[1]The authors acknowledge support from the German Research Foundation through SFB 631 and FE 1564/1-1, the EU project PROMISCE, the doctorate program ExQM of the Elite Network of Bavaria, and the German Excellence Initiative via the 'Nanosystems Initiative Munich' (NIM).

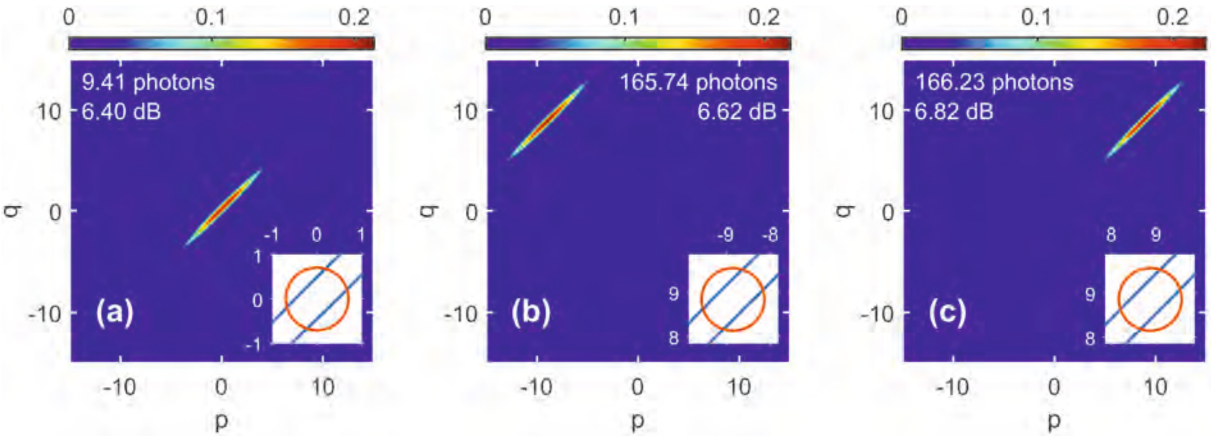

Figure 2: Reconstructed squeezed states at the input of the hybrid ring, p and q are dimensionless variables spanning the phase space. The JPA working frequency is $f_{\text{JPA}} = 5.573$ GHz, the applied pump power is $P_{\text{pump}} = -25$ dBm, which corresponds to a non-degenerate gain of $G = 9.9$ dB. The squeezing angle was stabilized at $\gamma = 45$. Wigner function of **(a)** a squeezed vacuum state, **(b)** a displaced squeezed vacuum state with a displacement angle $\theta = 135\ ^\circ$, **(c)** a displaced squeezed vacuum state with a displacement angle $\theta = 45\ ^\circ$. Numbers show the total number of photons in the states and the respective squeezing levels below vacuum in dB units. Insets illustrate $1/e$ contours for the ideal vacuum (red), and experimental squeezed states (blue).

performing a cross-correlation measurements. In this way, we can retrieve all the moments of the annihilation and creation operators, $\langle (a^\dagger)^n a^m \rangle$, of the signal mode and reconstruct a quasiprobability distribution (Wigner function) of the quantum signal incident to the hybrid ring.

We characterize the squeezing level of the reconstructed quantum state in decibel as $S = -10\log[(\Delta X_{sq})^2/0.25]$, where $(\Delta X_{sq})^2$ is the variance of the squeezed quadrature and the chosen vacuum reference is $(\Delta X_{vac})^2 \equiv 0.25$. We say that a state is squeezed below the vacuum level when $(\Delta X_{sq})^2 < 0.25$. Figure 2 illustrates Wigner functions of a squeezed vacuum, and a displaced squeezed vacuum for two different displacement angles. We observe that the directional coupler allows us to displace the propagating squeezed state with a high degree of control over both amplitude and phase of the displacement parameter α. Even for large displacement powers up to hundreds of photons, the squeezing remains unchanged within our experimental accuracy.

In conclusion, we have experimentally successfully realized the displacement of propagating squeezed states. In future experiments, we plan to use the displacement operation for quantum communication and information protocols with propagating squeezed states.

References

[1] U. L. Andersen, J. S. Neergaard-Nielsen, P. van Loock, and A. Furusawa, Nat. Phys. **11**, 713–719 (2015).

[2] E. P. Menzel, R. Di Candia, F. Deppe, P. Eder, L. Zhong, M. Ihmig, M. Haeberlein, A. Baust, E. Hoffmann, D. Ballester, K. Inomata, T. Yamamoto, Y. Nakamura, E. Solano, A. Marx, and R. Gross, Phys. Rev. Lett. **109**, 250502 (2012).

[3] L. Zhong, E. P. Menzel, R. D. Candia, P. Eder, M. Ihmig, A. Baust, M. Haeberlein, E. Hoffmann, K. Inomata, T. Yamamoto, Y. Nakamura, E. Solano, F. Deppe, A. Marx, and R. Gross, New Journal of Physics **15**, 125013 (2013).

[4] E. P. Menzel, F. Deppe, M. Mariantoni, M. A. Araque Caballero, A. Baust, T. Niemczyk, E. Hoffmann, A. Marx, E. Solano, and R. Gross, Phys. Rev. Lett. **105**, 100401 (2010).

Non-local magnetoresistance in YIG/Pt nanostructures

S. T. B. Goennenwein, R. Schlitz, M. Pernpeintner, K. Ganzhorn, M. Althammer, R. Gross, H. Huebl [1]

As described in the annual reports 2013 and 2014, we have discovered and modeled a novel magnetoresistance effect based on pure spin current transport back in 2013. This so-called spin Hall magnetoresistance (SMR) arises in thin non-magnetic metal films deposited onto an electrically insulating ferrimagnet [1, 2]. In most of our SMR experiments, we use yttrium iron garnet ($Y_3Fe_5O_{12}$, YIG) as the insulating magnet, and platinum (Pt) as the normal metal. The SMR in such YIG/Pt heterostructures manifests itself as a characteristic $\cos^2\alpha$-like modulation of the Pt resistance, as a function of the magnetization orientation α in the adjacent YIG. Systematic experiments performed at WMI show that the SMR is virtually independent of temperature (in the range $2\,\mathrm{K} \leq T \leq 300\,\mathrm{K}$) [3], and that it persists from DC up to frequencies of at least several GHz [4].

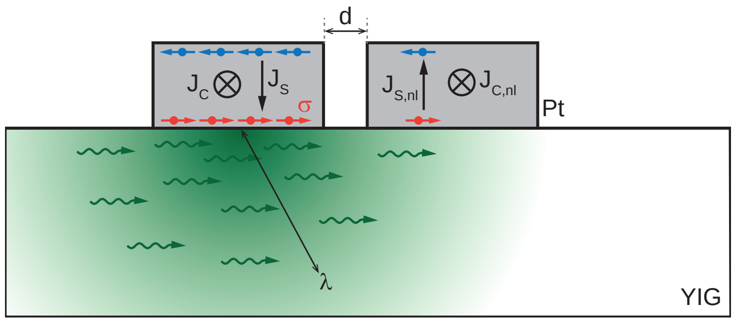

Figure 1: Sketch of the mechanism for non-local, magnon-mediated magnetoresistance in YIG/Pt nanostructures.

With the SMR effect now well established and understood, a logical next step is to investigate non-local magnetoresistance effects in YIG/Pt nanostructures. As illustrated in Fig. 1, the idea hereby is to electrically inject a non-equilibrium magnon accumulation in YIG (green wiggly arrows). This is achieved by driving a charge current J_C through a Pt strip (left gray box). Owing to the spin Hall effect, J_C is accompanied by a transverse spin current J_S, which in turn induces a spin accumulation σ (red arrows) in the Pt metal at the interface to YIG. According to theoretical work by Zhang & Zhang [5], a finite σ can induce in a finite magnon spin accumulation in the adjacent, electrically insulating YIG. The corresponding non-equilibrium magnons (green wiggly arrows) then will diffuse away and eventually reach a second Pt electrode (right gray box in Fig. 1), where they are converted back to a non-local charge current $J_{C,nl}$ (viz. open circuit voltage V_{nl}) by the inverse spin Hall effect. Given that the separation d between the 'magnon injection' and the 'magnon detection' Pt strip does not significantly exceed the magnon diffusion length $\lambda \lesssim 1\,\mu\mathrm{m}$ in YIG, one therefore expects a non-local, magnon-mediated electrical signal in nanoscale YIG/Pt devices.

Such a non-local, magnon-mediated magnetoresistance (MMR) signal is indeed observed in YIG/Pt nanostructures [6, 7]. Figure 2(a) shows a typical device, patterned at WMI using electron beam lithography and Argon ion beam milling. The two Pt wires are 100 µm long, 1 µm wide, and are separated by a gap $d = 200\,\mathrm{nm}$. We current-bias one wire, and detect the non-local voltage V_{nl} along the other. To infer the magneto-resistive response, we record V_{nl} at room temperature while rotating a magnetic field $\mathbf{H}$ in two different planes, as sketched in the insets of Fig. 2(b). The magnetic field magnitude $\mu_0 H = 2\,\mathrm{T}$ hereby is chosen large enough to saturate the YIG magnetization and align it along $\mathbf{H}$. As evident from Fig. 2(b), we observe a clear $\cos^2\alpha$-like modulation of V_{nl} when the magnetic field is rotated in the plane perpendicular to the direction of charge current flow (oopj), while V_{nl} vanishes when

[1] Financial support by the German Research Foundation via Priority Programme SPP 1538 "Spin Caloric Transport" (Project No. GO 944/4) and the Nanosystems Initiative Munich (NIM) is gratefully acknowledged

the magnetic field is rotated in the plane perpendicular to the **t** direction (oopt, see inset). Our experiments show that the non-local MMR signal exhibits exactly the same dependence on magnetization orientation as the (local) spin Hall magnetoresistance [7], for the magnetization both within as well as out of to the sample plane. This corroborates the conclusions drawn from the pioneering MMR experiments put forward by Cornelissen *et al.* [6], who investigated the MMR for the magnetization within the thin film plane only. In addition, we find a (quasi) exponential decay of the MMR signal with increasing Pt strip separation d in our sample, in good agreement with Cornelissen *et al.*.

Last but not least, we also studied the evolution of the MMR with temperature. As described in more detail in Ref. [7], the MMR decays as T^{β} with decreasing temperature, with a power law exponent $1 \leq \beta \leq 1.5$. For $T < 20\,\mathrm{K}$, the MMR signal V_{nl} drops to zero (within our experimental resolution of about 5 nV). In contrast, the SMR signal amplitude changes by at most a factor of two over the entire temperature range $5\,\mathrm{K} \leq T \leq 300\,\mathrm{K}$ studied. While the MMR thus can be naively understood as a non-local analogue of the SMR, the microscopic physics behind the two effects are markedly different. Since the MMR is intimately connected with magnon generation and propagation, MMR experiments hold the promise for all-electrical investigations of spin excitations in insulating magnets.

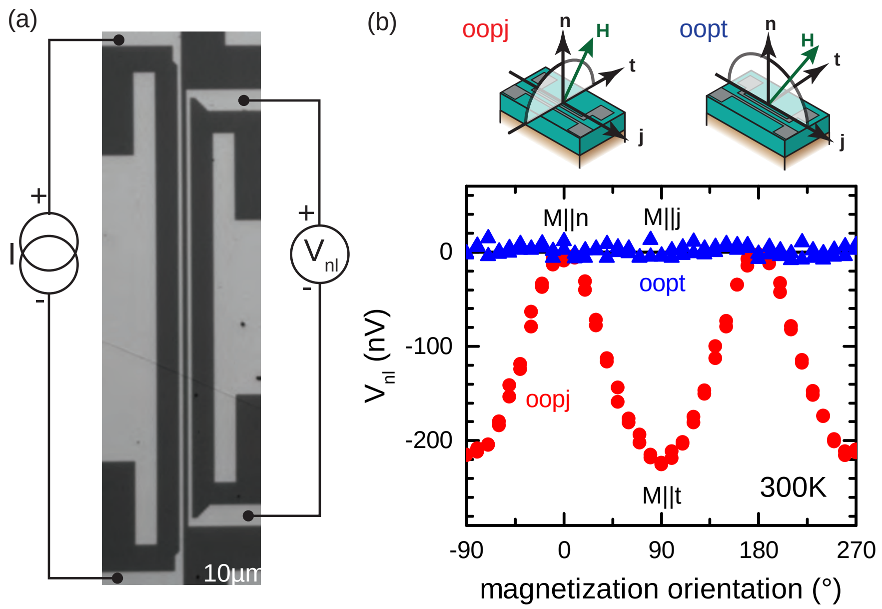

Figure 2: (a) Micrograph of a YIG/Pt nanostructure. Only the two narrow, vertical Pt lines (light gray) in the middle of the figure are connected to electronics and used for MMR experiments. The YIG surface appears as a dark gray background. (b) The non-local voltage V_{nl} (equivalent to $J_{\mathrm{C,nl}}$ for the open circuit conditions in our experiment) recorded in a YIG/Pt nanostructure at room temperature exhibits the dependence on magnetization orientation well-known from (local) spin Hall magnetoresistance. The insets on top show the magnetic field rotations planes used in the measurements.

References

[1] H. Nakayama, M. Althammer, Y.-T. Chen, K. Uchida, Y. Kajiwara, D. Kikuchi, T. Ohtani, S. Geprägs, M. Opel, S. Takahashi, R. Gross, G. E. W. Bauer, S. T. B. Goennenwein, and E. Saitoh, Phys. Rev. Lett. **110**, 206601 (2013).

[2] M. Althammer, S. Meyer, H. Nakayama, M. Schreier, S. Altmannshofer, M. Weiler, H. Huebl, S. Geprägs, M. Opel, R. Gross, D. Meier, C. Klewe, T. Kuschel, J.-M. Schmalhorst, G. Reiss, L. Shen, A. Gupta, Y.-T. Chen, G. E. W. Bauer, E. Saitoh, and S. T. B. Goennenwein, Phys. Rev. B **87**, 224401 (2013).

[3] S. Meyer, M. Althammer, S. Geprägs, M. Opel, R. Gross, and S. T. B. Goennenwein, Appl. Phys. Lett. **104**, 242411 (2014).

[4] J. Lotze, H. Huebl, R. Gross, and S. T. B. Goennenwein, Phys. Rev. B **90**, 174419 (2014).

[5] S. S.-L. Zhang, and S. Zhang, Phys. Rev. B **86**, 214424 (2012).

[6] L. J. Cornelissen, J. Liu, R. A. Duine, J. B. Youssef, and B. J. van Wees, Nat. Phys. **11**, 1022–1026 (2015).

[7] S. T. B. Goennenwein, R. Schlitz, M. Pernpeintner, K. Ganzhorn, M. Althammer, R. Gross, and H. Huebl, Appl. Phys. Lett. **107** (2015).

Current-induced spin torque resonance of a magnetic insulator

M. Schreier, A. Niedermayr, J. Lotze, H. Huebl, S. Geprägs, R. Gross, S. T .B. Goennenwein [1]
T. Chiba, S. Takahashi, G. E. W. Bauer [2,3]

Pure spin currents transport angular momentum without an associated charge flow. This makes them attractive for spintronics applications, such as torque-induced magnetization control in nanodevices [1], for sensing, data storage, interconnects, and logics. Up to now, however, most spin transfer torque studies focused on metallic ferromagnets [2–4], while magnetic insulators received much less attention [5, 6]. However, some magnetic insulators such as yttrium iron garnet (YIG) with extremely low magnetization damping, are well suited for the long-range transmission of signals via magnetization dynamics which are coupled to electronically by the spin transfer torque. To this end, the demonstration of electronic, spin transfer torque mediated magnetization manipulation in magnetic insulators is a critical open issue.

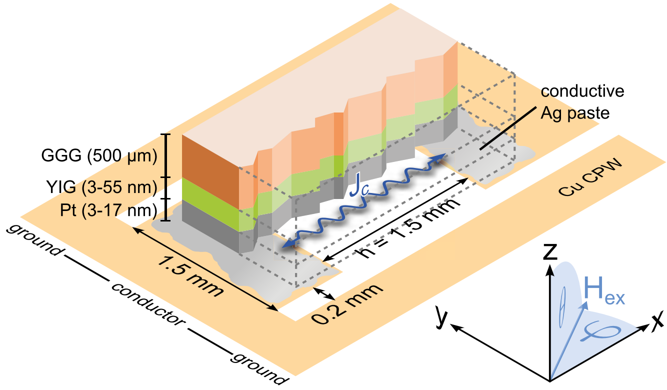

Figure 1: Samples are placed across a gap in the center conductor of a coplanar waveguide and contacted with conductive Ag paste. Figure adapted from Ref. [7].

In a recent article [7] we reported on the observation of spin torque-induced magnetization dynamics in a magnetic insulator. Applying a microwave-frequency (GHz) charge current to the Pt layer of a YIG/Pt sample (Fig. 1), we are able to drive ferromagnetic resonance by the combined action of Oersted fields and spin transfer torque. While Oersted fields drive bulk magnetization dynamics, the spin transfer torque is linked to the interface and is thus very effective for thin film structures that are of high importance for commercial applications. On resonance, a large DC voltage is measured in the Pt, which stems from electrically detected DC spin pumping [8] and rectification mediated by the AC spin Hall magnetoresistance (SMR) [9]. To single out the spin transfer torque contributions the experiment is modeled quantitatively [10, 11] and compared with the data. This allows to prove that in very thin YIG films, magnetization dynamics indeed are driven by spin transfer torque. In fact, they are substantially more efficient than the Oersted fields at actuating magnetization dynamics in thin films.

The measured DC voltage of a YIG(4 nm)/Pt(3 nm) sample is exemplarily shown in Fig. 2a. The broad positive voltage peak observed upon resonance is the fingerprint for a dominantly spin transfer torque driven excitation, as opposed to one driven by Oersted fields, which should be either negative or antisymmetric with respect to the resonance field. The simulation (solid line) then allows us to disentangle the measured V_{DC} regarding the contributions due to the Oersted field and those originating from spin transfer torque (Fig. 2b). As expected, the excitation in this sample is dominated by the spin transfer torque.

[1] Financial support from the German Research Foundation via SPP 1538 "Spin Caloric Transport", Project No. GO 944/4-2 is gratefully acknowledged.
[2] Institute for Materials Research, Tohoku University, Sendai, Japan
WPI Advanced Institute for Materials Research, Tohoku University, Sendai, Japan
Kavli Institute of NanoScience, Delft University of Technology, Delft, The Netherlands
[3] Financial support from the German Research Foundation via SPP 1538 "Spin Caloric Transport", Project No.BA 2954/1-2, FOM (Stichting voor Fundamenteel Onderzoek der Materie), the ICC-IMR, EU-FET grant InSpin 612759 and Grand-in-Aid for Scientific Research (KAKENHI) Nos. 22540346, 25247056, 25220910, and 268063 is gratefully acknowledged.

The shape of the V_{DC} resonance spectra and the dependence on the thicknesses of the yttrium iron garnet and platinum layers (not shown here), observed in the experiments and consistent with the theoretical modeling, is a strong indicator for the prominence of spin transfer torque driven magnetization dynamics in the samples. The result further implies that AC spin pumping [12–14] in magnetic insulators is reciprocal, as predicted by Onsager symmetry in the linear response regime. In particular, in magnetic insulators the spin transfer torque therefore provides an efficient link between pure magnonic and conventional electronic circuits. This opens new perspectives for the efficient integration of ferro-, ferri-, and antiferromagnetic insulators, in the form of e.g. spin transfer torque magnetic random access memory (STT-MRAM) or and spin-wave based interconnects, into electronic devices.

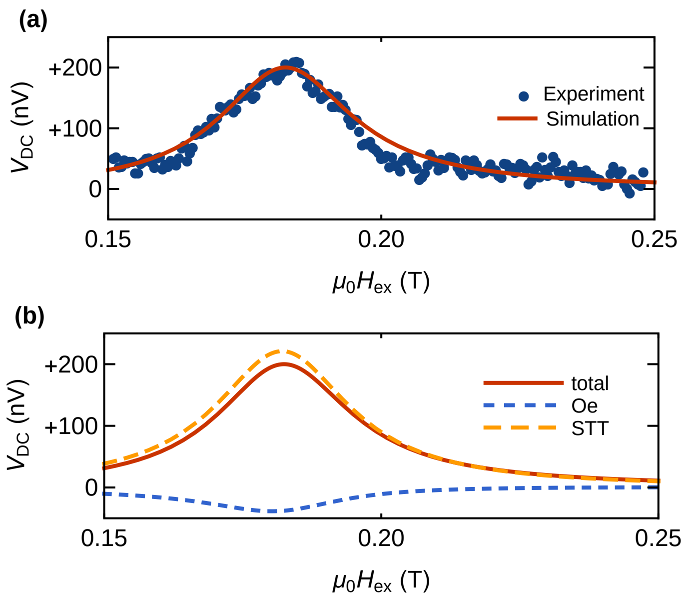

Figure 2: (a) Measured DC voltage V_{DC} of YIG(4 nm)/Pt(3 nm) under an AC current bias (full symbols). The solid/dashed red line is calculated from a simulation based on the Landau-Lifshitz-Gilbert-Slonczewski equation. The angle between the (in-plane) external magnetic field and the microwave current is $\varphi \cong -35°$ [$\theta = 90°$, Fig. 1]. **(b)** Contributions to the excitation by Oersted field and spin transfer torque to V_{DC}, according to the simulation. Figure adapted from Ref. [7].

References

[1] I. M. Miron, K. Garello, G. Gaudin, P.-J. Zermatten, M. V. Costache, S. Auffret, S. Bandiera, B. Rodmacq, A. Schuhl, and P. Gambardella, Nature **476**, 189–193 (2011).

[2] V. E. Demidov, S. Urazhdin, H. Ulrichs, V. Tiberkevich, A. Slavin, D. Baither, G. Schmitz, and S. O. Demokritov, Nat. Mater. **11**, 1028–1031 (2012).

[3] P. P. J. Haazen, E. Murè, J. H. Franken, R. Lavrijsen, H. J. M. Swagten, and B. Koopmans, Nat. Mater. **12**, 299–303 (2013).

[4] J. Ryu, K.-J. Lee, and H.-W. Lee, Appl. Phys. Lett. **102**, – (2013).

[5] A. Hamadeh, O. d'Allivy Kelly, C. Hahn, H. Meley, R. Bernard, A. H. Molpeceres, V. V. Naletov, M. Viret, A. Anane, V. Cros, S. O. Demokritov, J. L. Prieto, M. Muñoz, G. de Loubens, and O. Klein, Phys. Rev. Lett. **113**, 197203 (2014).

[6] T. Moriyama, S. Takei, M. Nagata, Y. Yoshimura, N. Matsuzaki, T. Terashima, Y. Tserkovnyak, and T. Ono, Appl. Phys. Lett. **106**, – (2015).

[7] M. Schreier, T. Chiba, A. Niedermayr, J. Lotze, H. Huebl, S. Geprägs, S. Takahashi, G. E. W. Bauer, R. Gross, and S. T. B. Goennenwein, Phys. Rev. B **92**, 144411 (2015).

[8] Y. Tserkovnyak, A. Brataas, and G. E. W. Bauer, Phys. Rev. Lett. **88**, 117601 (2002).

[9] H. Nakayama, M. Althammer, Y.-T. Chen, K. Uchida, Y. Kajiwara, D. Kikuchi, T. Ohtani, S. Geprägs, M. Opel, S. Takahashi, R. Gross, G. E. W. Bauer, S. T. B. Goennenwein, and E. Saitoh, Phys. Rev. Lett. **110**, 206601 (2013).

[10] T. Chiba, G. E. W. Bauer, and S. Takahashi, Phys. Rev. Applied **2**, 034003 (2014).

[11] T. Chiba, M. Schreier, G. E. W. Bauer, and S. Takahashi, J. Appl. Phys. **117**, – (2015).

[12] C. Hahn, G. de Loubens, M. Viret, O. Klein, V. V. Naletov, and J. Ben Youssef, Phys. Rev. Lett. **111**, 217204 (2013).

[13] D. Wei, M. Obstbaum, M. Ribow, C. H. Back, and G. Woltersdorf, Nat. Commun. **5**, – (2014).

[14] M. Weiler, J. M. Shaw, H. T. Nembach, and T. J. Silva, Phys. Rev. Lett. **113**, 157204 (2014).

Brillouin light scattering spectroscopy

Mathias Weiler, Stefan Klingler, Stephan Geprägs, Hannes Maier-Flaig, Hans Huebl, Sebastian T. B. Goennenwein and Rudolf Gross[1]

Recently, a Brillouin Light Scattering (BLS) spectroscopy setup was installed at the Center for Nanotechnology and Nanomaterials (CNN) as a central user facility supported by funding through the Excellence Cluster Nanosystems Initiative Munich (NIM). This tool opens an avenue to a whole new class of experiments that have previously not been possible at WMI.

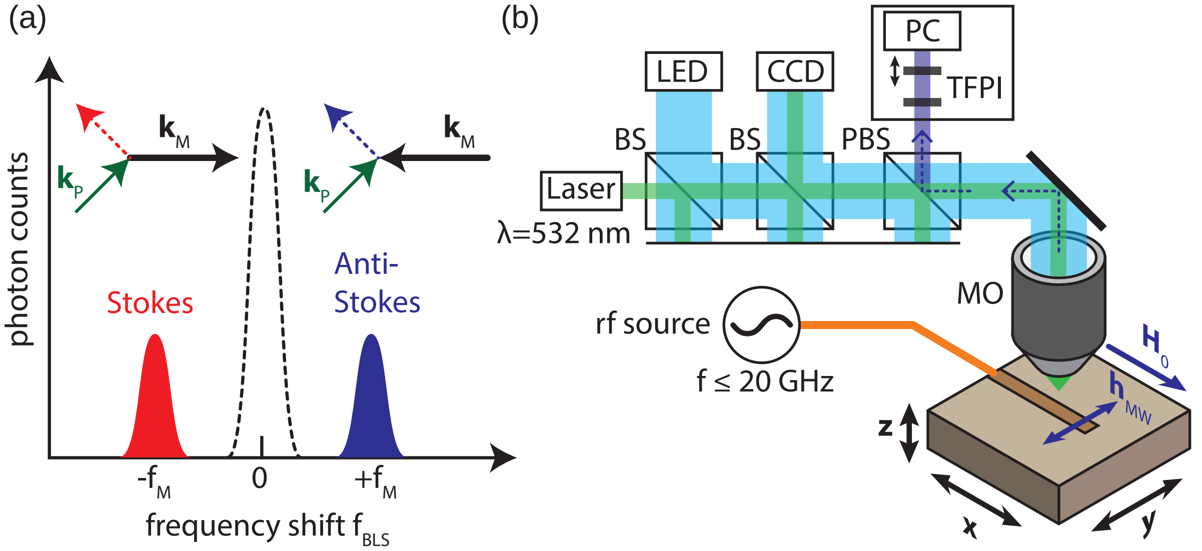

Figure 1: (a) Schematic depiction of the inelastic photon-magnon scattering process and the resulting frequency-shift of the scattered light. (b) Schematic view of the BLS setup.

BLS spectroscopy exploits the inelastic scattering of photons and quantized collective excitations in solids such as phonons and magnons. Here, we concentrate on photon-magnon scattering, as depicted schematically in Fig. 1(a). In a scattering process, an incident photon with momentum $\boldsymbol{k}_\mathrm{p}$ can either generate a magnon with momentum $\boldsymbol{k}_\mathrm{M}$ (Stokes process) or annihilate a magnon with momentum $-\boldsymbol{k}_\mathrm{M}$ (Anti-Stokes process), where $\boldsymbol{k}_\mathrm{p}$ and $\boldsymbol{k}_\mathrm{M}$ are uniquely determined by experimental geometry and momentum conservation, respectively. This $\boldsymbol{k}$-vector selectivity can be used to e.g. map magnon dispersions and thus determine symmetric and antisymmetric exchange constants [1]. Due to energy conservation, the frequency of the scattered photons is shifted with respect to the incoming photons by the magnon frequency f_M. Hence, by analyzing the frequency components of the scattered light, one can optically probe the magnonic excitations.

A simplified scheme of the corresponding experimental setup is shown in Fig. 1(b). A continuous wave laser with wavelength $\lambda = 532\,\mathrm{nm}$ and $10\,\mathrm{MHz}$ linewidth is used to provide the scattering photons. Magnons are generated above the thermal population in the sample by applying radio frequency (rf) power at frequency $f \leq 20\,\mathrm{GHz}$ to a microwave antenna patterned directly onto the sample. The laser beam position on the sample is controlled with 10 nm-precision by an xyz-stage. An external static magnetic field of $5\,\mathrm{mT} \leq \mu_0 H_0 \leq 200\,\mathrm{mT}$ can be applied. A CCD camera, LED illumination and two non-polarizing beam splitters (BS) provide an optical image of the laser spot position on the sample. The laser beam passes through a polarizing beam splitter (PBS) and is then focussed onto the sample using a microscope lens (MO) [2]. The polarization of photons that scatter inelastically off magnons is rotated by 90°,

[1]We acknowledge financial support by the German Excellence Initiative through the Nanosystems Initiative Munich (NIM)

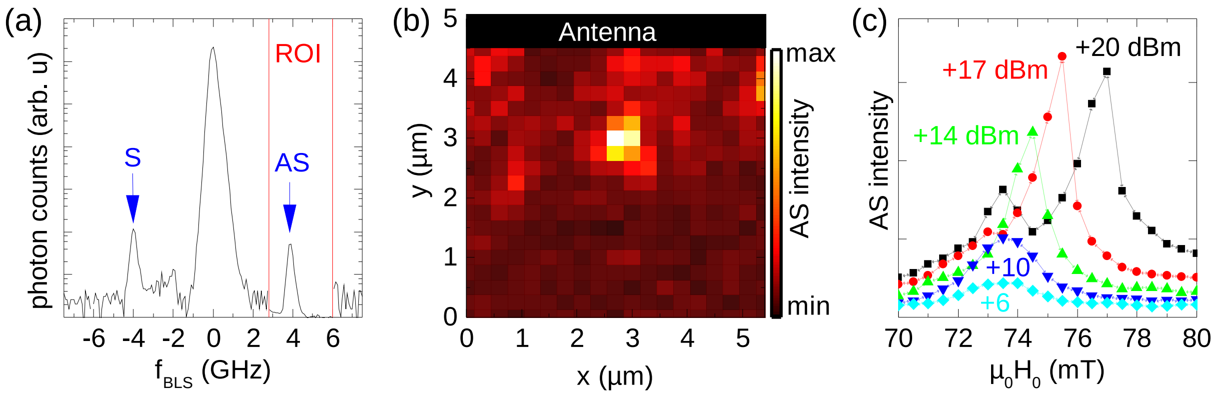

Figure 2: (a) Raw BLS spectrum acquired by scattering photons off a 30 nm thick Yttrium Iron Garnet film. The Stokes (S) and Anti-Stokes (AS) peaks are clearly visible at the microwave excitation frequency $f = 4\,\mathrm{GHz}$. Within a region of interest (ROI) around the AS peak the signal-to-noise ratio is improved by averaging. (b) Spatial map of the AS intensity obtained by scanning the laser beam across the sample. (c) AS intensity as a function of H_0 for several rf power levels.

allowing to separate them from the reflected photons by the PBS. The scattered light (dashed arrows) is then directed into a Tandem-Fabry-Perot Interferometer (TFPI) where it passes a total of six times through two Fabry-Perot interferometers. By simultaneously adjusting the mirror spacing of the two interferometers, the frequency of the transmittable light is selected with a frequency resolution of about 100 MHz. The transmitted photons are detected as a function of mirror spacing using a photon counter (PC).

To demonstrate some of the capabilities of this setup, we present BLS data obtained from an approximately 30 nm thick Yttrium Iron Garnet (YIG) film grown at WMI by pulsed laser deposition. A 10 µm wide Au antenna was lithographically prepared on the YIG film and connected to the rf source. A raw spectrum recorded with the laser spot directly next to the antenna and with $\mu_0 H_0 = 77\,\mathrm{mT}$, rf frequency $f = 4\,\mathrm{GHz}$ and rf power $P = 20\,\mathrm{dBm}$ is shown in Fig. 2(a). Besides the strong elastic peak at $f_{\mathrm{BLS}} = 0$, the Stokes (S) and anti-Stokes (AS) peaks stemming from light scattered off magnons with $f_{\mathrm{M}} = f = 4\,\mathrm{GHz}$ are clearly visible. In Fig. 2(b), we show the AS peak intensity recorded at $\mu_0 H_0 = 77\,\mathrm{mT}$, rf frequency $f = 4\,\mathrm{GHz}$ and rf power $P = 20\,\mathrm{dBm}$ as a function of laser spot position on the sample. The position of the microwave antenna is indicated by the black bar. Due to the finite magnon propagation length, the intensity decreases when moving the laser spot in y-direction away from the antenna. This data reveals that the AS intensity is not homogeneous along the x-direction, but rather reaches a maximum for $x \approx y \approx 3\,\mu\mathrm{m}$. This is indicative of spatially inhomogeneous magnetic properties of the YIG film. Finally, we investigated the rf power dependence of the AS peak intensity. To this end, we recorded BLS spectra at a fixed laser spot position $x = y = 3\,\mu\mathrm{m}$ as a function of H_0 for different rf powers, with results shown in Fig. 2(c). We find that for increasing rf power the line shape is distorted, in accordance with the observation of non-linear magnetic excitations.

In conclusion, we have demonstrated that the BLS tool is capable of recording spatially resolved (nonlinear) magnetic excitations in the YIG thin films grown at WMI. This opens the door to investigate magnetization dynamics in patterned thin film YIG structures to reveal, e.g., the coupling of magnonic and photonic modes in YIG-resonator hybrids.

References

[1] H. T. Nembach, J. M. Shaw, M. Weiler, E. Jue, and T. J. Silva, Nat. Phys. **11**, 825–829 (2015).
[2] T. Sebastian, K. Schultheiss, B. Obry, B. Hillebrands, and H. Schultheiss, Front. Phys. 3, 35 (2015).

Strongly anisotropic superconducting critical field in pressurised α-(BEDT-TTF)$_2$TlHg(SCN)$_4$

L. Höhlein, M. Kunz, W. Biberacher, K. Neumaier, M.V. Kartsovnik [1]
N.D. Kushch [2]

The organic charge transfer salt α-(BEDT-TTF)$_2$KHg(SCN)$_4$ (α-K) is a well studied compound with a lot of interesting physical properties [1]. It shows a competition of different ground states, entering a charge density wave (CDW) state at a low temperature $T_{\mathrm{CDW}} = 8.5\,\mathrm{K}$, as well as showing a transition into an inhomogeneous superconducting (SC) state below 0.3 K. Under a pressure above 2.5 kbar, the CDW state is suppressed giving way to a homogeneous bulk SC state [2] with the maximum critical temperature $T_c = 110\,\mathrm{mK}$. Earlier we reported on the critical field anisotropy of this high pressure SC state [3]. The sister compound α-(BEDT-TTF)$_2$TlHg(SCN)$_4$ (α-Tl) has a slightly higher CDW transition temperature, $T_{\mathrm{CDW}} \approx 10\,\mathrm{K}$, and a somewhat higher SC onset temperature of $\approx 0.6\,\mathrm{K}$ at ambient pressure [4]. Here, we report on studies of the superconducting state under pressure by resistance measurements. For our experiments, a plate-like sample of α-Tl was contacted in the interlayer resistance geometry and pressurised in a clamp pressure cell using the silicon oil GKZh as pressure medium. The pressure cell was mounted in our home-made dilution refrigerator and 2-axes superconducting vector magnet.

At zero pressure our sample shows a SC onset at $T = 0.68\,\mathrm{mK}$. The onset is suppressed by applying a small magnetic field of $B = 20\,\mathrm{mT}$ perpendicular to the layer. However, even above this magnetic field there is still some downturn in the $R(T)$ dependence below $T = 0.55\,\mathrm{K}$. This downturn keeps up to fields above 1 T. Therefore, it cannot be due to superconductivity. It shows a logarithmic T-dependence and, thus, may be a manifestation of the weak anti-localization effect [5]. Like in α-K we see a full SC transition under pressure with the highest $T_c = 70\,\mathrm{mK}$ at $p = 4.0\,\mathrm{kbar}$. Contrary to our expectations, T_c is lower than in α-K. Another drawback is the large transition width of $\approx 30\,\mathrm{mK}$ despite the proven high crystal quality.

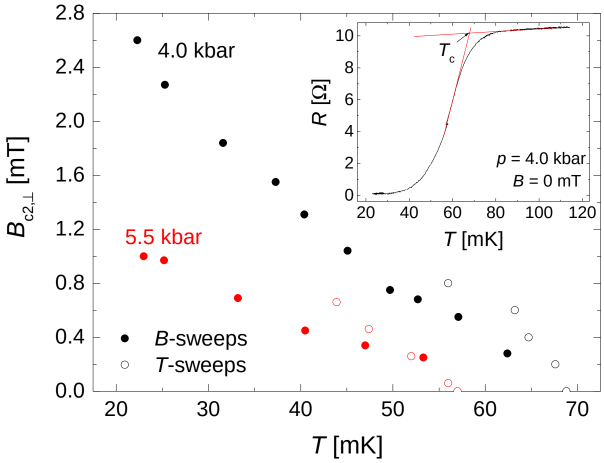

Figure 1: Temperature dependence of the critical field perpendicular to the layers for $p = 4.0$ (black symbols) and 5.5 kbar (red symbols). The filled and empty symbols are from field and temperature sweeps, respectively. Inset: an example of a temperature sweep. The red lines show the construction used to evaluate the critical field or temperature, respectively.

Fig. 1 shows the temperature dependence of the vertical critical field for pressures of 4.0 kbar and 5.5 kbar. Both T_c and $B_{c2,\perp}$ decrease at increasing pressure similarly to the case of α-K . The overall T-dependence of the critical field is linear, with a slight upturn at 4.0 kbar. This suggests a purely orbital pair-breaking mechanism, as expected. There is some discrepancy between the transition points determined from the field and temperature sweeps, respectively, as one can see in Fig. 1. This is obviously due to the rather large width of the transition in both, T- and B-sweeps. Therefore, the construction used for the evaluation of B_{c2} (see inset of Fig. 1) is not very precise. For 5.5 kbar the resistance is not zero even at the base temperature of the fridge, which makes the discrepancy even bigger.

[1] This work was supported by the German Research Foundation, grant number KA 1652/4-1.
[2] Institute of Problems of Chemical Physics, 142432 Chernogolovka, Russia

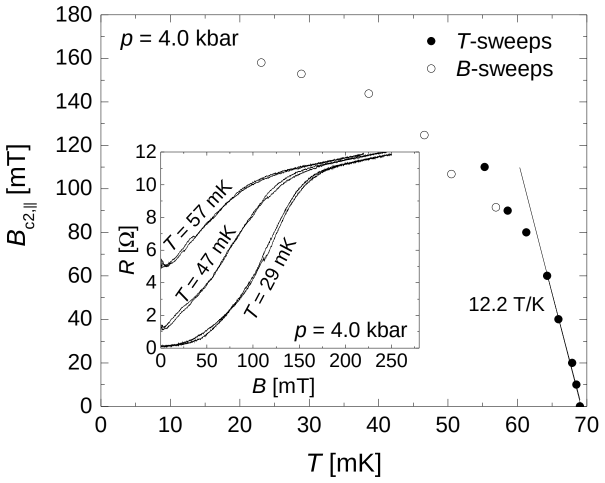

Figure 2: Temperature dependence of the in-plane critical field for $p = 4.0$ kbar. Inset: An example of field sweeps at different temperatures.

In Fig. 2 we show the temperature dependence of the critical field for magnetic field parallel to the conducting layers at $p = 4.0$ kbar. The maximum slope near T_c is $dB_{c2,\parallel}/dT = 12.2$ T/K. This value is very high and suggests a strong suppression of the shielding currents perpendicular to the conducting layers. Therefore, we expect that for low enough temperatures the critical field should be limited by the paramagnetic pair-breaking effect. Indeed, we observe a strong decrease of the slope at low temperatures. For 5.5 kbar the slope close to T_c decreases to 5.1 T/K. The low-temperature flattening of the $B_{c2,\parallel}(T)$ dependence is less pronounced at this pressure. This is easy to understand: the higher pressure makes the system more three-dimensional due to a bigger overlap of the π-orbitals from the different layers. Therefore, the orbital effect becomes stronger.

Fig. 3 shows the θ-dependence of the critical field, normalised to the perpendicular critical field, in the interval $87° < \theta < 95°$ ($\theta = 90° \Leftrightarrow \mathbf{B} \parallel$ layers) for 4.0 kbar. The inset shows the full angular range $0° < \theta < 180°$. We see a very sharp peak at the parallel orientation for the higher temperature, $T = 50$ mK. The anisotropy coefficient $B_{c2,\parallel}/B_{c2,\perp} = 160$ is very high at this temperature. At the lower temperature, the anisotropy is weaker and $B_{c2}(\theta)$ is rather flat at the angles $\pm 0.2°$ around the parallel orientation. This is again due to the paramagnetic pair-breaking mechanism coming into effect at low enough temperatures. Due to the lower T_c and the lower anisotropy these manifestations of the paramagnetic pair-breaking mechanism are weaker than in α-K.

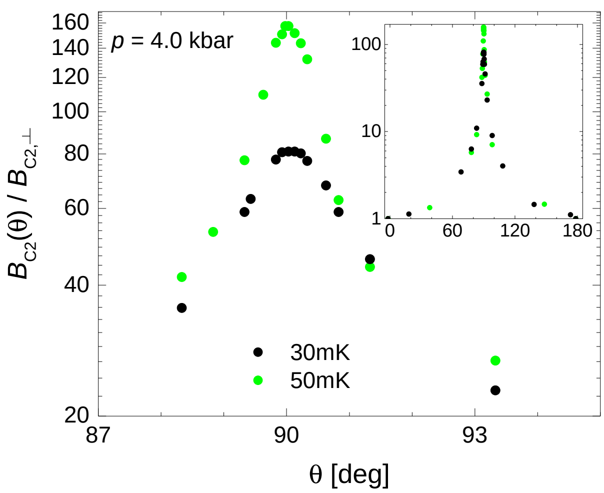

Figure 3: Normalised critical field versus the polar angle θ for $p = 4.0$ kbar. The black symbols were taken near the base temperature of the fridge and the green symbols near T_c. Inset: The full angle range of $R(\theta)$.

References

[1] M. V. Kartsovnik. *The Physics of Organic Superconductors and Conductors*, Ed. A. G. Lebed, chap. 8, Layered Organic Conductors in Strong Magnetic Fields, 185–246 (Springer Verlag, 2008).

[2] D. Andres, M. V. Kartsovnik, W. Biberacher, K. Neumaier, E. Schuberth, and H. Müller, Phys. Rev. B **72**, 174513 (2005).

[3] M. Kunz, W. Biberacher, K. Neumaier, V. N. Zverev, N. D. Kushch, H. Müller, and M. V. Kartsovnik, WMI Ann. Rep. **2011**, 31–33 (2011).

[4] H. Ito, M. V. Kartsovnik, H. Ishimoto, K. Kono, H. Mori, N. D. Kushch, G. Saito, T. Ishiguro, and S. Tanaka, Synth. Met. **70**, 899–902 (1995).

[5] G. Bergmann, Solid State Commun. **42**, 815–817 (1982).

Magnetic quantum oscillations of thermopower in the electron-doped cuprate superconductor $Nd_{0.85}Ce_{0.15}CuO_4$

T. Helm, V. Tzanos, M. Kartsovnik, W. Biberacher, A. Dorantes, A. Erb, and R. Gross [1]
S. Arsenijevic and G. Seyfarth [2]

Strong magnetic fields have proved to be a powerful tool for probing the anomalous "normal state" of the high-T_c cuprate superconductors. An impressive example is the discovery of magnetic quantum oscillations (MQO) in a number of hole- [1–3] and electron-doped [4, 5] cuprates, which provided essential information on the reconstruction of their Fermi surfaces in the vicinity of the superconducting instability. In the prototypical electron-doped compound $Nd_{2-x}Ce_xCuO_4$ (NCCO), the MQO observed in the overdoped regime are strongly suggestive of the reconstructed Fermi surface in the form shown in the inset in Fig. 1: the original quasi-two-dimensional simply-connected hole Fermi surface is folded by the $(\pi/a, \pi/a)$ superlattice potential (where a is the in-plane lattice constant), transforming into a set of small hole and electron pockets separated from each other by a small gap.

The interlayer magnetoresistance displays MQO of two frequencies. The low frequency $F_h \approx 300\,$T perfectly matches the expected size of the small hole Fermi pockets centered at $(\pm\pi/2a, \pm\pi/2a)$ [4]. The fast oscillations, $F_0 \simeq 11\,$kT, observed in fields above 40 T reveal a cyclotron orbit, which is geometrically equivalent to that on the large unreconstructed Fermi surface. This large orbit is understood as a result of magnetic breakdown through the small energy gap between the hole and electron-like subbands [5, 6]. Interestingly, no manifestation of the electron part of the reconstructed Fermi surface has been found in the oscillations of the interlayer magnetoresistance so far. The lack of MQO from the electron pockets may, at least partially, be caused by a relatively weak contribution of these parts of the Fermi surface to the interlayer conductivity, dictated by symmetry properties of the body-centered tetragonal crystal lattice. Indeed, the latter implies that the interlayer transfer integral, which gives rise to interlayer conduction, vanishes at the border of the (original) 1. Brillouin zone where the electron pockets are supposed to be located, see inset in Fig. 1. By contrast, the in-plane transport should be dominated by the electron pockets due to their relatively large size. While the in-plane resistivity of bulk NCCO crystals is very difficult to measure accurately due to the high electronic anisotropy and unavoidable (though minor, ~ 1%) presence of insulating Nd_2O_3 inclusions, the in-plane thermopower measurements should be much more reliable due to a more homogeneous heat flow distribution, as compared to a charge

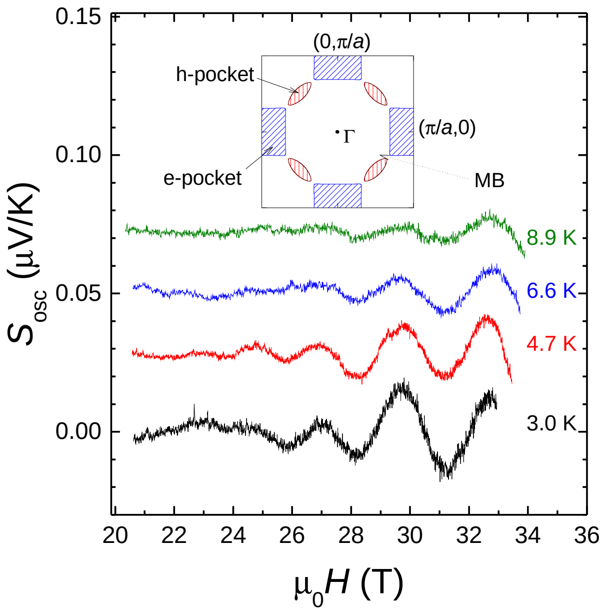

Figure 1: Magnetic quantum oscillations of the in–plane magnetothermopower in $Nd_{0.85}Ce_{0.15}CuO_4$ at different temperatures. The curves are displaced vertically for clarity. Inset: 2D view of the reconstructed Fermi surface consisting of electron (blue) and hole (red) pockets. The large magnetic-breakdown (MB) orbit identical to the unreconstructed Fermi surface is shown by the dotted line.

[1] The experiment in strong magnetic fields was done under support of the LNCMI-CNRS, member of the European Magnetic Field Laboratory (EMFL)
[2] Laboratoire National des Champs Magnétiques Intenses (LNCMI), CNRS, Grenoble, France

current. In addition, the MQO in magnetothermopower are often stronger than in magnetoresistance. We have, therefore, initiated high-field studies of the in-plane magneto-thermopower of NCCO single crystals at different doping levels.

Up to now we have performed measurements on two nearly optimally doped, $x = 0.15$, NCCO samples. Thanks to a very low noise level ($\lesssim$ 1 nV even at high fields), quantum oscillations of the Seebeck coefficient have been found and traced up to temperatures as high as 9 K, see Fig. 1. This is, in fact, the first evidence of MQO in an intralayer transport coefficient in NCCO. The fast Fourier transform (FFT) shown in Fig. 2 yields an oscillation frequency of $F_h \approx 290$ T, which is perfectly consistent with the interlayer magnetoresistance data [4, 7]. The effective cyclotron mass obtained from the temperature dependence of the oscillation amplitude (inset in Fig. 2), $m_c = (0.99 \pm 0.03)m_0$, where m_0 is the free electron mass, is also in very good agreement with the earlier experiments. The relative amplitude of the oscillations, $\widetilde{S}_h/S \simeq 10^{-2}$, is an order of magnitude higher than that of magnetoresistance oscillations at the same conditions.

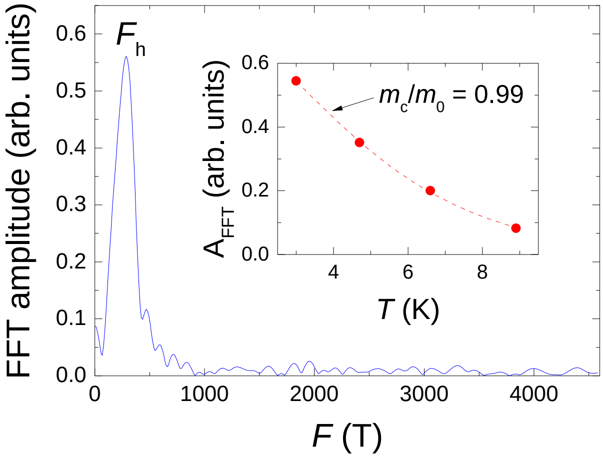

Figure 2: Fast Fourier transform (FFT) of the oscillatory thermopower signal at 3 K. Inset: Temperature dependence of the FFT amplitude at F_h (symbols) and the Lifshitz-Kosevich fit (dashed curve) yielding an effective cyclotron mass of $0.99m_0$.

Note that only one frequency peak is clearly seen in the oscillation spectrum in Fig. 2. It is obvious that the magnetic-breakdown frequency F_0 is not seen: given the high Dingle temperature, large cyclotron mass and relatively high breakdown field [7], the amplitude of these oscillations is estimated to be 6 orders of magnitude lower than that of $\widetilde{S}_h$ in fields $\sim$ 30T. On the other hand, the oscillations from the electron pockets of the reconstructed Fermi surface should be comparable in amplitude with those coming from the hole pockets [8]. Nevertheless, no contribution of the corresponding frequency $F_e \simeq 2.5$ kT is resolved in the FFT spectrum in Fig. 2. The present signal-to-noise level sets the upper limit for the relative amplitude of the MQO associated with the electron pockets as low as $\sim 0.03\widetilde{S}_h$. A possible explanation for this unexpected result may involve an anomalous damping of the oscillations associated, for example, with non-Fermi-liquid effects near the antiferromagnetic quantum critical point. Further studies are needed to clarify this issue.

References

[1] B. Vignolle, D. Vignolles, M. H. Julien, and C. Proust, C. R. Phys. **14**, 39–52 (2013).

[2] N. Barivsic, S. Badoux, M. K. Chan, C. Dorrow, W. Tabis, B. Vignolle, Y. G, J. Béard, X. Zhao, C. Proust, and M. Greven, Nat. Phys. **9**, 761–764 (2013).

[3] B. Vignolle, A. Carrington, R. A. Cooper, M. M. J. French, A. P. Mackenzie, C. Jaudet, D. Vignolles, C. Proust, and N. E. Hussey, Nature **455**, 952 (2008).

[4] T. Helm, M. V. Kartsovnik, M. Bartkowiak, N. Bittner, M. Lambacher, A. Erb, J. Wosnitza, and R. Gross, Phys. Rev. Lett. 157002 (2009).

[5] T. Helm, M. V. Kartsovnik, I. Sheikin, M. Bartkowiak, F. Wolff-Fabris, N. Bittner, W. Biberacher, M. Lambacher, A. Erb, J. Wosnitza, and R. Gross, Phys. Rev. Lett. **105**, 247002 (2010).

[6] J. Eun, and S. Chakravarty, Phys. Rev. B **84**, 094506 (2011).

[7] T. Helm, M. V. Kartsovnik, C. Proust, B. Vignolle, C. Putzke, E. Kampert, I. Sheikin, E.-S. Choi, J. S. Brooks, N. Bittner, W. Biberacher, A. Erb, J. Wosnitza, and R. Gross, Phys. Rev. B **92**, 094501 (2015).

[8] V. Tzanos. *High-Field Normal-State Magnetotransport Properties of Electron-Doped Cuprate Superconductors*. Master thesis, Technische Universität München (2014).

Application–Oriented Research

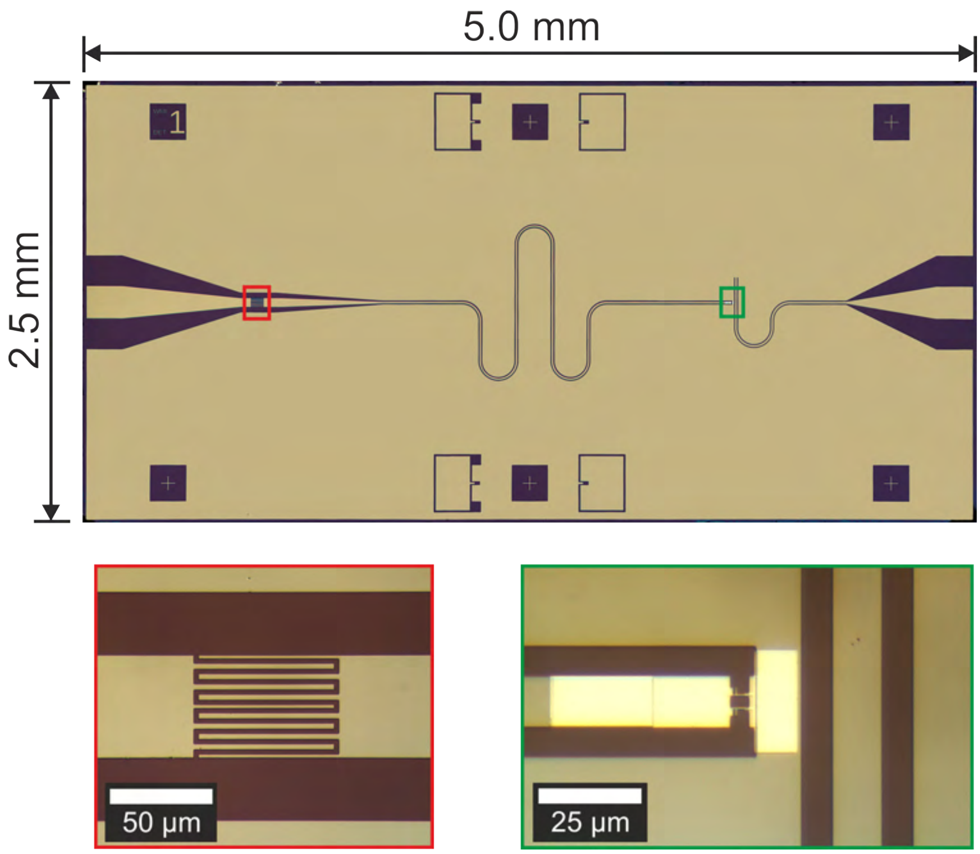

Optical micrographs of a superconducting Josephson Parametric Amplifier (JPA). The lower part is showing magnified views of the input coupling capacitor (left) and the dc-SQUID at the end of the quarter-wavelength coplanar waveguide resonator with the antenna for the JPA drive (right).

Nanomechanics probes magnetoelastics

M. Pernpeintner, R. B. Holländer, R. Gross, S. T. B. Goennenwein, H. Huebl [1]
M. J. Seitner, E. M. Weig [2,3]

Nanomechanical systems are an established platform for mass and force detection. In particular, the high quality factors of their vibrational modes [1] make them ideally suited for high-precision sensing applications [2, 3]. In solid state physics, nanomechanical sensors are utilized for the investigation of material properties of thin films [4–6].

Here, we employ nanomechanical sensing for the experimental investigation of magnetostriction in thin films. Our technique is based on a doubly-clamped silicon nitride (Si_3N_4) nanobeam covered with a thin magnetic layer. This approach allows to measure magnetostriction of thin film materials — conducting as well as insulating — which can be deposited on a Si_3N_4 nanobeam, using e. g. electron beam evaporation, thermal evaporation or sputtering. As the thin film deposition is the last step in the sample fabrication process, the ferromagnetic film is not exposed to etching solution or dry etch reactants, which allows us to apply this technique to a broad range of materials. In order to demonstrate the method we investigate a 10 nm thin cobalt film and find the magnetostrictive constant of bulk Co. For the readout of the sensing device we employ optical interferometry, but want to note, that depending on the measurement environment, also capacitive readout schemes can be applied.

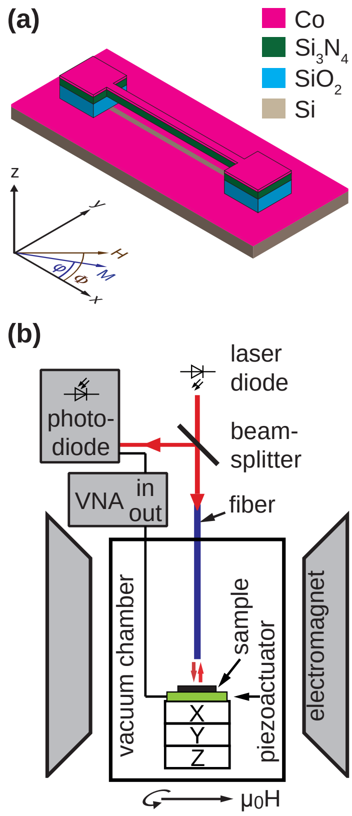

Figure 1: **(a)** Schematic of the doubly-clamped Si_3N_4 nanobeam (green) covered with a thin cobalt film (cyan). The magnetic field is applied in the x-y-plane with an angle Φ to the long axis (x-axis) of the beam. **(b)** Fiber interferometer used to characterize the sample in vacuum.

Conceptually, the idea of the measurement is to orient the magnetization of the magnetic thin film by an external magnetic field. As a consequence, inverse-magnetoelastic effect causes stress of the lattice of the magnetic material. As this thin film is in contact with the doubly-clamped nanobeam, the mechanical response, i.e. the resonance frequency ω_{res} is altered. By analyzing ω_{res} as function of the magnetization direction we observe a characteristic $\cos^2\phi$ dependence, where ϕ is the angle between the long axis of the beam and the magnetization direction. In detail, we find (see Ref. [7])

$$\frac{\omega_{\mathrm{res}}(\phi)}{2\pi} = \frac{1}{2l}\sqrt{\frac{\sigma_{\mathrm{eff}}}{\rho_{\mathrm{eff}}}} = \frac{1}{2l}\sqrt{\frac{\sigma_0 - \sigma_1\cos^2(\phi)}{\rho_{\mathrm{eff}}}}, \tag{1}$$

where l is the length, ρ_{eff} is the effective mass density, and σ_0 is the stress of the double layer nanobeam. $\sigma_1 = E t_{\mathrm{film}} \lambda_{\|} / (t_{\mathrm{SiN}} + t_{\mathrm{film}})$ is the additional stress stemming from the magnetostriction, which contains the Young's modulus E of the magnetic layer and the magnetostrictive constant $\lambda_{\|}$ beside geometric parameters of the double layer. For $\sigma_1/\sigma_0 \ll 1$, we obtain for the relative resonance frequency shift

$$\frac{\Delta\omega_{\mathrm{res}}(\phi)}{\omega_{\mathrm{res},0}} = \frac{\omega_{\mathrm{res}}(\phi) - \omega_{\mathrm{res},0}}{\omega_{\mathrm{res},0}} = -\frac{\sigma_1}{2\sigma_0}\cos^2(\phi) \tag{2}$$

with $\omega_{\mathrm{res},0}/2\pi = 1/(2l)\sqrt{\sigma_0/\rho_{\mathrm{eff}}}$ the resonance frequency at $\phi = 90^\circ$.

[1] We acknowledge financial support by the German Research Foundation via the Nanosystems Initiative Munich and the Priority Program SpinCAT (GO 944/4).
[2] Department of Physics, University of Konstanz, D-78457 Konstanz, Germany
[3] M.J.S. and E.M.W. greatfully acknowledge financial support by German Research Foundation via KO 416/18.

To spectroscopically investigate the mechanical properties of the nanobeam, we use a fiber interferometer as sketched in Fig. 1b operating at room temperature and in vacuum to avoid air damping. Using a piezoelectric actuator we can resonantly drive the flexural out-of-plane motion of the beam. To study the magnetostrictive impact we further need a magnetic field at the sample position to orient the magnetization of the magnetic film with respect to the long axis of the doubly clamped nanobeam. This is realized by a rotatable electromagnet providing a homogeneous magnetic field at the sample position.

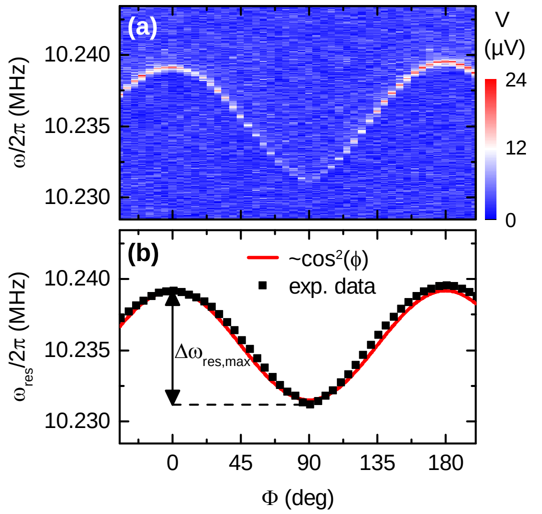

Figure 2: Resonance frequency of the fundamental flexural mode as a function of the external magnetic field orientation Φ for $\mu_0 H = 200\,\mathrm{mT}$. **(a)** shows the measured photovoltage V as a function of drive frequency and external field direction. In **(b)**, the fitted resonance frequency $\omega_{\mathrm{res}}(\Phi)$ is compared to the expected $\cos^2(\phi)$ behavior.

Figure 2a shows the interferometrically detected photovoltage, which corresponds to the amplitude of the out-of-plane mechanical response of the nanobeam as function of the magnetic field direction Φ and the actuator drive frequency. The experimental data confirm the expected $180°$-periodicity of the resonance frequency $\omega_{\mathrm{res}}(\Phi)$. From these data we extract the maximum resonance frequency shift $\Delta\omega_{\mathrm{res,max}}/2\pi = 8.00\,\mathrm{kHz}$ (see Fig. 2b), which allows us to determine the magnetostriction constant of $\lambda_{\parallel} = -79.7 \times 10^{-6}$ ($\lambda_{\perp} = 27.9 \times 10^{-6}$) [7]. These values are in very good agreement with the values we calculate for polycristalline cobalt $\lambda_{\parallel} = -78.4 \times 10^{-6}$ and $\lambda_{\perp} = 27.5 \times 10^{-6}$ following Ref. 8. The slight deviations between the measured $\omega_{\mathrm{res}}(\Phi)$ and the expected $\cos^2(\phi)$ behavior (see Eq. (2)) can be quantitatively understood as an imperfect parallel alignment between the magnetization and the external magnetic field.

In contrast to cantilever-based experiments, where magnetostriction causes a bending of the mechanical element, the present approach uses a pre-stressed, doubly-clamped nanobeam where the magnetostrictive stress modifies the total stress along the beam axis and therefore changes the resonance frequency of the bilayer beam. This stress-to-frequency conversion allows for an effective determination of the magnetostriction constants via a frequency measurement, which does not rely on a quantitative measurement of the beam displacement (as it is the case for cantilever-based techniques). The high quality factor of pre-stressed Si_3N_4 nanobeam resonators therefore allows for the precise investigation of magnetostriction in thin films.

References

[1] Q. P. Unterreithmeier, T. Faust, and J. P. Kotthaus, Phys. Rev. Lett. **105**, 027205 (2010).
[2] C. L. Degen, M. Poggio, H. J. Mamin, C. T. Rettner, and D. Rugar, PNAS **106**, 1313–1317 (2009).
[3] J. Moser, J. Güttinger, A. Eichler, M. J. Esplandiu, D. E. Liu, M. I. Dykman, and A. Bachtold, Nat. Nano. **8**, 493–496 (2013).
[4] R. B. Karabalin, L. G. Villanueva, M. H. Matheny, J. E. Sader, and M. L. Roukes, Phys. Rev. Lett. **108**, 236101 (2012).
[5] T. Faust, J. Rieger, M. J. Seitner, J. P. Kotthaus, and E. M. Weig, Phys. Rev. B **89**, 100102 (2014).
[6] S. C. Masmanidis, H. X. Tang, E. B. Myers, M. Li, K. De Greve, G. Vermeulen, W. Van Roy, and M. L. Roukes, Phys. Rev. Lett. **95**, 187206 (2005).
[7] M. Pernpeintner, R. B. Holländer, M. J. Seitner, E. M. Weig, R. Gross, S. T. B. Goennenwein, and H. Huebl. A universal platform for magnetostriction measurements in thin films. `arXiv:1509.00647` (2015).
[8] W. P. Mason, Phys. Rev. **96**, 302 (1954).

Time domain characterization of a transmon qubit

J. Goetz, M. Müting, F. Deppe, A. Marx, and R. Gross [1]

For many experiments and applications of circuit QED systems, the time evolution of the quantum system plays an important role. Therefore, studies of the quantum dynamics in the time domain are essential. Here, we present a time domain excitation and readout scheme, which allows us to investigate the quantum behavior of coupled qubit-resonator systems. We apply this scheme to perform Rabi and echo measurements fully characterizing the coherence properties of our device.

We analyze the coherence properties of a superconducting transmon qubit with a transition frequency $\omega_q/2\pi = 6.74\,\mathrm{GHz}$ which is strongly coupled with coupling strength $g/2\pi = 67\,\mathrm{MHz}$ to a quarter wavelength resonator of frequency $\omega_r/2\pi = 6.05\,\mathrm{GHz}$ [1]. The system Hamiltonian $\mathcal{H}_{tot} = \mathcal{H}_r + \mathcal{H}_q + \mathcal{H}_g + \mathcal{H}_d$ comprises the bare resonator Hamiltonian $\mathcal{H}_r = \hbar\omega_r \hat{a}^\dagger \hat{a}$, the qubit Hamiltonian $\mathcal{H}_q = \hbar\omega_q \hat{\sigma}_z/2$, the coupling Hamiltonian $\mathcal{H}_g = \hbar g(\hat{a}^\dagger\hat{\sigma}_- + \hat{a}\hat{\sigma}_+)$, and a driving term $\mathcal{H}_d = \hbar\Omega_d \cos(\omega_d t)\hat{\sigma}_x$. Here, $\hat{\sigma}_i$ are the Pauli operators, $\hat{a}^\dagger$ $(\hat{a})$ are the bosonic creation (annihilation) operators, and Ω_d defines the strength of the excitation drive. All our experiments are carried out in the dispersive limit where the resonator-qubit detuning $\Delta = \omega_q - \omega_r$ is much larger than their mutual coupling g. In this limit, we can use the qubit-state dependent ac-Stark shift for readout and describe the damping of the qubit by the master equation

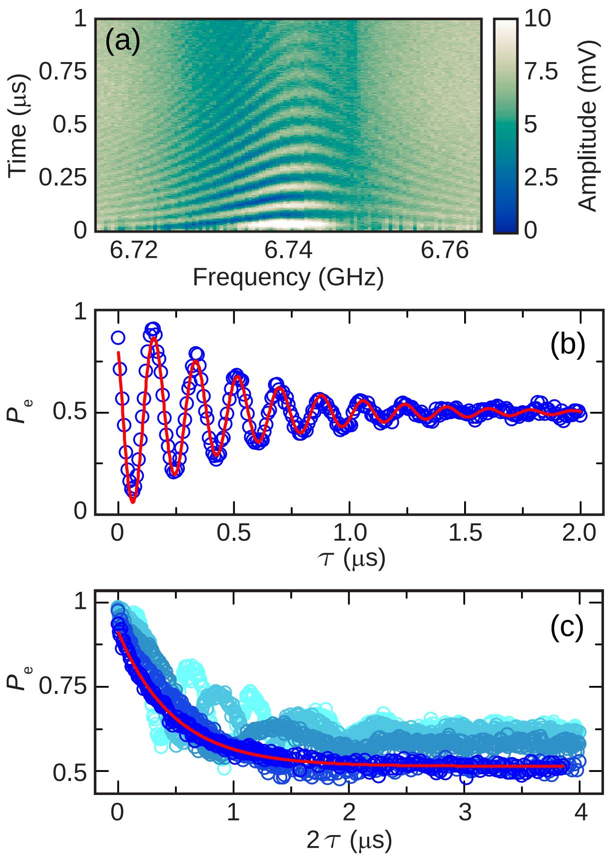

Figure 1: (a) Driven Rabi oscillations encoded in the frequency dependent transmission amplitude plotted versus time. (b) Qubit excited state probability for a Ramsey experiment plotted versus the waiting time between two $\pi/2$ pulses. Here, the detuning between the drive and the qubit frequency is 5 MHz. Solid line is a calculation using Eq. (1). (c) Qubit excited state probability for a spin-echo measurement sequence with a total waiting time 2τ.

$$\frac{\partial \hat{\rho}_q^D}{\partial t} = \frac{-i}{\hbar}[\mathcal{H}_q + \mathcal{H}_d, \hat{\rho}_q^D] + \frac{\Gamma_\phi}{2}\mathcal{D}[\hat{\sigma}_z] + \Gamma_r \mathcal{D}[\hat{\sigma}_-]\,. \tag{1}$$

Here, $\hat{\rho}_q^D = \mathrm{Tr}(\hat{\rho}_q)$ is the reduced density matrix of the qubit in the dispersive limit and $\mathcal{D}[\hat{L}] = (2\hat{L}\hat{\rho}\hat{L}^\dagger - \hat{L}^\dagger\hat{L}\hat{\rho} - \hat{\rho}\hat{L}^\dagger\hat{L})/2$ is the usual Lindblad damping superoperator. The qubit coherence properties are described by the pure dephasing and the intrinsic relaxation rate Γ_ϕ and Γ_r, respectively. In Fig. 1 (a) we show typical driven Rabi oscillations continuously recorded during a weak measurement with 0.5 readout photons on average. We measure an average Rabi decay time $\Gamma_{Rabi} = 1/\tau_{Rabi} \simeq 3.1\,\mathrm{MHz}$. To probe the influence of low-frequency

[1] The authors acknowledge support from the German Research Foundation through SFB 631 and FE 1564/1-1, the EU project PROMISCE, the doctorate program ExQM of the Elite Network of Bavaria, and the German Excellence Initiative via the 'Nanosystems Initiative Munich' (NIM).

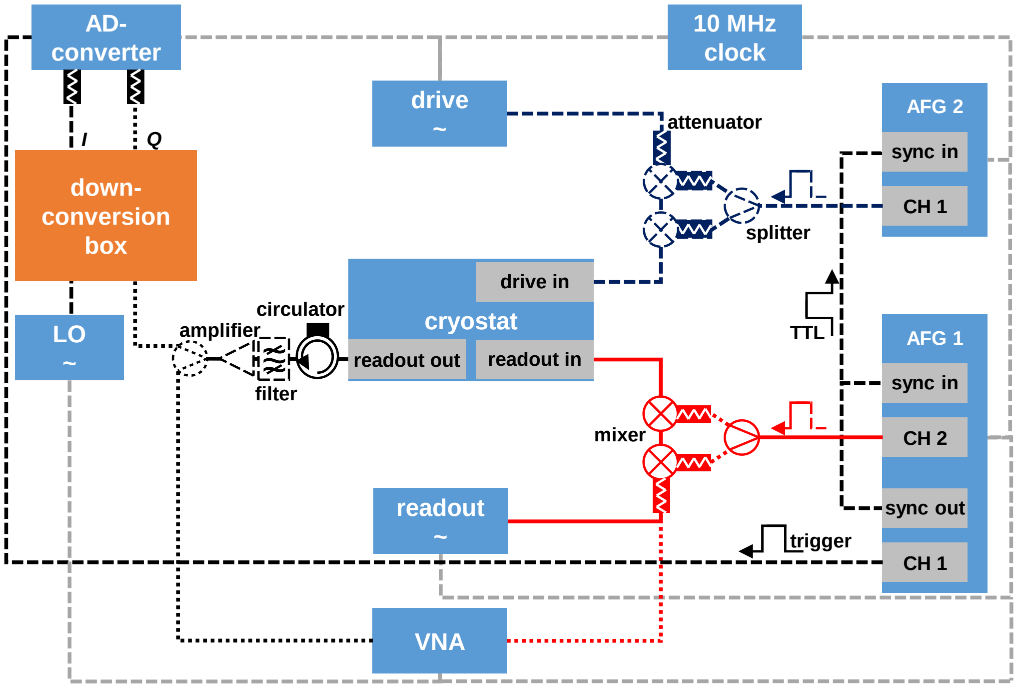

Figure 2: Time domain measurement setup. Red and dark blue lines belong to the pulse generation while dashed lines are used for synchronization. The down-conversion box contains a filter and a mixer to perform heterodyne down-conversion to the intermediate frequency and an amplifier to further increase the signal amplitude. The vector network analyzer (VNA) is used for a spectroscopic characterization of the qubit.

noise, we perform Ramsey type experiments as shown in Fig. 1 (b). Due to the Ramsey filter function, we can scan for low-frequency noise by adjusting the detuning between the drive frequency and the qubit frequency. Our sample shows a constant Ramsey decay rate $\Gamma_{\mathrm{Ramsey}} \simeq 2.1(1)$ MHz for detunings between 1 MHz and 20 MHz. Hence, noise in this frequency range is not dominant in our setup. To probe noise in the DC-limit, we perform spin-echo measurements as shown in Fig. 1 (c). All recorded spin-echo rates are approximately $\Gamma_{\mathrm{se}} \simeq 2.1(1)$ MHz and thus are very close to the Ramsey decay rates. These results show that the qubit coherence is dominated by high-frequency noise and consequently we measure a relaxation rate $\Gamma_{\mathrm{r}}^0 = 1/T_1 \simeq 3.9(1)\,\mathrm{MHz} \simeq 2/T_2$. However, this decay rate is still a factor of ten larger than the expected Purcell rate $\Gamma_{\mathrm{P}} = \kappa g^2/\Delta^2 \simeq 120$ kHz, where $\kappa/2\pi = 20$ MHz is the resonator bandwidth. Using the relation $\Gamma_\phi = \Gamma_{\mathrm{Ramsey}} - \Gamma_{\mathrm{r}}^0/2$ we find a pure dephasing rate of $\Gamma_\phi^0 = 150$ kHz.

The measurement setup used for theses measurements [2] is shown in Fig.2. We realize the time-resolved, phase-sensitive measurement of the in-phase and out-of-phase quadratures $I(t)$ and $Q(t)$ of the readout signal by heterodyne down-conversion to an intermediate frequency $\omega_{\mathrm{IF}} = 62.5$ MHz and a subsequent amplification. To generate pulsed sequences in the GHz-regime, we mix a continuous microwave signal to the envelope of a rectangular pulse generated by an arbitrary function generator (AFG). We digitize the signals and perform digital homodyning. In addition, we can readout the resonator via a vector network analyzer (VNA) for spectroscopic analysis of the sample.

References

[1] F. Wulschner, J. Puertas Martinez, E. P. Menzel, F. Deppe, A. Marx, and R. Gross, WMI Ann. Rep. **2014**, 19–20 (2014).

[2] M. Müting. *Time domain characterization of a transmon qubit*. Master's thesis, Technische Universität München (2015).

Loss mechanisms in superconducting thin film microwave resonators

J. Goetz, F. Deppe, A. Marx, and R. Gross [1]

We analyze internal losses of superconducting coplanar waveguide microwave resonators based on Nb thin films deposited on Si substrates. In particular, we study eddy current and quasiparticle losses at millikekvin temperatures in the gigahertz regime [1]. The clarification of the loss mechanisms is crucial for superconducting circuit-QED systems used for quantum information processing.

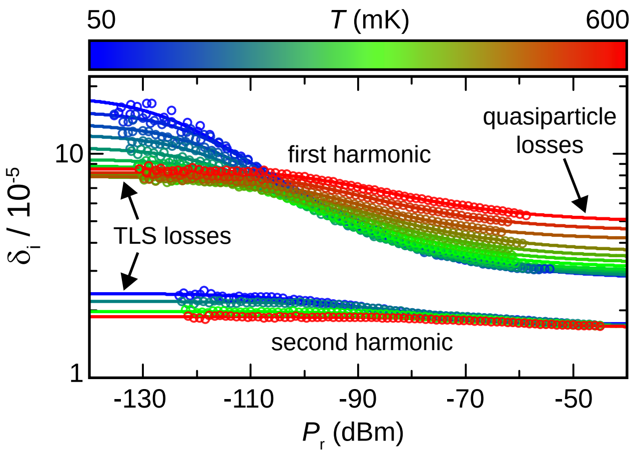

Figure 1: Internal losses plotted versus the circulating microwave power for the first two harmonic modes of sample VIII (no Ar ion cleaning) at temperatures between 50 mK and 600 mK.

To particularly study the influence of Al/Nb interfaces, we place an Al strip on purpose in the center conductor at the current antinode of the fundamental resonator mode. We treat the Nb/Al interfaces as large-area Josephson junctions which intrinsically contain two-level states (TLSs) in their oxide barrier. These TLSs are expected to result in additional losses. Our experimental findings that the quality of the resonator is reduced by more than one order of magnitude compared to pure Nb resonators shows that (i) the Nb oxides present at the interfaces are strong TLS sources and that (ii) these TLSs cause significant losses. This behavior is not immediately obvious, because the Nb/Al interfaces are placed at a voltage node of the first harmonic resonator mode. Consequently, the TLSs associated with the Nb oxides at these interfaces do not couple to the resonator electric field. Nevertheless, due to the electric field $\mathbf{E}_{\mathrm{Nb/Al}}$ between the Nb and the Al layer in the overlap area, we observe a pronounced power and temperature dependence of the internal loss rate δ_{i} (see Fig. 1). The field $\mathbf{E}_{\mathrm{Nb/Al}}$ is proportional to the resonator current which is maximum if the Nb/Al interface is placed at the current antinode (voltage node) of the resonator field.

In the next step, we confirm our model assumptions on TLS losses at the interfaces by analyzing the second harmonic mode of the resonator which has a voltage antinode at the interface position. As shown in Fig. 1, this mode shows significantly less internal losses than the first harmonic mode. This observation clearly contradicts the expectation $\delta_{\mathrm{i}} \propto n$ based on a model considering only a uniformly distributed residual conductivity. Evidently, we measure losses as small as those of the pure Nb resonator since for the second harmonic mode the interfaces are located at the current node, $I_{\omega_{\mathrm{r},2}} \simeq 0$, where the corresponding electric field $E^{\mathrm{rms}}_{\mathrm{Nb/Al}}$ is vanishingly small. Therefore, only the TLSs apart from the interface, which couple to the resonator electric field, introduce losses. These are expected to be comparable to those of a pure Nb resonator in agreement with our data. We note that also the power independent contribution δ_{c} is higher for the second harmonic mode than for the first harmonic mode. This behavior indicates that the interfaces are not only strong sources for the TLS losses but also for local resistive losses.

Next, we study the influence of the Nb/Al interfaces on the high power saturation value δ_{c}. For pure Nb resonators, we observe no significant change of δ_{c} in the temperature range

[1] The authors acknowledge support from the German Research Foundation through SFB 631 and FE 1564/1-1, the EU project PROMISCE, the doctorate program ExQM of the Elite Network of Bavaria, and the German Excellence Initiative via the 'Nanosystems Initiative Munich' (NIM).

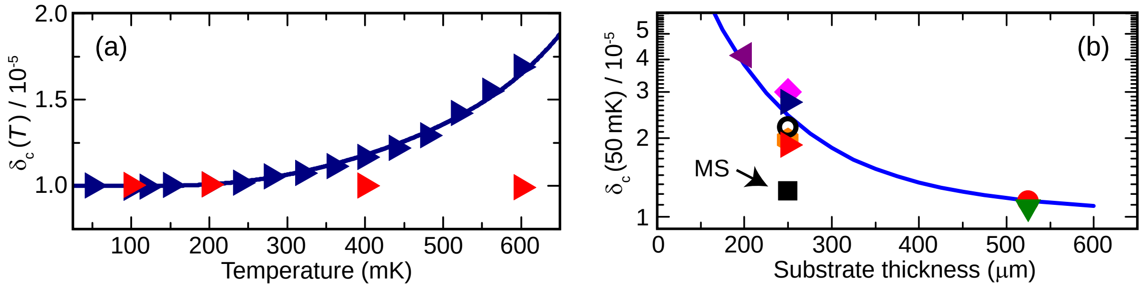

Figure 2: (a) High power losses δ_c plotted versus the sample temperature. Blue triangles correspond to the first and red triangles to the second harmonic mode. (b) Power independent losses δ_c measured at 50 mK plotted versus the substrate thickness.

between 50 mK and 600 mK. This behavior is expected because the number of quasiparticles is negligible for our experiments due to the high critical temperature $T_c \simeq 9$ K of the Nb films. However, the situation is different for samples including an Al strip, which has a much lower $T_c \simeq 1.5$ K. In Fig. 2 (a), we show the T dependence of δ_c for the first two modes. For the first harmonic mode, we observe a quasiparticle induced increase of δ_c which becomes relevant for $T > 200$ mK. We find a kinetic inductance fraction of $\gamma \simeq 3.5 \times 10^{-4}$, which is two orders of magnitude smaller than values reported in literature. We explain this difference by the fact that the length of the Al strip is only 1/100 of the total length of the center conductor. In contrast to the first harmonic mode, δ_c of the second harmonic mode shows no temperature dependence because the current distribution of the resonator has a node at the Al position in this case. Hence, the quasiparticles in the Al do not carry a significant amount of the current circulating inside the resonator.

We finally discuss the losses resulting from eddy currents induced in the conductive material on the backside of the substrate. To this end, we compare several CPW samples. We observe that δ_c shows a significant dependence on the substrate thickness as shown in Fig. 2 (b). We explain this effect by the finite conductivity of the silver glue used to fix the samples in the sample box. Our model results in a conductivity of $\sigma_{\omega_r} \simeq 7 \times 10^7\,\mathrm{S\,m^{-1}}$ of the silver glue. This value is about hundred times larger than the room temperature conductivity of our silver glue. However, since the conductivity of metals usually increases strongly with decreasing T, we safely can attribute the observed behavior to ohmic losses in the silver glue. The influence of eddy current losses depends on the material present underneath the sample. Compared to pure metals, silver glue has a relatively low conductivity and therefore larger losses. For samples with a substrate thickness of 525 μm the high power losses are already enhanced by 13 % compared to δ_0. Samples fabricated on 200 μm thick substrates show a loss increase by a factor of four compared to δ_0. The slight scatter in δ_c for $h = 250$ μm is attributed to our assumption of a universal δ_0. This assumption is, of course, only a rough estimation because the samples are fabricated with different cleaning methods. Losses caused by eddy currents can be avoided by using superconducting materials. This conclusion is supported by our measurements on a microstrip (MS) resonator, which is fabricated on a 250 μm thick substrate and employs a superconducting ground plane. For this sample, we measure a loss rate which is reduced by a factor of two compared to that of the samples fabricated on a 250 μm thick substrate, despite the fact that the field at the bottom surface of the substrate is an order of magnitude larger than for the CPW samples.

References

[1] J. Goetz, F. Deppe, M. Haeberlein, F. Wulschner, C. W. Zollitsch, S. Meier, M. Fischer, P. Eder, E. Xie, K. G. Fedorov, E. P. Menzel, A. Marx, and R. Gross. Loss mechanisms in superconducting thin film microwave resonators. Accepted for publication in J. Appl. Phys., arXiv:1510.05957 (2015).

Materials, Thin Film and Nanotechnology, Experimental Techniques

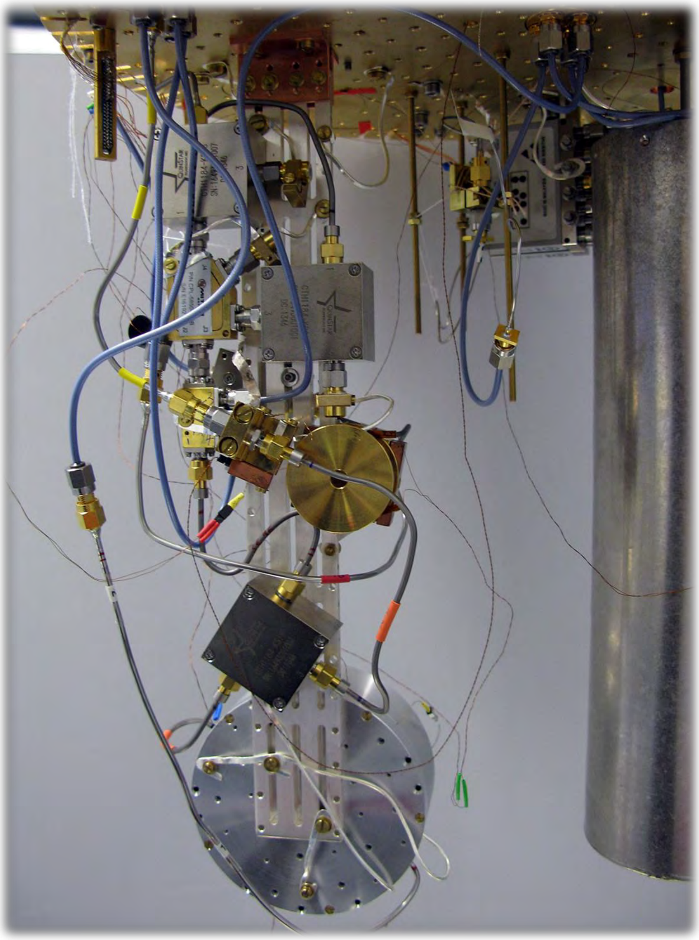

Installation of microwave cables and components on the mK part of a dilution refrigerator system used for experiments on solid state quantum systems.

Structural and magnetic properties of layered iridate thin films

S. Geprägs, J. Fischer, M. Opel, R. Gross [1]
B. Skovdal, D. Mannix [2]

Transition metal oxides (TMOs) are in the focus of research since many years due to their fascinating physical properties such as high-temperature superconductivity in cuprates, spin triplet superconductivity in ruthenates, colossal magnetoresistance in manganites, metal-insulator transition in vanadates, as well as the coupling of magnetism and ferroelectricity resulting from collective electric phenomena [1]. In contrast to TMOs based $3d$-metal ions, where the spin-orbit coupling (SOC) can be treated as a perturbation, the strong SOC in $5d$-TMOs drastically affects the electronic and magnetic structure. In particular, in iridates, novel physical properties emerge due to the entangled spin and orbital moments. Here, the prototype compound is the layered iridate Sr_2IrO_4 (cf. Fig. 1(a)), which has similar crystalline, electronic and magnetic structures as the high-temperature cuprates [2]. The physical properties of Sr_2IrO_4 are based on a splitting of the Ir $5d$-t_{2g} band due to the large SOC. This results in an effective $J_{\mathrm{eff}} = 1/2$ ground state leading to new quantum states including the unexpected Mott insulating phase [3].

Since the $5d$ orbitals are much more extended than those of the $3d$ and $4d$ states, the compound Sr_2IrO_4 is expected to be highly sensitive to strain effects, which modify the Ir-O-Ir bond length and angle. Indeed, recently, it has been found that strain can tune the magnetic coupling, modify the electronic states, change the octahedral rotation angle, and induce giant piezoresistive behaviour in Sr_2IrO_4 thin films [4]. To further investigate the strain dependence of the physical properties, we fabricated epitaxial Sr_2IrO_4 thin films on (001)-oriented, single-crystalline $SrTiO_3$ substrates by pulsed laser deposition (PLD). The growth was monitored *in-situ* by reflection high energy electron diffraction (RHEED). The best structural and magnetic properties were obtained by using a substrate temperature of 600 °C, an oxygen atmosphere of 25 μbar, and an energy fluence of the KrF excimer laser of 2 J cm^{-2} at the target surface. Using these deposition parameters, a two dimensional layer-by-layer growth mode is achieved, indicated by oscillations of the RHEED intensity (cf. Fig. 1(b)). The thus obtained Sr_2IrO_4 thin films exhibit a

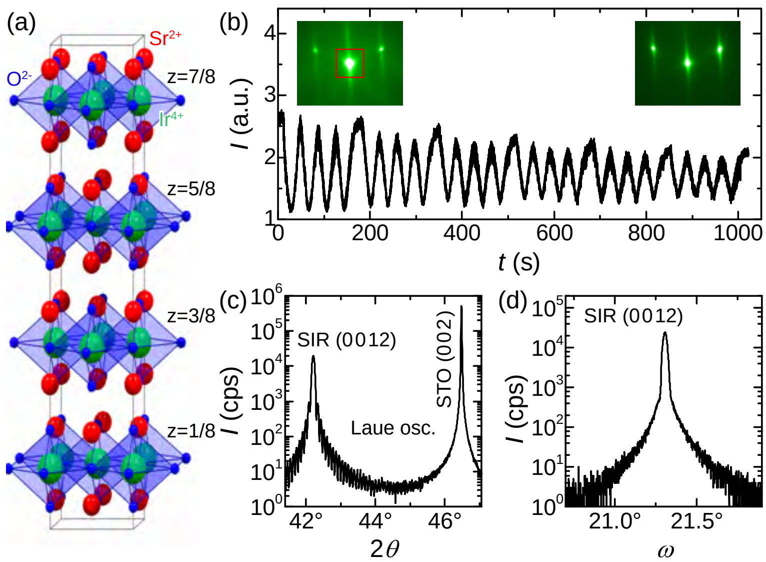

Figure 1: (a) Unit cell of Sr_2IrO_4 (red: Sr^{2+}, green: Ir^{4+}, blue: O^{2-}). The unit cell is built-up by four perovskite blocks separated by rock salt SrO layers. (b) RHEED intensity of the (0, 0) reflection recorded during the growth of a 50 nm thick Sr_2IrO_4 thin film. RHEED oscillations are clearly discernible demonstrating a two dimensional layer-by-layer growth. The insets show the RHEED patterns at the beginning (left) and at the end of the growth process (right). (c), (d) High resolution X-ray diffraction around the Sr_2IrO_4 (SIO) (0 0 12) reflection. The 2θ-ω-scan reveals finite thickness fringes (Laue oscillations), indicating a coherent growth of Sr_2IrO_4 on $SrTiO_3$. The high crystalline quality is further demonstrated by the narrow rocking curve around the SIR (0 0 12) reflection.

[1]This work was supported by the European Synchrotron Research Facility (ESRF) via HC-1821.
[2]Department of Physics, Lund University, Sweden.

high crystalline quality demonstrated by finite thickness fringes (Laue oscillations, cf. Fig. 1(c)) as well as a full width at half maximum of the rocking curve around the Sr_2IrO_4(0 0 12) reflection below 0.03° (cf. Fig. 1(d)).

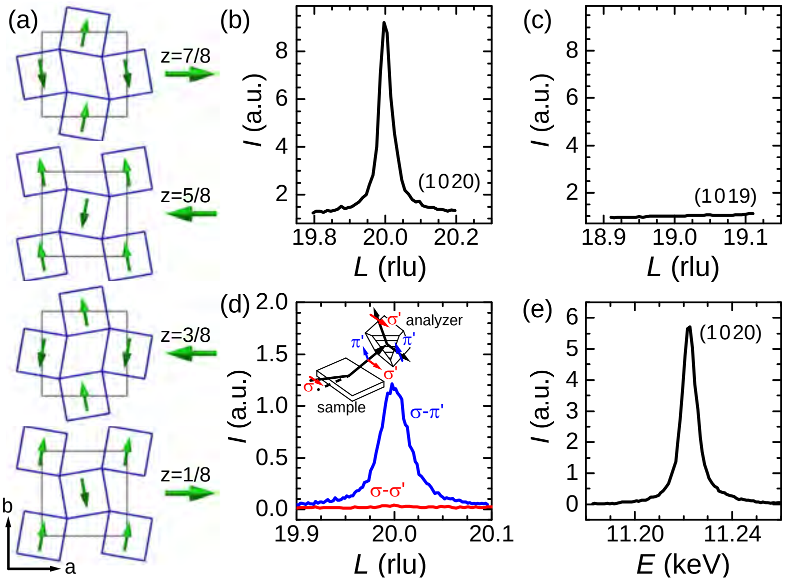

Figure 2: (a) Possible magnetic domain model of Sr_2IrO_4. The in-plane projections of the canted magnetic moments are shown for the different planes in the *c*-axis direction. (b)-(d) X-ray resonant magnetic scattering (XRMS) performed at the BM28 beamline at the European Synchrotron Radiation Facility (ESRF). A finite intensity is observed around the (1 0 20) reflection, but not around (1 0 19). The magnetic nature of the (1 0 20) reflection is proven by XRMS using a Au (333) analyzer crystal. The inset of (c) schematically shows the scattering geometry. A resonant enhancement is observed in energy scans around the Ir L_3-edge.

To investigate the magnetic structure of our Sr_2IrO_4 thin films we performed X-ray resonant magnetic scattering (XRMS) at the BM28 beamline at the European Synchrotron Radiation Facility (ESRF). A schematic diagram of the magnetic structure observed in bulk Sr_2IrO_4 is shown in Fig. 2(a). In general, two magnetic domains can exist due to the tetragonal structure of Sr_2IrO_4, which give rise to magnetic reflections either at $(1\,0\,4n{+}2)$ and $(0\,1\,4n)$ or at $(0\,1\,4n{+}2)$ and $(1\,0\,4n)$, respectively [5]. The results of our systematic search for magnetic reflections from our Sr_2IrO_4 films, are shown in Figs. 2(b) and (c). We find only magnetic reflections corresponding to $(1\,0\,L)$ and $(0\,1\,L)$ with L=even, which suggests that the magnetic structure of our films is similar to that of the bulk material. The magnetic nature of these reflections was further confirmed by polarization analysis using a Au (333) analyzer crystal shown in Fig. 2(d). The scans of the two different polarization channels (σ-σ' and σ-π') clearly demonstrate that the scattered intensity is in the σ-π' channel, confirming their magnetic origin. The energy dependence of the (1 0 20) reflection (Fig. 2(e)) shows a sharp resonant enhancement at the Ir L_3-edge (11.22 keV), consistent with electric dipole transitions probing the $J_{\mathrm{eff}} = 1/2$ $5d$-ground state of our Sr_2IrO_4 films.

In summary, we have fabricated epitaxial Sr_2IrO_4 thin films with high crystalline quality. X-ray resonant magnetic scattering experiments reveal a magnetic behavior very similar to that of bulk Sr_2IrO_4. In forthcoming experiments, we will systematically investigate the microscopic magnetic behavior of Sr_2IrO_4 thin films as a function of strain shedding new light on the rich, complex behavior of transition metal oxides and the physics of quantum materials.

References

[1] S.-W. Cheong, Nat. Mater. **6**, 927–928 (2007).
[2] B. J. Kim, H. Ohsumi, T. Komesu, S. Sakai, T. Morita, H. Takagi, and T. Arima, Science **323**, 1329–1332 (2009).
[3] Y. K. Kim, O. Krupin, J. D. Denlinger, A. Bostwick, E. Rotenberg, Q. Zhao, J. F. Mitchell, J. W. Allen, and B. J. Kim, Science **345**, 187–190 (2014).
[4] A. Lupascu, J. P. Clancy, H. Gretarsson, Z. Nie, J. Nichols, J. Terzic, G. Cao, S. S. A. Seo, Z. Islam, M. H. Upton, J. Kim, D. Casa, T. Gog, A. H. Said, V. M. Katukuri, H. Stoll, L. Hozoi, J. van den Brink, and Y.-J. Kim, Phys. Rev. Lett. **112**, 147201 (2014).
[5] C. Dhital, T. Hogan, Z. Yamani, C. de la Cruz, X. Chen, S. Khadka, Z. Ren, and S. D. Wilson, Phys. Rev. B **87**, 144405 (2013).

Cooldown of a cryogen-free 1K cryostat with an alumina shunt

K. Uhlig

One of the striking features of cryogen-free cryostats is their big experimental space. Diameters of up to 50 cm of the mixing chamber mounting plate in dilution refrigerators (DR) have become commercially available. For these cryostats, the precooling of additional cold stages in an inner vacuum vessel with exchange gas would be impractical as the wall thickness and, thus, the mass of an inner vacuum vessel would be too big to be precooled in a reasonable time by a pulse tube cryocooler (PTC) [1]. Cryogen-free cryostats usually have only one vacuum space and cold stages in addition to the PTC have to be cooled from 300 K to $\sim$ 15 K either by a separate ^{4}He precool loop, or by a set of gas heat switches, or by a mechanical switch. For example, both of the WMI cryogen free DRs are equipped with precool loops. These precooling devices have their drawbacks. Whereas the construction and operation of precool loops and mechanical switches is quite involved, gas heat switches suffer from low thermal conductivity.

Here a different approach is described. In a first attempt, we have constructed and operated a thermal shunt from sintered alumina (SA) to cool the 1 K-stage of our dry DR from 300 K to 3 K. To demonstrate the effectiveness of this shunt, we have added a ballast of 3 kg of copper to the 1 K-pot.

SA has high thermal conductivity κ at high temperatures, whereas κ decreases proportional to T^{-3} at low temperatures and thus has the properties required for the thermal shunt. The heat capacity of metals also drops steeply at low temperatures, so it can be cooled via a sintered alumina shunt. It is important to note that the drop-off of the specific heat of metals occurs at higher temperatures than the drop-off of κ of SA. At low enough temperatures, the heat leak through the thermal shunt is so small that it barely affects the performance of a powerful ^{4}He-1 K-loop. The heat conductivity of SA and the specific heat of copper are depicted in Fig. 1. The values of κ of our shunt are also included in the figure.

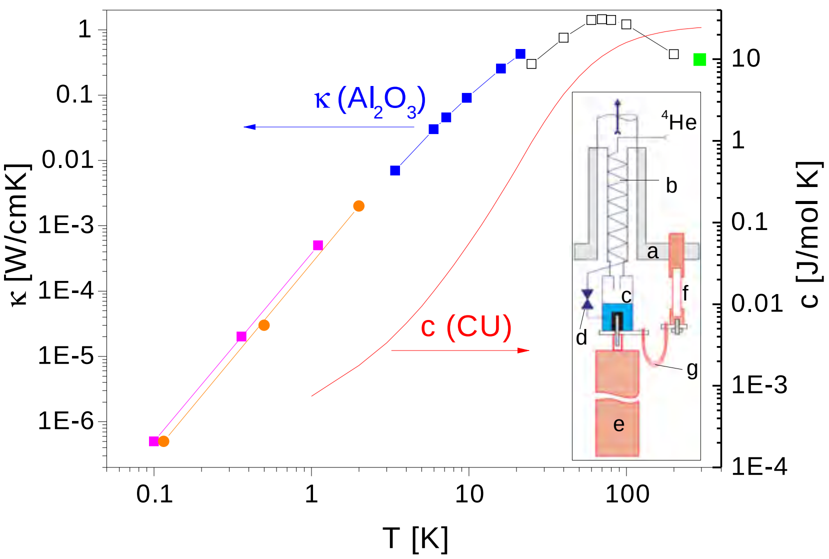

Figure 1: Thermal conductivity κ of SA (left scale) and specific heat c of copper (right scale). Data for κ are measurements on our alumina shunt (blue), data from various textbooks [2, 3] and the room temperature value of a manufacturer (green) [4]. Insert: Sketch of the 1 K-stage with SA shunt (**a**: second stage of PTC; **b**: counterflow heat exchanger; **c**: 1 K-pot; **d**: flow restriction; **e**: Cu ballast; **f**: alumina shunt; **g**: thermal connection made from Cu wires).

In the insert of Fig. 1 a sketch of our experimental set-up is given. The figure shows the ^{4}He-1 K-stage with the thermal shunt and its copper ballast, and a thermal connection between the alumina shunt and the 1 K-stage. The alumina shunt has a free length of 40 mm and a diameter of 8 mm. To measure its heat conductivity, two calibrated germanium resistors and a heater made from metal film resistors were used. The thermal connection between the 1 K-stage and the shunt were made from a bundle of 8 annealed Cu wires (each 1.35 mm thick). The 1 K-loop has been described in detail in [5] and the references therein. Its maximum refrigeration power is 100 mW.

In Fig. 2 cooldown curves of our cryostat are shown. Black symbols show the temperature of the 2nd stage of the PTC (T_{PT2}). They are close to the temperature of the top end of the shunt. The red symbols represent the temperature of the 1 K-pot and its ballast. Blue squares are for the bottom end of the shunt. Obviously, for a wide temperature range they lie between the temperatures of the 1 K-pot and T_{PT2} and thus indicate temperature gradients across the shunt and the connector between shunt and 1 K-pot ("g" in Fig. 1). For temperature measurements we used platinum sensors (PT 100) and ruthenium oxide resistors.

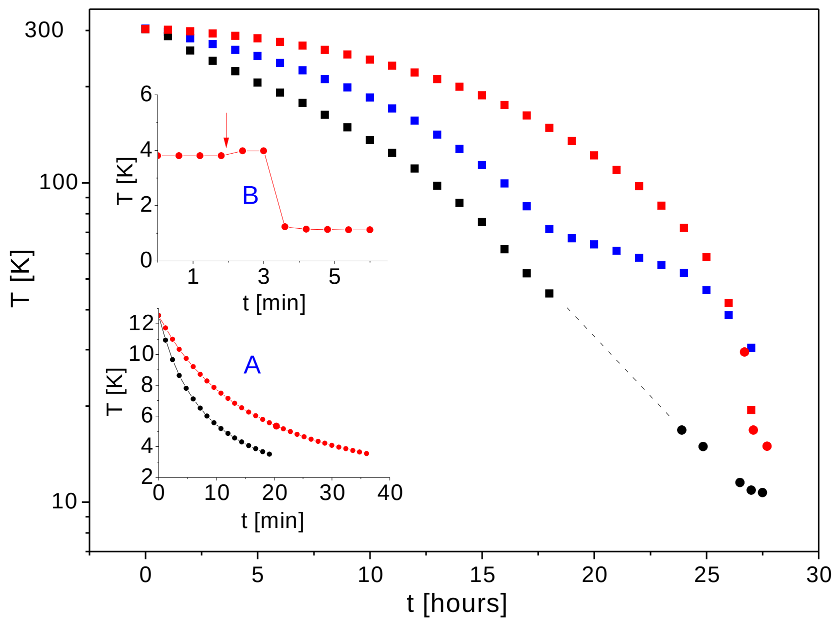

Figure 2: Cooldown curve of the 1K-stage from room temperature to 12 K. Black: Cold side of the alumina shunt. Blue: Hot side of the alumina shunt. Red: 1K-refrigerator with ballast. Insert A: Cooldown from 12 K to ~ 3 K (base temperature of the PTC). Black: 2nd stage of the PTC. Red: 1K-refrigerator. Insert B: Cooling of the 1K-stage after starting the ^{4}He circulation in the 1K-loop (arrow).

Insert A in Fig. 2 shows that the cooldown of the 1 K-stage from 12 K to 4 K takes 30 minutes. From insert B it is seen that within a minute the 1 K-loop cools from 4 K to 1 K. The residual heat leak through the shunt can be calculated by using the κ-curve of Fig. 1. At $T_{PT2} = 3$ K we find the heat leak of $Q = 0.6$ mW (for $T_{PT2} = 4$ K: $Q = 1.9$ mW).

In summary, we have shown that a SA shunt is perfectly suited for convenient and failure-free operation to precool a 1 K-refrigerator to $T_{PT2} \sim 3$ K. Cooling a dry DR without a 1 K-stage would be a different problem. This is because the total mass of dry DRs with heavy heat shields can be sizeable (e.g., the still shield of our cryogen-free DR weighs 20 kg) and, therefore, the q/L-ratio of the shunt would have to be increased. On the other hand, the refrigeration power of the still of dry DRs is typically an order of magnitude smaller than the one of 1 K-coolers. But the SA shunt could make sense in dry fridges with 1 K-stage.

References

[1] Cryomech Inc., Syracuse N.Y.; www.cryomech.com.
[2] R. C. Richardson. Experimental Techniques in Condensed Matter Physics at Low Temperatures. Addison-Wesley Publishing Company, Inc. (1988).
[3] F. Pobell. Matter and Methods at Low Temperatures. Springer-Verlag, Third edition (2006).
[4] FRIATEC AG; www.friatec.de.
[5] K. Uhlig, Cryogenics **66**, 6–12 (2015).

Construction of a new ^{3}He-^{4}He dilution refrigerator

E. Xie, C. Probst, J. Höß, F. Deppe, A. Marx, R. Gross [1]

Quantum information processing with superconducting qubits is a promising candidate for a future quantum computer. At WMI, we use Josephson-junction based qubits to study light-matter interaction. For these experiments to be carried out and the quantum nature of light to be revealed, low temperatures below 50 mK are necessary along with microwave signal access and sufficient sample space. To this end, several dilution refrigerators have been set up at WMI in the last 10 years. At the moment, two "wet" fridges [1] and one "dry" fridge [2] are available for long-term experiments on the order of months.

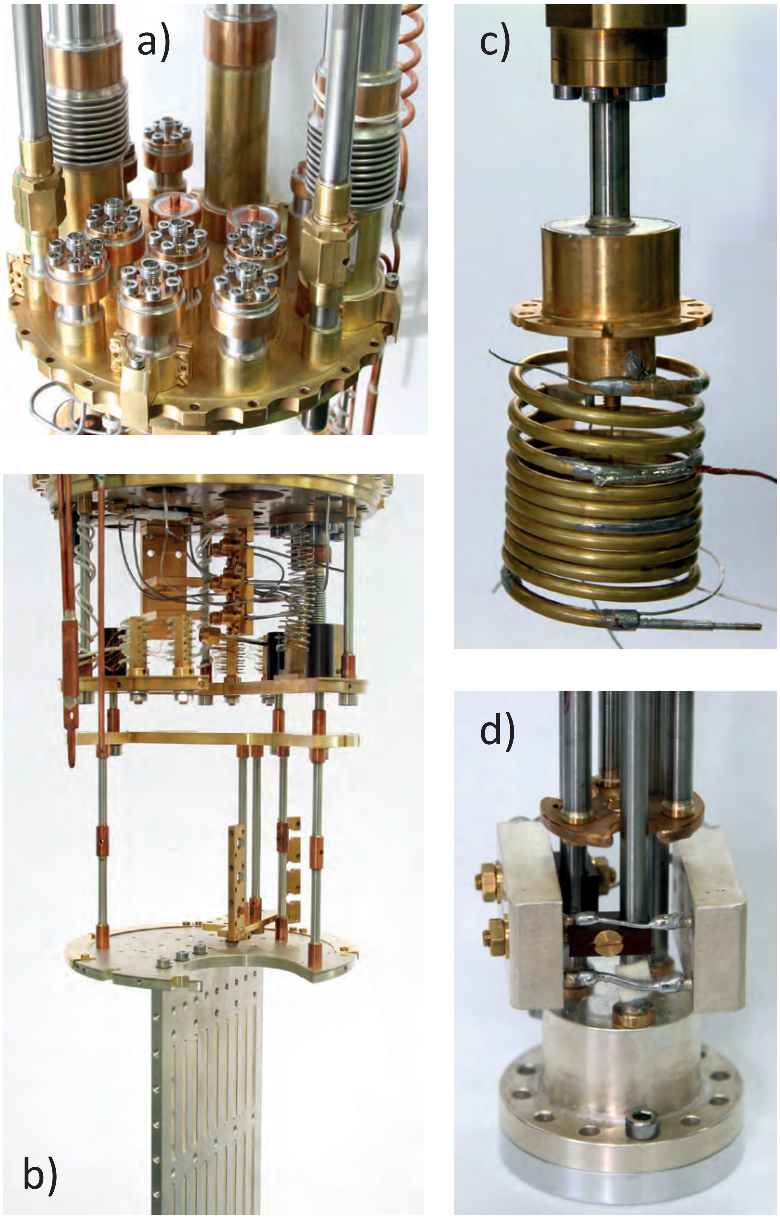

Figure 1: Photographs of the insert: **(a)** 4 K-stage with 8 vacuum tight RF feedthroughs. **(b)** Experimental setup with the dilution unit detached: Stages below 4 K (from bottom to top): the mixing chamber stage along with the sample rod, the distillation stage and the 1 K stage. The 1 K stage is equipped with the 1 K pot. Anchoring of RF and DC cables is in progress. **(c)** The distillation pot and the coil heat exchanger. **(d)** Compact two-stage step exchanger (boxes) mounted above the mixing chamber.

Here, we present progress on an additional "wet" cryostat suitable for experiments with superconducting qubits. Its compact design makes the facility ideal for pre-characterization experiments on a timescale of a few weeks. It features six coaxial input and two output lines for microwave signals. The latter made of superconducting NbTi material and run through circulators and HEMT amplifiers to enhance the signal-to-noise ratio. Differently from previous setups, the circulators and amplifiers are chosen to cover a broad frequency range from 4 to 16 GHz which is suitable for pre-characterization measurements.

Inside a vacuum can, which is surrounded by liquid ^{4}He, we find a 4 K stage, a 1 K pot, a ^{3}He

[1]The authors acknowledge support from the German Research Foundation through SFB 631, the EU project PROMISCE, and the German Excellence Initiative via the ‘Nanosystems Initiative Munich’ (NIM).

distillation stage, a coil heat exchanger followed by a step exchanger and, finally, a ^{3}He-^{4}He mixing chamber (cf. Fig. 1). Following the overall design idea of particular compactness, the step exchanger is split in two stages mounted above the mixing chamber lid. Based on experience from previous cryostats, we use a modular design, where experimental components and the dilution unit are disentangled as much as possible. As a consequence, the dilution unit can be detached from the main setup (cf. Fig. 1b) and tested separately. Moreover, 48 filtered DC lines can be used for thermometry and DC signals. For protection from thermal radiation, we mount a copper shield at the 1 K stage and an aluminum shield at the mixing chamber stage. The measurement lines are anchored at several temperatures before reaching the experiment at the sample stage. With this setup, we aim to reach a cooling power of approximately 50 µW at a base temperature of 20 mK. Currently, we are conducting final leak tests and planning the first cooldown of the cryostat.

For this new fridge, we are able to make use of (otherwise quite expensive) components from previous setups, such as the gas handling system and the ^{4}He dewar. However, several measures are taken to upgrade the laboratory to match upcoming experimental demands. Future experiments will be done in a screening chamber to reduce RF noise (cf. Fig. 2a). Moreover, multiple layers of µ-metal around the dewar screen the experiment from magnetic stray fields. The screening chamber is now equipped with a robust sliding shelf for the dewar and an electrical lift for handling the insert. The ^{3}He pump and the 1 K pump have been moved to an equipment room outside the lab in favour of reduced noise and mechanical vibrations (cf. Fig. 2b). A turbo molecular pump is added to the ^{3}He cycle to achieve higher throughput and hence a better cooling performance.

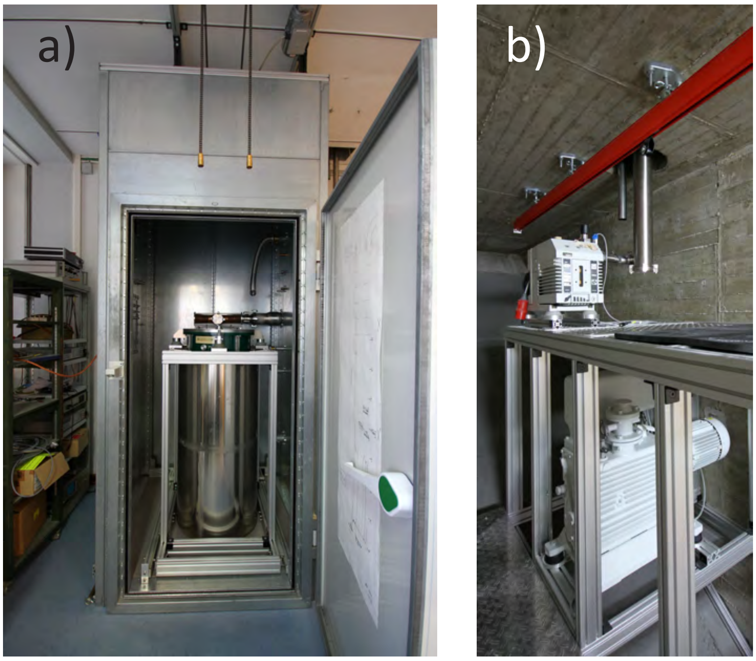

Figure 2: Photographs of the laboratory and the equipment room: **(a)** Screening chamber with the dewar on the sliding shelf. The dewar is shielded by a triple µ-metal shield. Chains coming from the ceiling are part of the motorized lift for insert handling. **(b)** Pumps are placed in a renovated, separate equipment room. The upper pump is used for the ^{3}He cycle, the lower for the 1 K pot.

In conclusion, we have advanced significantly on setting up a new compact dilution refrigerator for characterization experiments of superconducting quantum circuits. We plan to conduct first experiments in spring 2016.

References

[1] J. Goetz, F. Wulschner, J. Höß, K. Neumaier, C. Probst, F. Deppe, A. Marx, and R. Gross, WMI Ann. Rep. **2013**, 75–76 (2013).
[2] A. Marx, J. Höß, and K. Uhlig, WMI Ann. Rep. **2013**, 77–78 (2013).

Experimental Facilities

Overview of Key Experimental Facilities and Infrastructure

In the following basic information on the key experimental facilities and components of the technical infrastructure installed at the Walther-Meißner-Institute (WMI) is given.

UHV Laser-MBE

The WMI operates an UHV Laser-Molecular Beam Epitaxy (L-MBE) system for the growth of complex oxide heterostructures. The system has been designed to meet the special requirements of oxide epitaxy. The UHV cluster tool consists of the following main components:

- central transfer chamber;
- load-lock chamber with a heater system for substrate annealing;
- laser deposition chamber with a KrF excimer laser, *in-situ* reflection high energy electron diffraction (RHEED) system, laser substrate heating system, and atomic oxygen/nitrogen source; the RHEED system has been modified to allow for the operation at high oxygen partial pressure up to 0.5 mbar;
- surface characterization chamber with UHV scanning atomic force microscope (Omicron);
- metallization chamber with a four heart electron gun system and a liquid nitrogen cooled sample stage. The sample holder can be tilted for shadow evaporation.

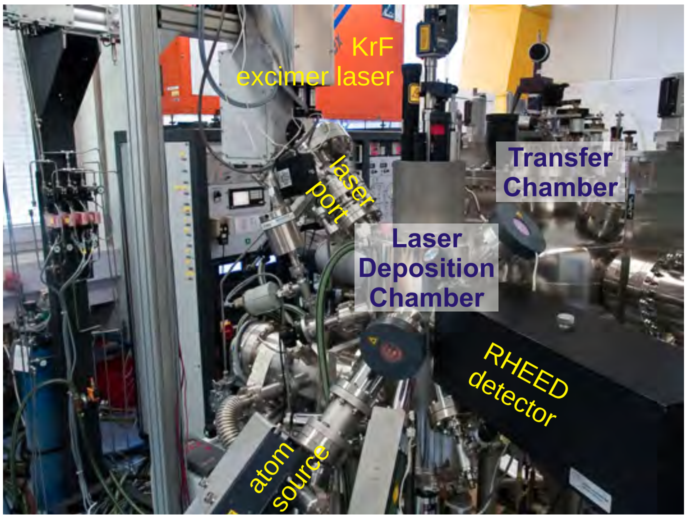

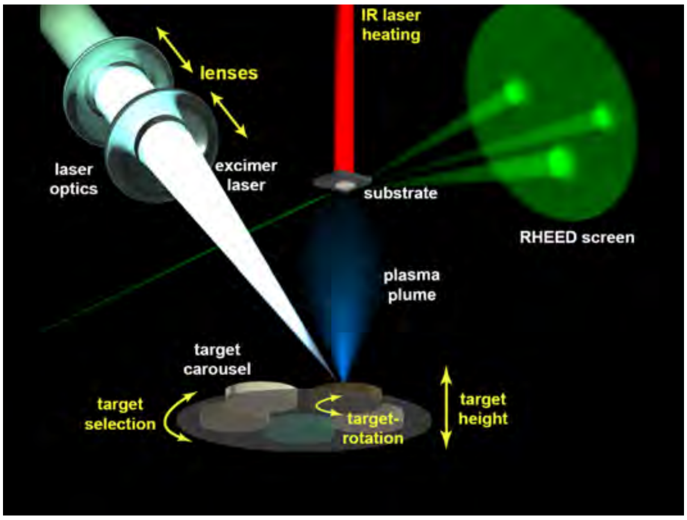

Figure 1: Top: UHV laser-molecular beam epitaxy system. Bottom: principle of the deposition process.

The system is used for the growth of complex oxide heterostructures consisting of superconducting, ferromagnetic, ferroelectric, and semiconducting materials such as high-temperature superconductors, doped manganites, (double) perovskites, magnetite, zinc oxide, rare earth iron garnets, pyrochlore iridates, etc.

The original laser molecular beam epitaxy system (laser-MBE) designed already in 1995/96 has been continuously upgraded and modified until now. In particular, the substrate heating system and the temperature control unit were changed from a resistive radiation heater to an infrared laser heating system (see Fig. 3, left) including a pyrometer for determining the sample temperature. In addition, a source for atomic oxygen and nitrogen has been installed. The main advantage of the new heating system is that only the substrate is heated while the surrounding parts are hardly affected (Fig. 3, right). In this way one can achieve a substantially better vacuum at temperatures well above 1000 °C. The achievable substrate temperature is limited by the melting point and the size of the substrate material (approx. 1410 °C for a 5 mm × 5 mm silicon substrate). The laser heating system has already been successfully used for removing the amorphous silicon oxide layer from the surface of silicon substrates at 1150 °C.

Figure 2: Pulsed Laser Deposition (PLD): When the pulse of the UV laser (KrF excimer laser, 248 nm) hits the target, the target material is ablated and the so-called laser "plume" containing highly excited atoms and molecules is formed.

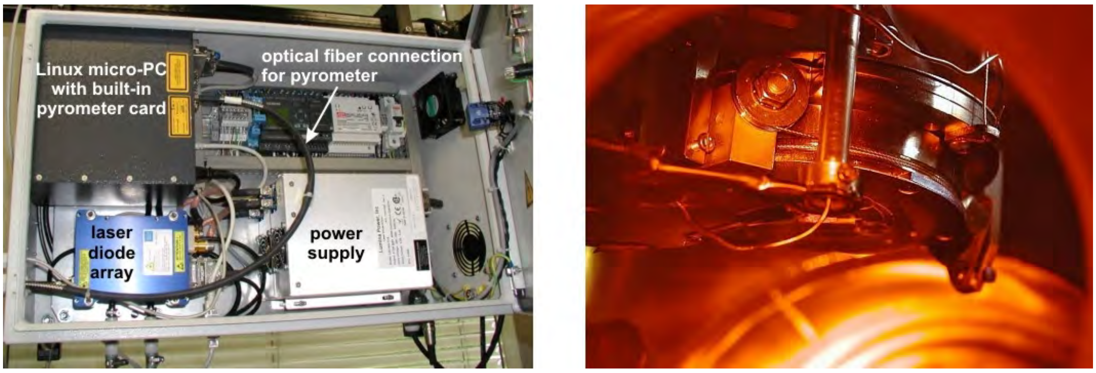

Figure 3: Components of the laser heating system: The substrate is heated using an IR diode laser head that is located in a separate box far away from the deposition chamber (left). The laser light is brought to the substrate (right) via an optical fiber.

We have further developed and installed a home-made telescope zoom optics for the pulsed UV laser light, consisting of in total five lenses on sliding lens holders allowing for a movement over a total distance of 1200 mm. The lens holders are attached to independent stepper motors, each connected to a controller providing an accurate positioning precision. The controllers are driven via a PC, thus allowing for a full automation of the lens system itself. With this telescope zoom optics we are able to change the area of the UV laser spot on the target, resulting in an accessible range of laser fluences from $\rho_L = 0.5\,\mathrm{J/cm^2}$ to $5\,\mathrm{J/cm^2}$. To maintain a stable laser fluence at the target, we have installed a so-called *intelligent* window (PVD Products) at the laser entrance port combining two unique features. First, it keeps the inner side of the entrance window free of coatings by blocking the ablated plasma plume via a rotatable disc consisting of UV grade fused silica. Second, an insertable mirror positioned in the light path after the disc allows to guide the incoming UV laser pulse through a side window, where its energy is determined by a pyroelectric detector. These measures help to improve the deposition processes by accurately monitoring ρ_L as one of the most critical process parameters.

UHV Electron Beam Evaporation System

The UHV metal MBE system allows for the growth of high quality metallic thin films by electron beam evaporation and molecular beam epitaxy. The system is optimized for the fabrication of superconducting persistent current qubits by aluminum shadow evaporation. It is equipped with an improved substrate holder allowing for multi-angle shadow evaporation. The main components of the system are:

- UHV system with a process chamber with a base pressure of $\sim 1 \times 10^{-8}$ mbar pumped by a 1000 l/s turbo molecular pump with magnetic suspension of the rotor adequate for corrosive gases.
- Load-lock chamber equipped with a magnetic transfer system (push-pull positioner) for sample transfer without breaking the vacuum in the process chamber.
- Downstream pressure control by an adaptive pressure controlled gate valve.
- Electron beam evaporator with six 8 cm^3 crucibles embedded in a linearly movable water cooled rail providing six different materials.
- Film thickness measurement and closed loop evaporation rate control by a quartz crystal microbalance in combination with the evaporation controller.
- Effusion cell for molecular beam epitaxy processes.
- Ion sputtering gun for in-situ sample cleaning
- Manipulator with UHV stepping motors for automated and precise sample tilt and options for rotating and cooling the sample.

A precise and reproducible tilt of the sample is realized by a sample manipulator with process specific degrees of freedom. The downstream pressure control allows for a fast adjustment and precise control of the oxygen partial pressure. This is crucial for a well-defined oxidation process of the Josephson junctions barriers. The entire process can be performed fully automated via a touch screen and is controlled by a LabView program. Up to six effusion cells can be optionally added to the system allowing for further materials. The manipulator allows for further degrees of freedom that can be used to align the sample to the effusion cells, the ion sputtering gun and to measuring equipment such as ellipsometry or RHEED.

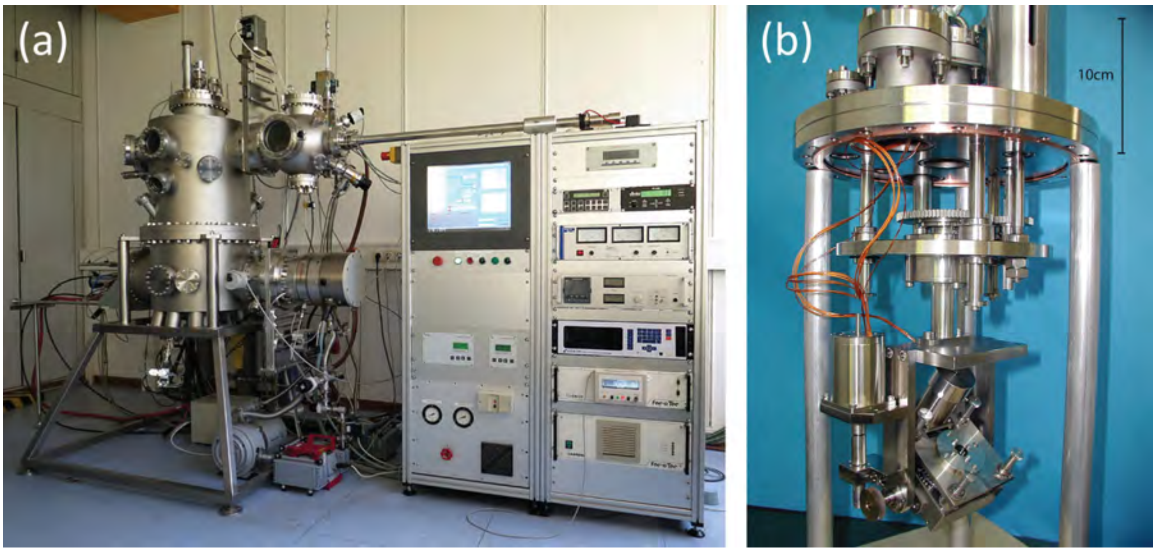

Figure 4: (a) Photograph of the UHV electron beam evaporation system. (b) Manipulator with UHV stepping motors for automated and precise sample tilt and options for rotation.

Single Crystal Growth and Synthesis of Bulk Materials

Transition metal oxides are of great interest due to their various interesting physical properties (e.g. high temperature superconductivity, colossal magnetoresistance, ferroelectricity, nonlinear optical properties etc.) and their high potential for applications. Therefore, the WMI operates a laboratory for the synthesis of bulk materials and single crystals of transition metal oxides. Besides various chamber- and tube furnaces a four-mirror image furnace is used for the crystal growth of various oxide systems. With this furnace crystals of many different compounds of the high temperature superconductors and various other transition metal oxides have been grown as single crystals using the traveling solvent floating zone technique. The furnace consists basically of 4 elliptical mirrors with a common focus on the sample rod and with halogen lamps in their other focus. By irradiation of the focused light the sample rod is locally heated and eventually molten. The molten zone can be moved up and down along the entire sample rod under simultaneous rotation. Due to the anisotropic growth velocity a preferential growth of those grains with the fastest growth velocity along the pulling direction is obtained and the formerly polycrystalline rod is transformed into a single crystal. Single crystal growth can be performed with this furnace at maximum temperatures up to 2200 °C in the pressure range from 10^{-5} mbar up to 10 bar and in oxidizing, reducing as well as inert atmosphere.

Figure 5: The four-mirror image furnace installed at the crystal laboratory of the WMI. Crystals can be grown by the floating zone and traveling solvent floating zone techniques at temperatures up to 2200 °C and pressures up to 10 bar.

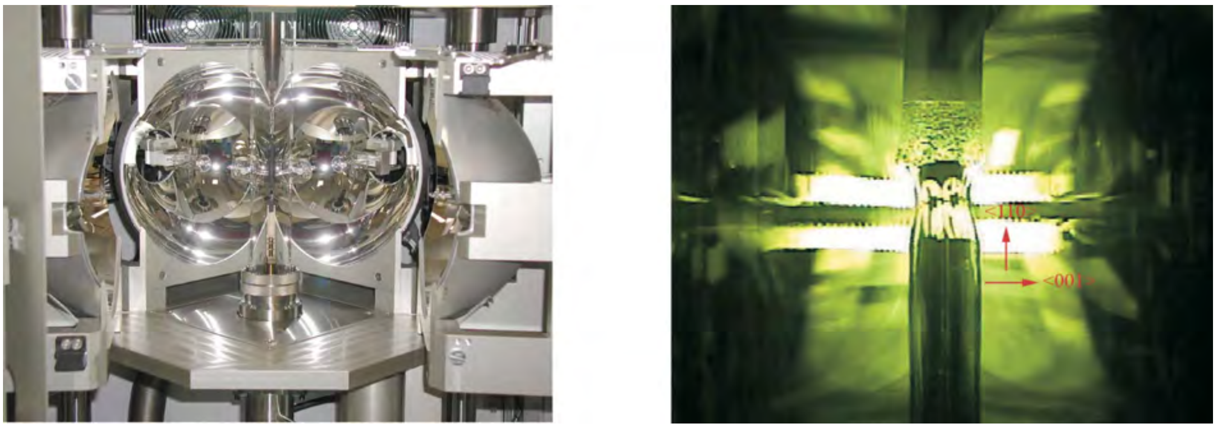

Figure 6: Left: Central part of the image furnace with four elliptical mirrors. In the center one can see the quartz tube with a polycrystalline rod. Right: View on the molten zone of $Pr_{2-x}Ce_xCuO_4$ (melting point: 1280 °C) obtained by a CCD camera.

The X-ray diffraction systems

For X-ray analysis the WMI operates two X-ray diffractometers (Bruker D8 Advance and D8 Discover). The two-circle system is used for powder diffraction. In this system the samples can be heated in oxygen atmosphere up to 1600 °C. It is equipped with a Göbel mirror and an area detector to save measuring time. The second system is a high resolution four-circle diffractometer that can be used for reciprocal space mappings. It is equipped with a Göbel mirror and an asymmetric two-fold Ge monochromator and allows for the texture analysis of thin film heterostructures, superlattices and single crystalline materials. In both systems measurements can be carried out fully computer controlled.

Beside these two Bruker X-ray systems a Laue camera for single crystal analysis and a Debye-Scherrer camera are available.

Figure 7: The two-circle X-ray diffractometer Bruker D8 Advance.

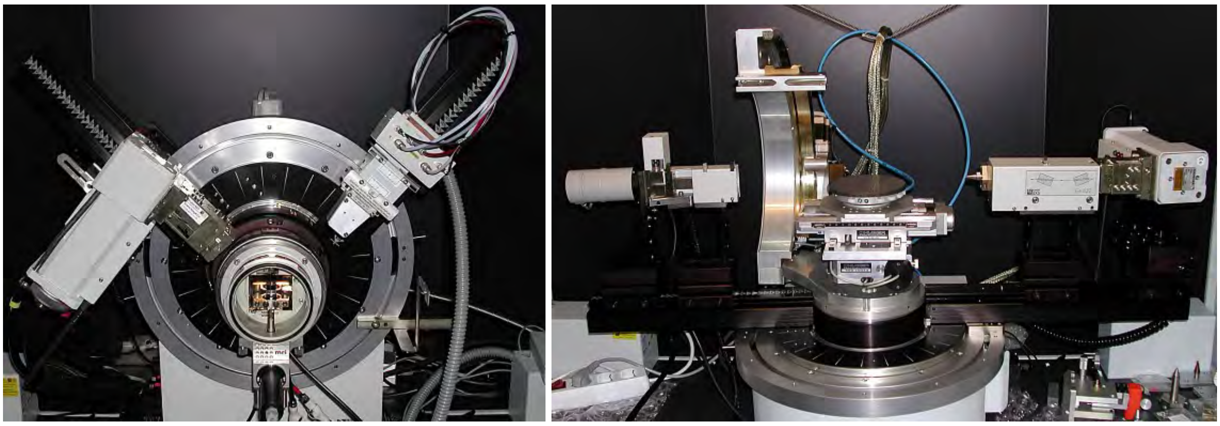

Figure 8: Left: High temperature sample holder of the D8 Advance system. Right: Four-circle high resolution X-ray diffractometer Bruker D8 Discover.

Figure 9: Quantum Design SQUID magnetometer.

The SQUID magnetometer

For the analysis of the magnetic properties of materials, a Quantum Design SQUID magnetometer system (Fig. 9) is operated at the WMI. The SQUID magnetometer allows for measurements in the temperature regime from 1.8 to 400 K and provides excellent sensitivity particularly in the low field regime. Due to the excellent sensitivity of the system, thin film samples with a very small sample volume can be analyzed. The SQUID magnetometer is equipped with a superconducting solenoid allowing for a maximum field of 7 T. At present, the magnetometer is used for the characterization of magnetic and superconducting materials (both in bulk and thin film form). Examples are the cuprate high temperature superconductors, the doped manganites, magnetite, the double perovskites, magnetic semiconductors, or multiferroics.

The High Field Laboratory

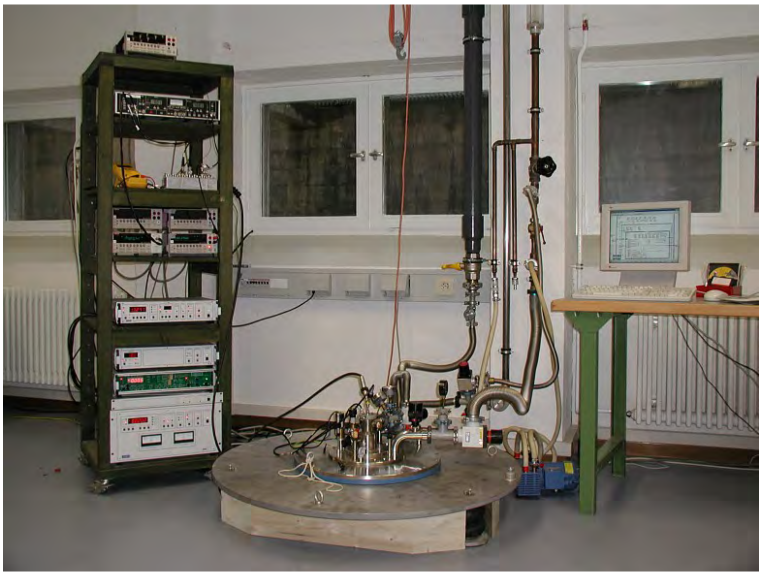

Figure 10: High field laboratory with Oxford 17 T magnet system.

Transport and thermodynamic properties of samples are often studied as a function of the applied magnetic field. For such measurements several superconducting magnets are available at the WMI. Two of them (8/10 and 15/17 Tesla magnet system) are located in the high magnetic field laboratory in the basement of the WMI. The magnet systems are installed below the floor level to facilitate the access to the top flange and the change of the sample sticks. The magnet systems are decoupled from the building to avoid noise due to mechanical vibrations. A variety of sample holders can be mounted allowing for e.g. sample rotation during the measurement. For standard sample holders the accessible temperature regime is $1.5\,\mathrm{K} < T < 300\,\mathrm{K}$. However, also ^{3}He/^{4}He dilution refrigerator inserts ($T > 20\,\mathrm{mK}$) or high temperature units ($T < 700\,\mathrm{K}$) can be mounted. All measurements are fully computer controlled (by the use of the LabView software tool) allowing for remote control and almost continuous measurements.

Since 2012, a 3D vector magnet with variable temperature insert, allowing for 2 T in-plane and 6 T out-of-plane magnetic fields is available for thermal and electrical transport experiments. This system has been named "Chaos" cryostat (acronym for "Cold, Hot And Other Secret experiments"). It consists of a ^{4}He flow cryostat with a liquid nitrogen shield and includes a vertically oriented 6 T solenoid combined with two horizontally oriented split coil pairs. The magnet system can be operated in two ways:

- in a single axis mode: up to 6(2) T are provided in the vertical (horizontal) direction.
- in a arbitrary axis mode: the flux density vector can be oriented in arbitrary directions and the magnitude of the flux density is limited to 2 T.

The magnetic field is controlled by a Mercury IPS superconducting magnet power supply master/slave system. It provides output currents of up to 120 A in bipolar operation for each magnet axis. The control of the system is feasible either directly via touch-screen or remote using a LabView based software.

Figure 11: The 3D vector magnet with control electronics in the "CHAOS" Laboratory.

The Chaos cryostat has a IN100 variable temperature insert (VTI), enabling an operation for temperature setpoints between 1.5 K and 300 K. The temperature control of the sample space inside the VTI can be achieved via an automatic needle valve drive for helium flow control and/or an automatic heater system. The temperature of the VTI is read via a Cernox sensor fitted to the heat exchanger. A remote control of the system is realized by a LabView based software. It provides control of the VTI (heater, needle valve, temperature setpoint) and the IPS (control of the magnetic field setpoints and energizing rates for the three vector components of the field) as well as the display of the actual He and liquid nitrogen levels.

A further 3D vector magnet allowing for 1 T in-plane and 6 T out-of-plane magnetic fields is installed in the WMI Quantum Laboratories as part of a cryogen-free dilution system.

The Clean Room Facility

For the fabrication of solid state nanostructures and quantum circuits including superconducting, spintronic and nanomechanical devices the WMI operates a class 1000 clean room facility with an area of about 50 m^2. This clean room facility has been put into operation at the WMI within the year 2001. The clean room is subdivided into two parts for optical lithography and electron beam lithography, respectively. The clean room facility is equipped with the standard tools for optical lithography such as resist coaters, hot plates, wet benches, a Karl Süss MJB3 mask aligner and an optical projection lithography system. The technical infrastructure for the clean room is located in the basement of the WMI directly below the clean room area.

Figure 12: Top: Part of the clean room facility with optical lithography equipment and clean room benches. Bottom: Resist coater and hot plates.

The clean room also is equipped with a reactive ion etching system, Plasmalab 80 Plus with ICP plasma source (Oxford Instruments Plasma Technology).

Electron Beam Lithography

A 100 kV Electron Beam Lithography System nB5 fabricated by NanoBeam Ltd., UK, is installed in the second part of the clean room facility. The nB5 is a round-beam step-and-repeat system oriented towards high-end R&D applications at universities and research institutes. It is designed for nanopatterning and mix-and-match lithography. The innovative design of the electron optics and automation system enhances its throughput and reliability. It is an ideal tool

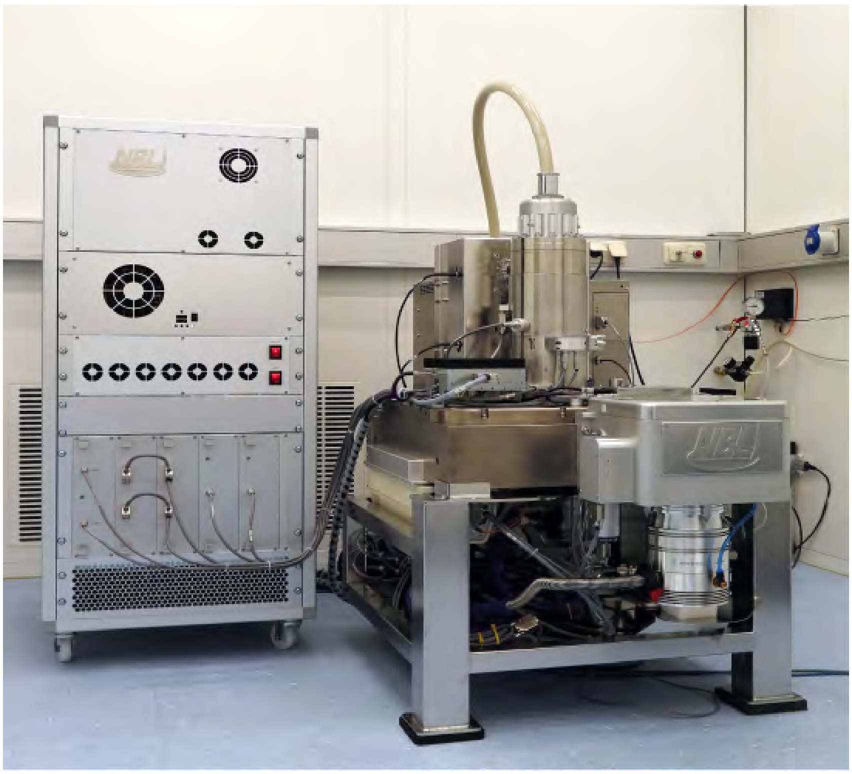

Figure 13: 100 kV Electron Beam Lithography System nB5 of NanoBeam Ltd., UK, inside the WMI cleanroom facility.

for nano-device research and production. The electron beam lithography is used for the fabrication of nanostructures in metallic and oxide systems required for the study of quantum effects in mesoscopic samples.

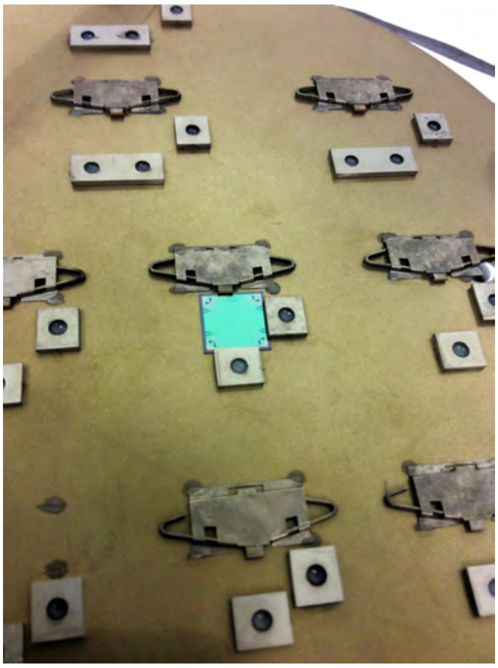

Figure 14: Chuck of the nB5 e-beam lithography system with a mounted $12 \times 12\,\mathrm{mm}^2$ silicon wafer.

The nB5 Electron Beam Lithography System employs low Coulomb-effect electron optics and sophisticated column designs to reduce beam size. The shorter optical column eliminates column bending and reduces system vibration. The modern electronics has low noise and low thermal effects. The perfectly integrated machine structure greatly improves system settling time and total stage move time. The advanced vibration tracking design enables the nB5 system to write on the fly. All these features combined with the fast deflection speed and high data processing rate make the nB5 the highest throughput system available today. Moreover, the nB5 requires undemanding cleanroom conditions, in particular regarding temperature stability, stray field magnitude, and floor vibration level.

The nB5 system is equipped with a thermal field emitter (TFE), an electrostatic lens and magnetic condenser lens, a conjugate beam blanking at $<$ 5 ns slew rate and a dual beam deflection. The latter is used to achieve ultra-high deflection speed for beam writing (clock rate: 55 MHz). The total deflection coverage is combined with the mainfield and the subfield and controlled by two independent deflection sub-systems (field size: 1000 μm, address resolution: 1 nm). The characteristic performance parameters of the electron optics of the nB5 system are: (i) beam voltage range: 20 kV to 100 kV, (ii) minimum beam current: 0.1 nA, (iii) maximum beam current: 100 nA, (iv) theoretical beam size: 2.3 nm at 100 kV, (v) guaranteed writing beam size: $<$ 5 nm at 2 nA, (vi) beam current drift: $<$ 0.5%/hour at 5 nA, (vii) beam position drift: $<$ 50 nm/hour for 3 nA beam current, including blanking, deflection and stage move.

The XY-stage allows for a traversal distance of 200 mm with a total stage move time of only 150 ms for 1 mm stage movement and a position measurement resolution of 0.3 nm using laser interferometry. The maximum substrate sizes are $2-8$ in for round substrates, $2-5$ for square glass masks up to 3 mm thickness. Finally, the nB5 system has airlock operation with automatic loading robotics with a loading cassette for 6 chucks with a maximum diameter of 8 inch.

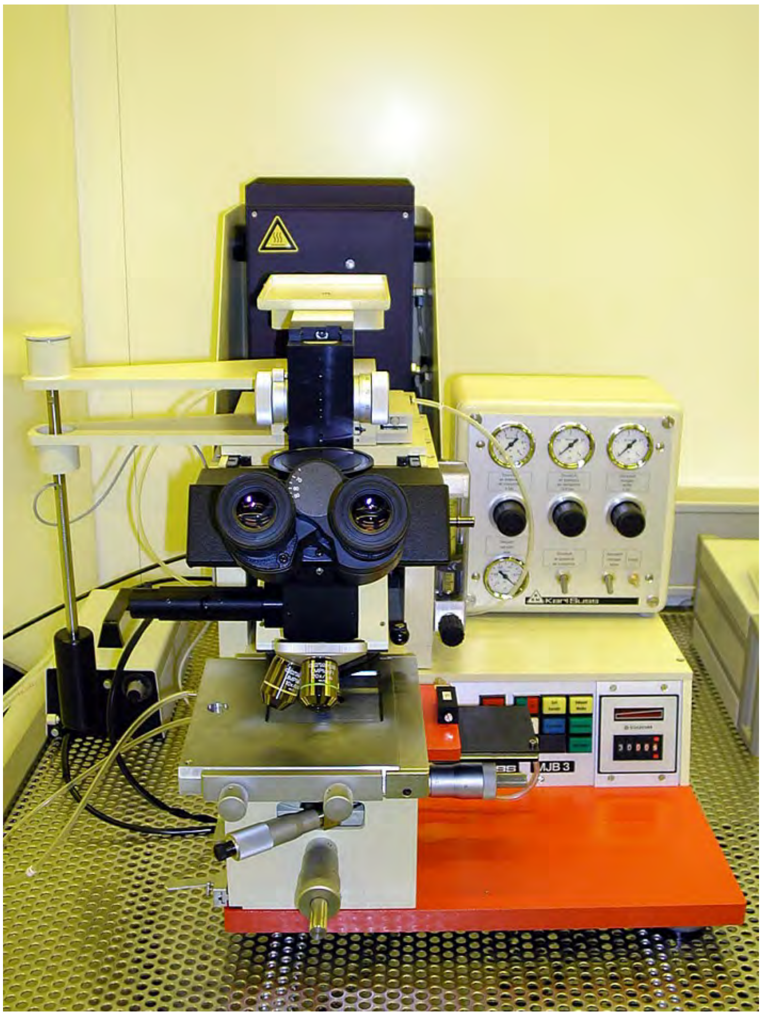

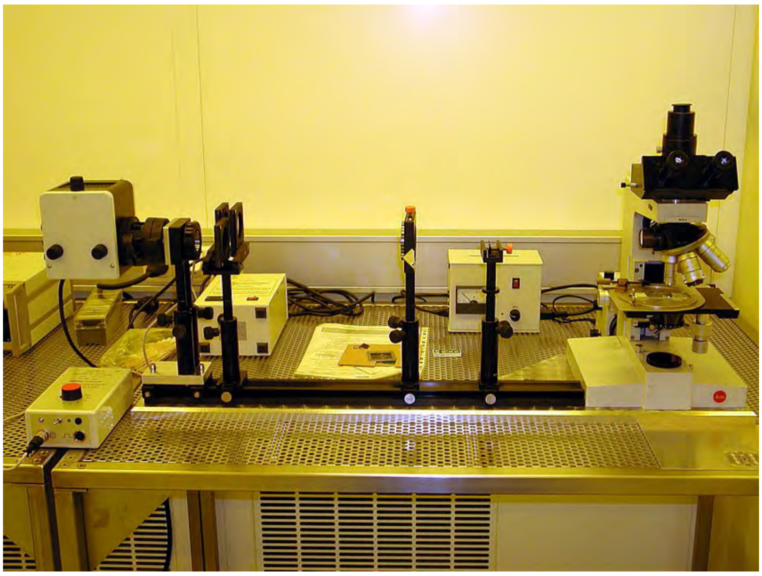

Figure 15: Top: Süss MJB 3 maskaligner for optical lithography. Bottom: Optical projection lithography based on an optical microscope.

Optical Lithography

For optical lithography, a Karl Süss MJB 3 maskaligner or an optical microscope based projection system are used. The maskaligner operates in the 1 : 1 soft or hard contact mode and uses chromium metal masks. In the projection system the mask pattern is demagnified by a factor of 5 to 100. Therefore, cheap foil masks can be used. With both systems microstructures with a lateral dimension down to 1 µm can be fabricated.

Low and Ultra-Low Temperature Facilities

At the WMI, we have constructed the first dilution refrigerator with pulse tube pre-cooling for ultra-low temperature experiments. This type of refrigerator works without cryo-liquids, and thus is a lot more practical, more economical and more reliable than cryostats with liquid helium pre-cooling. These days, all major cryo-engineering companies are offering commercial versions of this Millikelvin cooler, and these so-called "dry" refrigerators outsell conventional refrigerators by a wide margin. The general construction concept of most manufacturers is unchanged from our original prototype, where the refrigerator consists of three basic components. The first cooling stage is a commercial pulse tube cryocooler which reaches a base temperature of 2.5 K. The second stage is a Joule-Thomson stage, and the last stage is a dilution refrigeration stage, where the lowest temperature of the cryostat is about 0.01 K (Fig. 16).

Figure 16: The "dry" dilution refrigerator of the WMI.

Figure 17: Low-temperature unit of a WMI dilution refrigerator ready to go into a cryostat.

Figure 18: Two mixing chamber mounting plates with silver sponges. Those are needed to overcome the thermal resistance (Kapitza resistance) between the liquid ^{3,4}He and the mounting plate of the mixing chamber. To fabricate the mounting of the sponge (square pins embedded in the sponge) a spark erosion technique has been employed.

In many low temperature applications high refrigeration capacities are required. Our design allows for a high circulation rate of ^{3}He which in the end determines the cooling power of a dilution refrigerator. Presently our "dry" fridge reaches a refrigeration capacity of 700 µW at a temperature of the mixing chamber of 0.1 K, seven times the cooling power of the WMI nuclear demagnetization cryostat. Goals of our present work are a further increase of cooling power and a lower base temperature of the dry dilution refrigerator.

A smaller version of our cryogen-free fridge has become commercially available by *Oxford Instruments* (formerly *VeriCold Technologies, Ismaning*). It has a refrigeration capacity of 250 µW at a mixing chamber temperature of 0.1 K (Fig. 17).

The WMI also develops and fabricates dilution refrigerator inserts for temperatures down to about 20 mK. The inserts fit into all cryogenic systems (e.g. superconducting magnets) having a two inch bore. They allow fast sample change and rapid cool down cycles of less than five hours. The dilution refrigerator inserts are engineered and fabricated in-house and are also provided to other low temperature laboratories for ultra-low temperature experiments.

Millikelvin Temperatures in Combination with 3D Vector Magnetic-Fields

Figure 19: The dilution refrigerator with the 3D vector magnet located in the Quantum Laboratories.

In one room of the WMI Quantum Laboratories a cryogen-free dilution refrigerator is installed. This system is equipped with a 3D vector magnet allowing for 1 T in-plane and 6 T out-of-plane magnetic fields. Additional microwave coaxial lines allow for the microwave spectroscopy up to 18 GHz under these experimental conditions.

Scientifically, several directions in the field of fundamental light-matter interaction are envisaged:

(i) Circuit quantum electrodynamics (circuit QED), where superconducting qubits form hybrids with microwave resonators. These experiments are time consuming, because quantum effects arise in the limit of low excitation numbers. Hereby, challenging requirements are imposed on the detection systems allowing to detect microwave signals in the attowatt regime.

(ii) Storage of quantum states. One possibility is the transfer of the quantum information contained in photons to long-lived spin states. Additionally, exchange coupled systems or ferromagetic systems come into focus, because the effective coupling strength scales with the square-root of the number of spins contributing. In general, we study the light-matter interaction with long-lived spin systems and integrate them into superconducting quantum circuits.

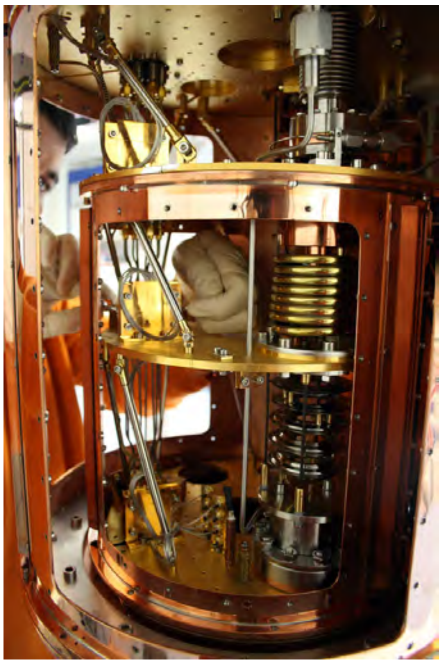

Figure 20: Inside of the dilution system. The windows of the 4 K and the still shield are removed providing access to the low temperature stages.

(iii) Spin systems. Here, our studies are not limited to paramagnetic spin systems, but also involve exchange coupled (ferro- or ferri-) magnetic systems. Hereby, magnetization damping can be investigated as a function of temperature, frequency and magnetic field direction.

(iv) Circuit electro-mechanical hybrid systems consisting of a nano-mechanical element coupled to a superconducting microwave resonator. In this context, sideband cooling of the mechanical system into its ground state and pulsed spectroscopy of hybrid system are performed and will be extended.

WMI Millikelvin Facilities for Experiments with Superconducting Quantum Circuits

The research on superconducting quantum circuits at WMI focuses mainly on systems sensitive to externally applied flux (flux qubits), circuit QED systems where flux qubits are coupled to transmission line resonators, squeezing physics in flux driven Josephson parametric amplifiers, and propagating quantum microwaves (e.g., quantum state reconstruction methods). In order to further develop our activities on quantum effects in the microwave regime, additional cryogenic capacities at millikelvin temperatures have been established. In addition to sufficient cooling power, the specifications for these cryostats are mainly dictated by the dimensions (typically a few centimeters in each direction) of bulky microwave components such as circulators or microwave switches.

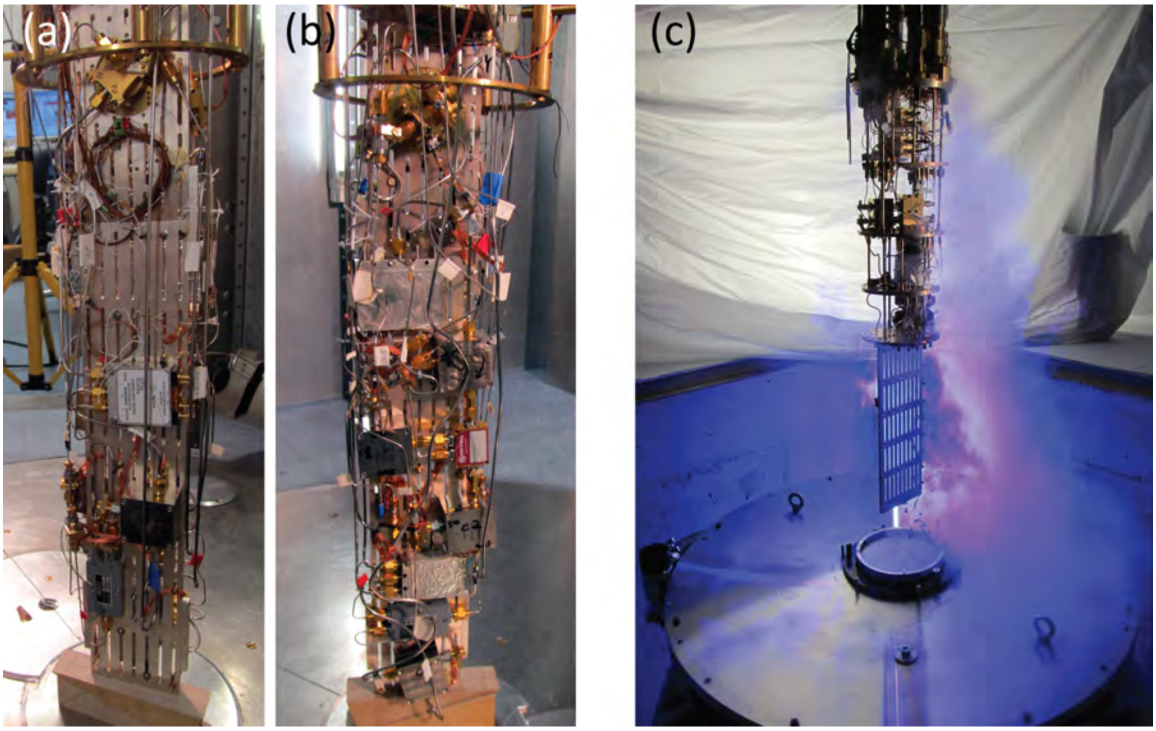

Figure 21: Liquid-helium precooled dilution refrigerators for experiments with superconducting quantum circuits. (a), (b) Back and front sides of the sample stage of the K12-refrigerator equipped with four circuit QED experiments. The height of the silver rod is 50 cm. (c) Sample stage and dewar of the dilution refrigerator in the quantum laboratory K04.

Two liquid-helium precooled dilution refrigerators are available for experiments with superconducting quantum circuits. The dilution refrigerator in laboratory K12 provides a sample space with a cylindrical volume with 11 cm diameter 55 cm height. The refrigerator is equipped with four microwave amplifiers at the 4 K-stage, seven broadband input lines and 80 twisted pair DC lines. This allows for mounting four experiments simultaneously to avoid idle times by interleaved measurements (see Fig. 21(a) and (b)). The base temperature of this refrigerator is 20 mK.

A new liquid-helium precooled dilution refrigerator for experiments with superconducting quantum circuits has been set up in the quantum laboratory K04. To provide enough space at the sample stage we have installed a Cryogenic Ltd. stainless steel dewar with a ^{4}He volume of 89 l. The time between two refills exceeds nine days. The cryostat is equipped with 16 coaxial measurement lines suitable for microwave frequencies down to the mixing chamber stage and low-noise cryogenic high electron mobility transistor (HEMT) amplifiers. Presently up to four samples can be mounted simultaneously to the sample stage. By expanding the number of input lines in the near future a more complex experiment can be set up. The cooling power of the mixing chamber at 100 mK was determined to about 140 µW.

A new cryogen-free dilution refrigerator with a pulse tube refrigerator (PTR) for precooling and with a large sample stage has been set up in room K21 of the WMI Quantum Laboratories using the longstanding experience in dry dilution refrigerators at WMI. This refrigerator features large diameters (tens of centimeters) of all temperature stages providing sufficient space for advanced quantum experiments. The main components of the refrigerator are the PTR, a 1 K-stage and a dilution unit. The two stages of the PTR cool the incoming ^{4}He and the ^{3}He/^{4}He mixture as well as one radiation shield at each stage. To provide sufficiently high cooling power near 1 K to cool microwave components and cables, this refrigerator has been equipped with a 1 K-stage operating in a closed cycle. A refrigeration capacity of the 1 K-stage of up to 100 mW could be reached. The dilution refrigerator is precooled by a dedicated ^{4}He circuit. The minimum base temperature of the refrigerator is below 11 mK. The cooling power at 100 mK was determined to about 300 μW at the maximum ^{3}He flow rate.

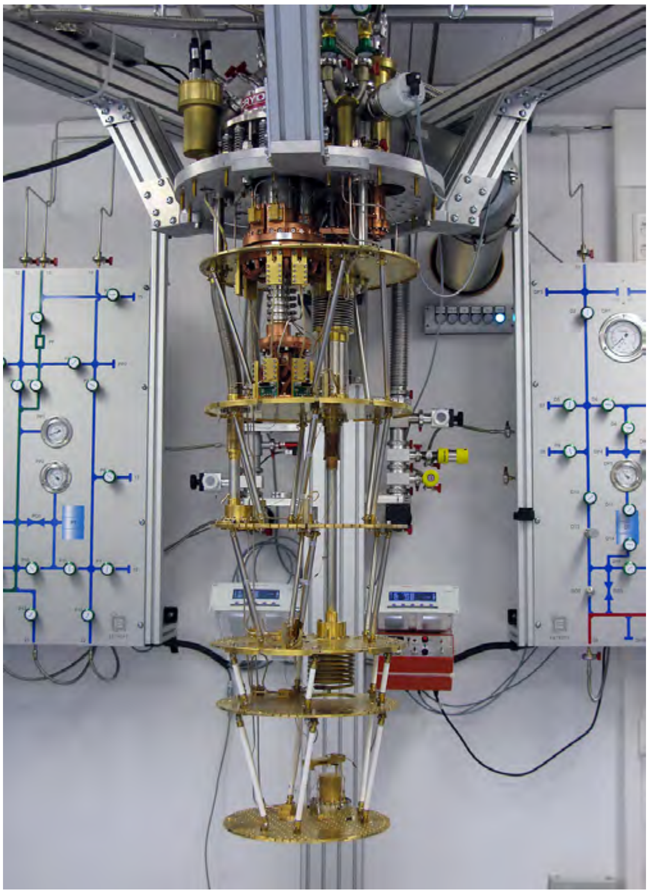

Figure 22: Dry dilution refrigerator with a large sample space.

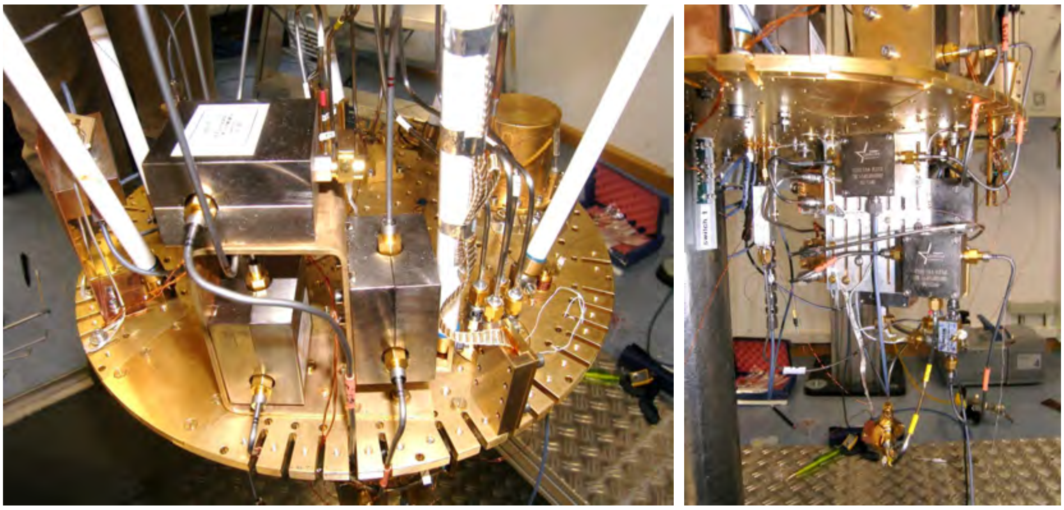

Figure 23: Low temperature platform of K21 dilution refrigerator with experimental setup for circuit QED experiments.

Statistics

Publications

1. **Anomalous Hall effect in YIG | Pt bilayers**
Sibylle Meyer, Richard Schlitz, Stephan Geprägs, Matthias Opel, Hans Huebl, Rudolf Gross, Sebastian T. B. Goennenwein
Appl. Phys. Lett. **106**, 132402 (2015).

2. **Sign of inverse spin Hall voltages generated by ferromagnetic resonance and temperature gradients in yttrium iron garnet | platinum bilayers**
Michael Schreier, Gerrit E. W. Bauer, Vitaliy Vasyuchka, Joost Flipse, Ken-ichi Uchida, Johannes Lotze, Viktor Lauer, Andrii Chumak, Alexander Serga, Shunsuke Daimon, Takashi Kikkawa, Eiji Saitoh, Bart J. van Wees, Burkard Hillebrands, Rudolf Gross, Sebastian T. B. Goennenwein
Phys. D: Appl. Phys. **48**, 025001 (2015).

3. **Tunable and Switchable Coupling Between Two Superconducting Resonators**
A. Baust, E. Hoffmann, M. Haeberlein, M. J. Schwarz, P. Eder, E. P. Menzel, K. Fedorov, J. Goetz, F. Wulschner, E. Xie, L. Zhong, F. Quijandria, B. Peropadre, D. Zueco, J.-J. Garcia Ripoll, E. Solano, F. Deppe, A. Marx, R. Gross
Phys. Rev. B **91**, 014515 (2015).

4. **Quantum State Engineering with Circuit Electromechanical Three-Body Interactions**
Mehdi Abdi, Matthias Pernpeintner, Rudolf Gross, Hans Huebl, Michael J. Hartmann
Phys. Rev. Lett. **114**, 173602 (2015).

5. **Single Crystal Growth of the High Temperature Superconducting Cuprates**
Andreas Erb
Applied Superconductivity: Handbook on Devices and Applications, vol. 2, editor Paul Seidel, Wiley-VCH (2015), pp. 222-246.

6. **Low-Temperature Scintillation Properties of $CaWO_4$ Crystals for Rare-Event Searches**
M. v. Sivers, M. Clark, P.C.F. Di Stefano, A. Erb, A. Gütlein, J.-C. Lanfranchi, A. Münster, P. Nadeau, M. Piquemal, W. Potzel, S. Roth, K. Schreiner, R. Strauss, S. Wawoczny, M. Willers, A. Zöller
J. Appl. Phys. **118**, 164505 (2015).

7. **Spin Pumping**
M. Althammer, M. Weiler, H. Huebl, S.T.B. Gönnenwein in Spintronics for Next Generation Innovative Devices, Katsuaki Sato (Editor), Eiji Saitoh (Editor), Arthur Willoughby (Series Editor), Peter Capper (Series Editor), Safa Kasap (Series Editor), Wiley Series in Materials for Electronics and Optoelectronic Applications, Wiley, Chichester UK (2015), ISBN: 978-1-118-75191-6.

8. **Exchange magnon-polaritons in microwave cavities**
Yunshan Cao, Peng Yan, Hans Huebl, Sebastian T.B. Goennenwein, Gerrit E.W. Bauer
Physical Review B **91**, 094423 (2015).

9. **Pulsed Low-Field Electrically Detected Magnetic Resonance**
L. Dreher, F. Hoehne, H. Morishita, H. Huebl, M. Stutzmann, K. M. Itoh, M. S. Brandt
Physical Review B **91**, 075314 (2015).

10. **Ultrafast Electronic Read-Out of Diamond NV Centers Coupled to Graphene**
Andreas Brenneis, Louis Gaudreau, Max Seifert, Helmut Karl, Martin S. Brandt, Hans Huebl, Jose A. Garrido, Frank H.L. Koppens, Alexander W. Holleitner
Nature Nanotechnology **10**, 135 (2015).

11. **Dry dilution refrigerator with ^{4}He-1K-loop**
K. Uhlig
Cryogenics **66**, 6-12 (2015).

12. **Dry Dilution Refrigerator for Experiments on Quantum Effects in the Microwave Regime**
A. Marx, J. Hoess, K. Uhlig
Cryocoolers **18**, 481 (2015).

13. **Towards on-chip generation, routing, and detection of non-classical light**
F. Flassig, M. Kaniber, G. Reithmaier, K. Mueller, A. Andrejew, R. Gross, J. Vuckovic, J. Finley

Proc. of SPIE **9373**, 937305 (2015).

14. **Arrangement of Maghemite Nanoparticles via Wet Chemical Self-Assembly in PS-b-PNIPAM Diblock Copolymer Films**
Yuan Yao, Ezzeldin Metwalli, Volker Körstgens, Daniel Moseguí González, Anna Miasnikova, Andre Laschewsky, Matthias Opel, Gonzalo Santoro, Stephan V. Roth, Peter Müller-Buschbaum
ACS Appl. Mater. Interfaces **7**, 13080-13091 (2015).

15. **Signatures of nematic quantum critical fluctuations in the Raman spectra of lightly doped cuprates**
S. Caprara, M. Colonna, C. Di Castro, R. Hackl, B. Muschler, L. Tassini, and M. Grilli
Phys. Rev. B **91**, 205115 (2015).

16. **On-chip generation, routing and detection of quantum light**
Günther Reithmaier, Michael Kaniber, Fabian Flassig, Stefan Lichtmannecker, Kai Müller, Alexander Andrejew, Jelena Vuckovic, Rudolf Gross, Jonathan Finley
Nano Letters **15**(8), 5208–5213 (2015).

17. **Scanning Probe Microscopy in an Ultra-Low Vibration Closed-Cycle Cryostat: Skyrmion Lattice Detection and Tuning Fork Implementation**
Francesca Paola Quacquarelli, Jorge Puebla, Thomas Scheler, Dieter Andres, Christoph Bödefeld, Balazs Sipos, Claudio Dal Savio, Andreas Bauer, Christian Pfleiderer, Andreas Erb, Khaled Karrai
Microscopy Today **23**, 12-17 (2015).

18. **Torque differential magnetometry using quartz tuning forks**
Akashdeep Kamra, Stefan von Hoesslin, Niklas Roschewsky, Johannes Lotze, Michael Schreier, Rudolf Gross, Sebastian T. B. Goennenwein, Hans Huebl
Eur. Phys. J. B **88**, 224 (2015).

19. **Correlation between Fermi surface transformations and superconductivity in the electron-doped high-T_c superconductor $Nd_{2-x}Ce_xCuO_4$**
T. Helm, M. V. Kartsovnik, C. Proust, B. Vignolle, C. Putzke, E. Kampert, I. Sheikin, E.-S. Choi, J. S. Brooks, N. Bittner, W. Biberacher, A. Erb, J. Wosnitza, R. Gross
Phys. Rev. B **92**, 094501 (2015).

20. **Spin pumping in YIG/Pt bilayers as a function of layer thickness**
M. Haertinger, C. H. Back, J. Lotze, M. Weiler, S. Geprägs, H. Huebl, S. T. B. Goennenwein, and G. Woltersdorf
Phys. Rev. B **92**, 054437 (2015).

21. **Radiative damping in waveguide-based ferromagnetic resonance measured via analysis of perpendicular standing spin waves in sputtered permalloy films**
M. A. W. Schoen, J. M. Shaw, H. T. Nembach, M. Weiler, and T. J. Silva
Phys. Rev. B **92**, 184417 (2015).

22. **Perpendicular Magnetic Anisotropy and Easy Cone State in $Ta/Co_{60}Fe_{20}B_{20}/MgO$**
J. M. Shaw, H. T. Nembach, M. Weiler, T. J. Silva, M. Schoen, J. Z. Sun, and D. C. Worledge
IEEE Magnetics Letters **6**, 1 (2015).

23. **Impact of Coherent Neutrino Nucleus Scattering on Direct Dark Matter Searches based on $CaWO_4$ Crystals**
A. Gütlein, G. Angloher, A. Bento, C. Bucci, L. Canonica, A. Erb, F. v. Feilitzsch, N. Ferreiro Iachellini, P. Gorla, D. Hauff, J. Jochum, M. Kiefer, H. Kluck, H. Kraus, J.-C. Lanfranchi, J. Loebell, A. Münster, F. Petricca, W. Potzel, F. Pröbst, F. Reindl, S. Roth, K. Rottler, C. Sailer, K. Schäffner, J. Schieck, S. Schönert, W. Seidel, M. v. Sivers, L. Stodolsky, C. Strandhagen, R. Strauss, A. Tanzke, M. Uffinger, A. Ulrich, I. Usherov, S. Wawoczny, M. Willers, M. Wüstrich, A. Zöller
Astroparticle Physics **69**, 44-49 (2015).

24. **Longitudinal spin Seebeck effect contribution in transverse spin Seebeck effect experiments in Pt/YIG and Pt/NFO**
Daniel Meier, Daniel Reinhardt, Michael van Straaten, Christoph Klewe, Matthias Althammer, Michael Schreier, Sebastian T. B. Goennenwein, Arunava Gupta, Maximilian Schmid, Christian H. Back, Jan-Michael Schmalhorst, Timo Kuschel, Günter Reiss

Nature Communications **6**, 8211 (2015).

25. **Electrical signal picks up a magnet's heartbeat**
Hans Huebl, Sebastian T.B. Gönnenwein
Physics **8**, 51 (2015).

26. **Junction size dependence of ferroelectric properties in e-beam patterned $BaTiO_3$ ferroelectric tunnel junctions**
A. V. Singh, M. Althammer, K. Rott, G. Reiss, and A. Gupta
Applied Physics Letters **107**, 122903 (2015).

27. **Study of structural and ferromagnetic resonance properties of spinel lithium ferrite ($LiFe_5O_8$) single crystals**
N. Pachauri, B. Khodadadi, M. Althammer, A. V. Singh, B. Loukya, R. Datta, M. Iliev, T. Mewes, and A. Gupta
Journal of Applied Physics **117**, 233907 (2015).

28. **Electron/gamma and alpha backgrounds in CRESST-II Phase 2**
R. Strauss, G. Angloher, A. Bento, C. Bucci, L. Canonica, A. Erb, F. v. Feilitzsch, N. Ferreiro Iachellini, P. Gorla, A. Gütlein, D. Hauff, J. Jochum, M. Kiefer, H. Kluck, H. Kraus, J.-C. Lanfranchi, J. Loebell, A. Münster, F. Petricca, W. Potzel, F. Pröbst, F. Reindl, S. Roth, K. Rottler, C. Sailer, K. Schäffner, J. Schieck, S. Scholl, S. Schönert, W. Seidel, M. v. Sivers, L. Stodolsky, C. Strandhagen, A. Tanzke, M. Uffinger, A. Ulrich, I. Usherov, S. Wawoczny, M. Willers, M. Wüstrich, A. Zöller
Journal of Cosmology and Astroparticle Physics vol. **2015** (6), (2015).

29. **Current-induced spin torque resonance of a magnetic insulator**
Michael Schreier, Takahiro Chiba, Arthur Niedermayr, Johannes Lotze, Hans Huebl, Stephan Geprägs, Saburo Takahashi, Gerrit E. W. Bauer, Rudolf Gross, Sebastian T. B. Goennenwein
Phys. Rev. B **92**, 144411 (2015).

30. **Manifestation of nematic degrees of freedom in the Raman response function of iron pnictides**
Una Karahasanovic, Florian Kretzschmar, Thomas Boehm, Rudi Hackl, Indranil Paul, Yann Gallais, Joerg Schmalian
Phys. Rev. B **92**, 075134 (2015).

31. **High cooperativity coupling between a phosphorus donor spin ensemble and a superconducting microwave resonator**
Christoph W. Zollitsch, Kai Mueller, David P. Franke, Sebastian T. B. Goennenwein, Martin S. Brandt, Rudolf Gross, Hans Huebl
Appl. Phys. Lett. **107**, 142105 (2015).

32. **Leggett Modes and the Anderson-Higgs Mechanism in Superconductors without Inversion Symmetry**
Nikolaj Bittner, Dietrich Einzel, Ludwig Klam, and Dirk Manske
Phys. Rev. Lett. **115**, 227002 (2015).

33. **Antiferromagnetic fluctuations in the quasi-two-dimensional organic superconductor detected by Raman spectroscopy**
N. Drichko, R. Hackl, J. A. Schlueter
Phys. Rev. B **92**, 161112(R) (2015).

34. **Non-local magnetoresistance in YIG/Pt nanostructures**
Sebastian T.B. Goennenwein, Richard Schlitz, Matthias Pernpeintner, Matthias Althammer, Rudolf Gross, Hans Huebl
Appl. Phys. Lett. **107**, 172405 (2015).

35. **Supraleitung unter Hochdruck**
R. Hackl, B. Büchner
Physik Journal **14** (11), 22-23 (2015).

36. **A detector module with highly efficient surface-alpha event rejection operated in CRESST-II Phase 2**

R. Strauss, G. Angloher, A. Bento, C. Bucci, L. Canonica, A. Erb, F. v. Feilitzsch, N. Ferreiro, P. Gorla, A. Gütlein, D. Hauff, J. Jochum, M. Kiefer, H. Kluck, H. Kraus, J.-C. Lanfranchi, J. Loebell, A. Münster, F. Petricca, W. Potzel, F. Pröbst, F. Reindl, S. Roth, K. Rottler, C. Sailer, K. Schäffner, J. Schieck, S. Scholl, S. Schönert, W. Seidel, M. v. Sivers, M. Stanger, L. Stodolsky, C. Strandhagen, A. Tanzke, M. Uffinger, A. Ulrich, I. Usherov, S. Wawoczny, M. Willers, M Wüstrich, A. Zöller
Eur. Phys. J. C **75**, 352 (2015).

37. **Antiferromagentic resonance detected by DC voltages in MnF_2/Pt bilayers**
Philipp Ross, Michael Schreier, Johannes Lotze, Hans Huebl, Rudolf Gross, Sebastian T. B. Goennenwein
J. Appl. Phys. **118**, 233907 (2015).

38. **Focus on cavity and circuit quantum electrodynamics in solids**
Yasuhiko Arakawa, Jonathan Finley, Rudolf Gross, Fabrice Laussy, Enrique Solano, Jelena Vuckovic
New J. Phys. **17**, 010201 (2015).

39. **Quantum teleportation of propagating quantum microwaves**
R. Di Candia, K. G. Fedorov, L. Zhong, S. Felicetti, E. P. Menzel, M. Sanz, F. Deppe, A. Marx, R. Gross, E. Solano
EPJ Quantum Technology **2**, 25 (2015).

40. **Origin of the spin Seebeck effect probed by temperature dependent measurements in $Gd_3Fe_5O_{12}$**
Stephan Geprägs, Andreas Kehlberger, Tomek Schulz, Christian Mix, Francesco Della Coletta, Sibylle Meyer, Akashdeep Kamra, Matthias Althammer, Gerhard Jakob, Hans Huebl, Rudolf Gross, Sebastian T.B. Goennenwein, Mathias Kläui
Nature Communications, accepted for publication (2015).

41. **Bosons and Fermions**
B. S. Chandrasekhar, Deccan Herald, School Edition, Bangalore (2015).

42. **Dark Matter and Dark Energy**
B. S. Chandrasekhar, Deccan Herald, School Edition, Bangalore (2015).

43. **LIGO**
B. S. Chandrasekhar, Deccan Herald, School Edition, Bangalore (2015).

44. **Superconductors, Superfluids**
B. S. Chandrasekhar, Deccan Herald, School Edition, Bangalore (2015).

45. **Precision Measurements of Light Quenching in $CaWO_4$ Crystals at mK Temperatures**
R. Strauss, G. Angloher, A. Bento, C. Bucci, L. Canonica, A. Erb, F. v. Feilitzsch, P. Gorla, A. Gütlein, D. Hauff, J. Jochum, H. Kraus, J.-C. Lanfranchi, J. Loebell, A. Münster, F. Petricca, W. Potzel, F. Pröbst, F. Reindl, S. Roth, K. Rottler, C. Sailer, K. Schäffner4 J. Schieck, S. Scholl, S. Schönert, W. Seidel, M. v. Sivers, L. Stodolsky, C. Strandhagen, A. Tanzke, M. Uffinger, A. Ulrich, I. Usherov, S. Wawoczny, M. Willers, M. Wüstrich, A. Zöller, W. Carli, C. Ciemniak, H. Hagn, D. Hellgartner
Eur. Phys. J. C **74**, 2957 (2014).

46. **Glassiness induced by charge stripe order in 1/8-doped lanthanum cuprates**
S.-H. Baek, M. Hücker, A. Erb, G. D. Gu, B. Büchner, H.-J. Grafe
arXiv:1402.3077, submitted for publication (2014).

47. **Ultrastrong coupling in two-resonator circuit QED**
A. Baust, E. Hoffmann, M. Haeberlein, M. J. Schwarz, P. Eder, J. Goetz, F. Wulschner, E. Xie, L. Zhong, F. Quijandria, D. Zueco, J.-J. Garcia Ripoll, L. Garcia-Alvarez, G. Romero, E. Solano, K. G. Fedorov, E. P. Menzel, F. Deppe, A. Marx, R. Gross
arXiv:1412.7372, submitted for publication (2014).

48. **Probing Low WIMP Masses with the Next Generation of CRESST Detector**
The CRESST Collaboration: G. Angloher, A. Bento, C. Bucci, L. Canonica, A. Erb, F. v.Feilitzsch, N. Ferreiro Iachellini, P. Gorla, A. Gütlein, D. Hauff, J. Jochum, M. Kiefer, H. Kluck, H. Kraus, J.-C. Lanfranchi, J. Loebell, A. Münster, F. Petricca, W. Potzel, F. Pröbst, F. Reindl, K. Schäffner, J.

Schieck, S. Scholl, S. Schönert, W. Seidel, L. Stodolsky, C. Strandhagen, R. Strauss, A. Tanzke, M. Uffinger, A. Ulrich, I. Usherov, S. Wawoczny, M. Willers, M. Wüstrich, A. Zöller
arXiv:1503.08065, submitted for publication (2015).

49. **In-Situ Performance Characterization of CRESST Detector Modules**
The CRESST Collaboration: M. Kiefer, G. Angloher, A. Bento, C. Bucci, L. Canonica, A. Erb, F. v. Feilitzsch, N. Ferreiro Iachellini, P. Gorla, A. Gütlein, D. Hauff, J. Jochum, H. Kluck, H. Kraus, J.-C. Lanfranchi, J. Loebell, A. Münster, F. Petricca, W. Potzel, F. Pröbst, F. Reindl, S. Roth, K. Rottler, C. Sailer, K. Schäffner, J. Schieck, S. Schönert, W. Seidel, M. v. Sivers, L. Stodolsky, C. Strandhagen, R. Strauss, A. Tanzke, M. Uffinger, A. Ulrich, I. Usherov, S. Wawoczny, M. Willers, M. Wüstrich, A. Zöller
arXiv:1503.07806, submitted for publication (2015).

50. **Spin-boson model with an engineered reservoir in circuit quantum electrodynamics**
Max Haeberlein, Frank Deppe, Andreas Kurcz, Jan Goetz, Alexander Baust, Peter Eder, Kirill Fedorov, Michael Fischer, Edwin P. Menzel, Manuel J. Schwarz, Friedrich Wulschner, Edwar Xie, Ling Zhong, Enrique Solano, Achim Marx, Juan-José García-Ripoll, Rudolf Gross
arXiv:1506.09114, submitted for publication (2015).

51. **New twist on the vortex-core tunneling spectroscopy in $YBa_2Cu_3O_{7-\delta}$**
Jens Bruér, Ivan Maggio-Aprile, Nathan Jenkins, Andreas Erb, Christophe Berthod, Øystein Fischer, Christoph Renner
arXiv:1507.06775, submitted for publication (2015).

52. **Nematic fluctuations and the magneto-structural phase transition in $Ba(Fe_{1-x}Co_x)_2As_2$**
F. Kretzschmar, T. Böhm, U. Karahasanovic, B. Muschler, A. Baum, D. Jost, J. Schmalian, S. Caprara, M. Grilli, C. Di Castro, J. G. Analytis, J.-H. Chu, I. R. Fisher, R. Hackl
arXiv:1507.06116, submitted for publication (2015).

53. **Theory of spin Hall magnetoresistance (SMR) and related phenomena**
Y. T. Chen, S. Takahashi, H. Nakayama, M. Althammer, S. T. B. Goennenwein, E. Saitoh, and G. E. W. Bauer
arXiv:1507.06054, submitted for publication (2015).

54. **Tunable coupling of transmission-line microwave resonators mediated by an rf SQUID**
F. Wulschner, J. Goetz, F. R. Koessel, E. Hoffmann, A. Baust, P. Eder, M. Fischer, M. Haeberlein, M. J. Schwarz, M. Pernpeintner, E. Xie, L. Zhong, C. W. Zollitsch, B. Peropadre, J.-J. Garcia Ripoll, E. Solano, K. Fedorov, E. P. Menzel, F. Deppe, A. Marx, R. Gross
arXiv:1508.06758, submitted for publication (2015).

55. **A universal platform for magnetostriction measurements in thin films**
Matthias Pernpeintner, Rasmus B. Holländer, Maximilian J. Seitner, Eva M. Weig, Rudolf Gross, Sebastian T. B. Goennenwein, Hans Huebl
arXiv:1509.00647, submitted for publication (2015).

56. **Results on Light Dark Matter Particles with a Low-Threshold Cresst-II Detector**
The CRESST Collaboration: G. Angloher, A. Bento, C. Bucci, L. Canonica, X. Defay, A. Erb, F. v. Feilitzsch, N. Ferreiro Iachellini, P. Gorla, A. Gütlein, D. Hauff, J. Jochum, M. Kiefer, H. Kluck, H. Kraus, J. C. Lanfranchi, J. Loebell, A. Münster, C. Pagliarone, F. Petricca, W. Potzel, F. Pröbst, F. Reindl, K. Schäffner, J. Schieck, S. Schönert, W. Seidel, L. Stodolsky, C. Strandhagen, R. Strauss, A. Tanzke, H.H. Trinh Thi, C. TürkoÄ§lu, M. Uffinger, A. Ulrich, I. Usherov, S. Wawoczny, M. Willers, M. Wüstrich, A. Zöller
arXiv:1509.01515, submitted for publication (2015).

57. **The CRESST Dark Matter Search - Status and Perspectives**
The CRESST Collaboration: F. Reindl, G. Angloher, A. Bento, C. Bucci, L. Canonica, X. Defay, A. Erb, F. v. Feilitzsch, N. Ferreiro Iachellini, P. Gorla, A. Gütlein, D. Hauff, J. Jochum, M. Kiefer, H. Kluck, H. Kraus, J. C. Lanfranchi, J. Loebell, A. Münster, C. Pagliarone, F. Petricca, W. Potzel, F. Pröbst, K. Schäffner, J. Schieck, S. Schönert, W. Seidel, L. Stodolsky, C. Strandhagen, R. Strauss, A. Tanzke, H.H. Trinh Thi, C. TürkoÄ§lu, M. Uffinger, A. Ulrich, I. Usherov, S. Wawoczny, M. Willers, M. Wüstrich, A. Zöller
arXiv:1509.09124, submitted for publication (2015).

58. **Loss mechanisms in superconducting thin film microwave resonators**
Jan Goetz, Frank Deppe, Max Haeberlein, Friedrich Wulschner, Christoph W. Zollitsch, Sebastian Meier, Michael Fischer, Peter Eder, Edwar Xie, Kirill G. Fedorov, Edwin P. Menzel, Achim Marx, Rudolf Gross
arXiv:1510.05957, submitted for publication (2015).

The accompanying diagram shows the development of the total number of citations per year of papers published by members of WMI since 1996. This number has about tripled within the last fifteen years and is exceeding 1800 in 2015.

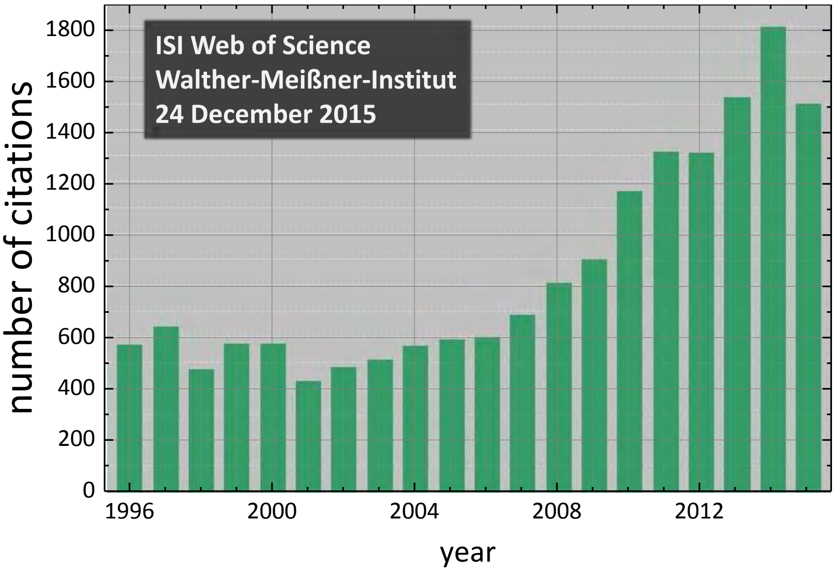

Completed and Ongoing Ph.D. Theses

Completed Ph.D. Theses:

1. **Gradiometric Tunable-Gap Flux Qubits in a Circuit QED Architecture**
   Manuel Schwarz, TU München, Januar 2015.
2. **Tunable Coupling and Ultrastrong Interaction in Circuit Quantum Electrodynamics**
   Alexander Theodor Baust, TU München, Juni 2015.
3. **Spin Pumping in Ferrimagnet/Normal Metal Bilayers**
   Johannes Lotze, TU München, Juli 2015.
4. **Generation and Reconstruction of Propagating Quantum Microwaves**
   Ling Zhong, TU München, August 2015.
5. **Nematic Fluctuations, Fermiology and the Pair Breaking Potential in Iron-Based Superconductors**
   Florian Kretschmar, TU München, August 2015.
6. **Spin Caloritronics in Ferromagnet/Normal Metal Hybrid Structures**
   Sybille Meyer, TU München, Dezember 2015.

The six Ph.D. students of the Walther-Meißner-Institute finishing their Ph.D. theses in 2015.

Ongoing Ph.D. Theses:

7. **All Optical Quantum Computing**
   Max Häberlein, TU München, seit Dezember 2009.
8. **Vibrational Investigations of Luminescence Molecules**
   Nitin Chelwani, TU München, seit September 2010.

9. **Superconducting Quantum Circuits for Qunatum Electrodynamics Experiments**
   Karl Friedrich Wulschner, TU München, seit Januar 2012.
10. **Circuit Quantum Electrodynamics Experiments with Tunable Flux Qubits**
    Jan Goetz, TU München, seit Januar 2012.
11. **Single Excitation Transfer in the Quantum Regime: A Spin-Based Solid State Approach**
    Christoph Zollitsch, TU München, seit Januar 2012.
12. **Untersuchung der verschiedenen Phasen eisenbasierter Supraleiter mittels Raman-Streuung**
    Andreas Baum, TU München, seit April 2012.
13. **Superconducting Properties of Organic Metals in the Vicinity of Ordering Instabilities**
    Michael Kunz, TU München, seit August 2012.
14. **Quantum Information Processing with Propagating Quantum Microwaves**
    Peter Eder, TU München, seit November 2012.
15. **Coupled Electro-Nanomechanical Systems**
    Matthias Pernpeintner, TU München, seit November 2012.
16. **Spin Transport in Ferrromagnetic Microsturctures**
    Michael Schreier, TU München, seit Dezember 2012.
17. **Spin dynamics and spin transport in solid state systems**
    Hannes Maier-Flaig, TU München, seit November 2013.
18. **A Comparative Study of the Phase Diagrams of CuO_2 and Fe-based Compounds**
    Thomas Böhm, TU München, seit Dezember 2013.
19. **Circuit Quantum Electrodynamics with Three-dimensional Cavities**
    Edwar Xie, TU München, seit Dezember 2013.
20. **Spin Currents in Ferrimagnetic Materials**
    Kathrin Ganzhorn, TU München, seit Dezember 2014.
21. **Chains of Nonlinear and Tunable Superconducting Resonators**
    Michael Fischer, seit Januar 2015.
22. **Magnetization Dynamics in Coupled Photon/Phonon-Magnon Systems**
    Stefan Klingler, seit Februar 2015.
23. **Nanomechanical Quantum Systems**
    Philip Schmidt, seit Oktober 2015.
24. **Magnetic Resonance at Millikelvin Temperatures**
    Stefan Weichselbaumer, seit Dezember 2015.

Completed and Ongoing Bachelor and Master Theses

Completed Master Theses:

1. **Quantenelektrodynamik supraleitender Schaltkreise am Beispiel eines Transmon-Qubits / Circuit quantum electrodynamics with transmon qubits**
   Javier Puertas Martínez, Masterarbeit, TU München, Februar 2015.
2. **Circuit Quantum Electrodynamics with a Transmon Qubit in a 3D Cavity**
   Gustav Andersson, Masterarbeit, TU München, März 2014.
3. **Untersuchung der Dotierungsabhängigkeit der Wechselwirkungspotentiale von $Ba_{1-x}K_xFe_2As_2$ / Analysis of the doping dependence of the interaction potentials of $Ba_{1-x}K_xFe_2As_2$**
   Michael Rehm, Masterarbeit, TU München, März 2015.
4. **Weiterentwicklung eines Schärfemessverfahrens für Kameras mit Fischaugenobjektiven / Further Developement of sharpness measurements for cameras using fish eye lenses**
   Marc Andreas Schneider, TU München, April 2015.
5. **Charakterisierung von Hochleistungspermanentmagneten für elektrische Antriebe**
   Michael Tillinger, Diplomarbeit, TU München, Mai 2015.
6. **Spin Seebeck Effect in Rare Earth Iron Garnets**
   Francesco Della Coletta, Masterarbeit, TU München, Mai 2015.
7. **Inductive Switchable Cavity Electromechanics**
   Philipp Schmidt, Masterarbeit, TU München, Juni 2015.
8. **Fabrication Stability of Josephson Junctions for Superconducting Qubits**
   Lujun Wang, Masterarbeit, TU München, seit Mai 2014.
9. **Magnetresonanzspektroskopie mit zirkularpolarisierter Mikrowellenanregung / Circularly polarized microwaves for magnetic resonance experiments**
   Sho Watanabe, Masterarbeit, TU München, August 2015.
10. **Zeitaufgelöste Spin-Seebeck-Effekt-Messungen / Time-Resolved Spin Seebeck Effect Experiments**
    Franz-Georg Kramer, Masterarbeit, TU München, August 2015.
11. **Tip-Enhanced Raman Spectroscopy**
    David Hoch, Masterarbeit, TU München, September 2015.
12. **Displacement of Squeezed Propagating Microwave States**
    Stefan Pogorzalek, Masterarbeit, TU München, Oktober 2015.
13. **Time Domain Characterization of a Transmon Qubit**
    Miriam Müting, Masterarbeit, TU München, Oktober 2015.
14. **Charakterisierung von hysteretischen flussgetriebenen parametrischen Josephson-Verstärkern / Characterization of hysteretic flux-driven Josephson parametric amplifier**
    Martin Betzenbichler, Masterarbeit, TU München, Oktober 2015.
15. **Spin-Hall-Magnetwiderstand in Bilagen aus Normal-Metallen und kompensierten Seltenerd-Eisengranaten / Spin Hall Magnetoresistance in Normal Metal | Compensated Rare Earth Iron Garnet Bilayers**
    Michaela Lammel, Masterarbeit, TU München, November 2015.
16. **Spin Transport Experiments in Hybrid Nanostructures**
    Richard Schlitz, Masterarbeit, TU München, November 2015.

Completed Bachelor Theses:

17. **Optische Interferometrie spinmechanischer Nanostrukturen**
Lisa Rosenzweig, Bachelorarbeit, TU München (2015).

18. **Shubnikov-de Haas Oszillationen in dem Organischen Supraleiter κ-(ET)$_2$Cu[N(CN)$_2$]Cl nahe des Mott-Isolator-Übergangs / Shubnikov-de Haas Oscillations in the Organic Superconductor κ-(ET)$_2$Cu[N(CN)$_2$]Cl near the Mott-Insulating Transition**
Sebastian Oberbauer, Bachelorarbeit, TU München (2015).

19. **Herstellung und Spin Hall Magnetwiderstand von Pt|$ErFeO_3$ Bilagen / Fabrication and Spin Hall Magnetorestistance of Pt|$ErFeO_3$ bilayers**
Sarah Gelder, Bachelorarbeit, TU München (2015).

20. **Aufbau für breitbandige ferromagnetische Resonanz / Broadband Ferromagnetic Resonance Setup**
Johannes Küchle, Bachelorarbeit, TU München (2015).

21. **Aufbau eines Freistrahl-Interferometers zur Untersuchung nanomechanischer Resonatoren im Magnetfeld / Free space interferometry stage for nano-mechanics experiments**
Peter Joerg, Bachelorarbeit, TU München (2015).

22. **Rekonstruktion von lokalisierten und sich ausbreitenden Mikrowellenzuständen / Reconstruction of Propagating and Confined Microwave States**
Daniel Arweiler, Bachelorarbeit, TU München (2015).

23. **Hohlraumresonator- und Qubitdesign für dreidimensionale Schaltkreisquantenelektrodynamik / Cavity and Qubit Design for 3D Circuit QED**
Jonas Lederer, Bachelorarbeit, TU München (2015).

24. **Untersuchung des Wärmehaushalts an Strukturen mit ungünstiger Wärmeableitung bei Additive Manufacturing / Investigation of the thermal balance at structures with less favorable heat dissipation at addictive manufacturing**
Markus Full, Bachelorarbeit, TU München (2015).

25. **Grundlegende Betrachtung der Eigenschaften verschiedener Linsentypen für LWL-Steckverbinder**
Stefanie Blob, Bachelorarbeit, TU München (2015).

26. **Aufbau eines Messstabs für winkelaufgelöste Magnetotransportmessungen**
Claudio De Rose, Bachelorarbeit, TU München (2015).

Ongoing Master Theses:

27. **Untersuchung nematischer Fluktuationen in FeAs**
Daniel Jost, seit Januar 2015.

28. **Superconductivity versus Charge Density Wave in the Organic Metal α-(BEDT-TTF)$_2$TlHg(SCN)$_4$**
Luzia Höhlein, Masterarbeit, seit November 2014.

29. **Ladungsbasierte Messung von ultrafeinen Partikeln und Nanopartikeln in Verbrennungsmotorabgasen / Charge-based Measurement of Ultrafine- and Nano-Particles in Combustion Engine Exhaust**
Philipp Link, Masterarbeit, TU München, seit Februar 2015.

30. **Breitbandspektroskopie von magnetischen Dünnfilmen bei tiefen Temperaturen / Broadband Spectroscopy of Magnetic Thin Film Materials at Low Temperatures**

Philip Louis, Masterarbeit, TU München, seit März 2015.

31. **Unconventionally Coupled Nanoelectromechanics**
    Daniel Schwienbacher, Masterarbeit, TU München, seit Mai 2015.

32. **Quasiteilcheneigenschaften von überdotierten Kupraten / Quasiparticle properties of overdoped cuprates**
    Ramez Hosseinian Ahangharnejhad, Masterarbeit, TU München, seit August 2015.

33. **LASER ARPES investigation of correlated electron systems**
    Irene Cucchi, Masterarbeit, TU München, seit August 2015.

34. **Thin Film Fabrication for Spin Caloritronic Experiments/Herstellung dünner Schichten für spinkaloritronische Experimente**
    Johanna Fischer, Masterarbeit, TU München, seit August 2015.

35. **Fabrication of ferromagnetic insulator/normal metal hybrid structures for pure spin current experiments**
    Hiroto Sakimura, Masterarbeit, TU München, seit Oktober 2015.

36. **Tomografie von einem Zwei-Moden-Gequetschten Zustand / Tomography of a two-mode squeezed state**
    Patrick Yard, Masterarbeit, TU München, seit Oktober 2015.

37. **Characterization of a single photon**
    Le anh Tuan, Masterarbeit, TU München, seit November 2015.

38. **Electronic properties of an organic superconductor in the vicinity of the Mott-insulating transition**
    Sergej Fust, Masterarbeit, TU München, seit November 2015.

39. **Spintransport in magnetischen Nanostrukturen/Spin Transport in magnetic Nanostructures**
    Tobias Wimmer, Masterarbeit, TU München, seit Dezember 2015.

Research Projects and Cooperations

A large number of our research projects are benefiting from the collaboration with external groups in joint research projects, as well as from individual collaborations, exchange programs and visitors. Most collaborations are based on joint projects, which are funded by different research organizations (see list below). A considerable number of collaborations also exists with universities, other research institutions and industry without direct financial support.

Funded Projects

A. German Research Foundation: Excellence Initiative

Cluster of Excellence "Nanosystems Initiative Munich"

1. Research Area I: *Quantum Nanophysics*
   F. Deppe, S.T.B. Gönnenwein, R. Gross, H. Huebl, A. Marx
2. Research Area II: *Hybrid Nanosystems*
   S.T.B. Gönnenwein, R. Gross, H. Huebl

B. German Research Foundation: Collaborative Research Centers

Collaborative Research Center 631: "Solid-State Quantum Information Processing: Physical Concepts and Materials Aspects"

1. Project A3: *Superconducting Quantum Circuits as Basic Elements for Quantum Information Processing*
   R. Gross, A. Marx
2. Project A8: *Cavity Quantum Electrodynamics with Superconducting Devices*
   A. Marx, R. Gross
3. Project C3: *Fundamentals of Quantum Logic Gates in Silicon*
   M. Brandt, H. Huebl, M. Stutzmann
4. Project S: *Coordination of the Collaborative Research Center*
   R. Gross

Transregional Collaborative Research Center TRR 80: "From Electronic Correlations to Functionality"

1. Project A2: *Spatially and Momentum Resolved Raman Studies of Correlated Systems*
   R. Hackl

C. German Research Foundation: Priority Programs

1. Pulsed Electron Paramagnetic Resonance at Millikelvin Temperatures
   within the DFG Priority Program 1601 *New frontiers in sensitivity for EPR spectroscopy: from biological cells to nano materials*
   H. Huebl (Az. HU 1896/2-1)
2. Spin-dependent thermo-galvanic effects: experiment
   within the DFG Priority Program 1538 *Spin-Caloric Transport – SpinCAT*
   S.T.B. Gönnenwein, R. Gross (Az. GO 944/4-1, GO 944/4-2)

3. Project: *Raman study of electron dynamics and phase transitions in iron-pnictide compounds* within the DFG Priority Program 1458 *"High-Temperature Superconductivity in Iron-Pnictides"*
   R. Hackl, R. Gross, B. Büchner, D. Johrendt, C. Honerkamp (Az. HA 2071/7-1, HA 2071/7-2)

D. German Research Foundation: Research Projects

1. Project: *Correlated Quantum Microwaves: Continuous-Variables for Remote State Preparation and Quantum Illumination*
   K.G. Fedorov (Az. FE 1564/1-1)
2. Project: *Exotic Superconductivity in Strongly Anisotropic Correlated Organic Metals in the Vicinity of Insulating Phases*
   M. Kartsovnik, W. Biberacher, R. Gross (Az. KA 1652/4-1)
3. Project: *Interaction Between Spin, Lattice, and Charge in Non-Centrosymmetric Correlated Metals*
   R. Hackl, R. Gross (Az. HA 2071/5-1)

E. European Union

1. EU Collaborative Project (call identifier FP7-ICT-2011-C), project title *Quantum Propagating Microwaves in Strongly Coupled Environments – PROMISCE*
   F. Deppe, A. Marx, R. Gross, Grant Agreement no. 284566
   partners: several European Universities and research institutions.
2. Marie Curie Network for Initial Training (call identifier FP7-PEOPLE-2010-ITN), project title *Circuit and Cavity Quantum Electrodynamics (CCQED)*
   R. Gross, A. Marx, F. Deppe, Grant Agreement No. PITN-GA-2010-264666
   partners: several European Universities and research institutions.

F. Free State of Bavaria

1. International PhD Programme of Excellence *Exploring Quantum Matter (ExQM)* within the Elite Network of Bavaria, Project No. K-NW-2013-231
   R. Gross, A. Marx, F. Deppe, K. Fedorov
   Partners: jointly with 12 quantum physics research groups at the TU Munich, the LMU Munich, and the Max Planck Institute of Quantum Optics.

G. Max Planck Society

1. International Max Plank Research School for *Quantum Science and Technology (QST)*, Spokesman: Prof. Dr. J. Ignacio Cirac
   R. Gross, A. Marx, F. Deppe, K. Fedorov
   Partners form Max Planck Institute of Quantum Optics, Ludwig-Maximilians-Universität München and Technische Universität München, including Walther-Meißner-Institute (WMI) and Walter Schottky Institute (WSI).

H. Bavaria California Technology Center (BaCaTeC)

1. Project: *Nematic Order and New Phases in Quantum Materials*
   R. Hackl,
   partners: Profs. Thomas Devereaux, Steve Kivelson, and Sri Raghu (Stanford University)

I. German Academic Exchange Service

1. Project-based Personnel Exchange Programme (PPP) with Serbia (project 56267076: Fe-based superconductors), collaboration with the Institute of Physics, University of Belgrade (Dr. Z.V. Popovic).
   R. Hackl
2. Project-based Personnel Exchange Programme (PPP) with India (project 57085749: Spin Current Generation and Detection Using FMI/NM Hybrids), collaboration with the IIT Madras, Chennai (Prof. Dr. M. S. Ramachandra Rao).
   R. Gross

Conferences, Workshops, Public Outreach

The Walther-Meißner-Institute has organized/co-organized several conferences, workshops and symposia in 2015. It also was participating in several public outreach events aiming at making science accessible to the public.

International Workshop "Spin Mechanics 3" (22 – 26 June 2015, Munich Residence, Munich, Germany)

The International Workshop "Spin Mechanics 3" was organized by Sebastian Gönnenwein, Hans Hübl and Rudolf Gross of Walther-Meißner-Institute jointly with Eva Weig of University of Konstanz at the Munich Residence. The emerging field of spin mechanics addresses the basic physics questions arising from the interaction between spin angular momenta and mechanical degrees of freedom. Research related to Spin Mechanics draws from different areas in modern solid state physics, ranging from magnetism and spintronics over material science and spectroscopy to nanoelectromechanical systems and scanning probe techniques.

The meeting was bringing together experts from the different fields of research representing the various points of view on spin mechanics. The five day workshop stimulated interactions between the fields of (a) optomechanics, (b) spintronics (explicitly including antiferromagnets), (c) torques and forces on spins and mechanical systems, (d) spin-caloritronics, and (e) spin orbit torques. Since researchers from various fields in solid state physics participated, each of the above mentioned topics was introduced in an extensive tutorial. They provided a thorough introduction into the respective fields for non-experts, in particular for young PhD students. The sessions consisted of invited talks, complemented by poster presentations. Considering the set of tutorials, the ample time slots reserved for discussions, and the interdisciplinary scope, the Spin Mechanics 3 workshop also served as a summer-school like introduction to a variety of modern and active fields in solid state physics.

International NIM Conference on Resonator QED (03 – 07 August 2015, Lietraturhaus, Munich, Germany)

The International NIM Conference on Resonator Quantum Electrodynamics (Resonator QED 2015) was organized by Rudolf Gross (WMI) jointly with Jonathan Finley (Walter Schottky Institute, TU Munich) and Gerhard Rempe (Max Planck Institute of Quantum Optics, Garching). Achim Marx and Frank Deppe of WMI were members of the local organisation team. It was the first conference within a research conference series started by the Excellence Cluster

"Nanosystems Initiative Munich". It took place in the Literaturhaus at Munich from 03 – 07 August 2015. The Resonator QED 2015 conference was a continuation of the highly successful Resonator QED 2013 conference, also taking place at Munich from 09–13 September 2013. The Resonator QED 2015 conference consisted of tutorials and invited talks, as well as a small number of contributed talks and poster presentations.

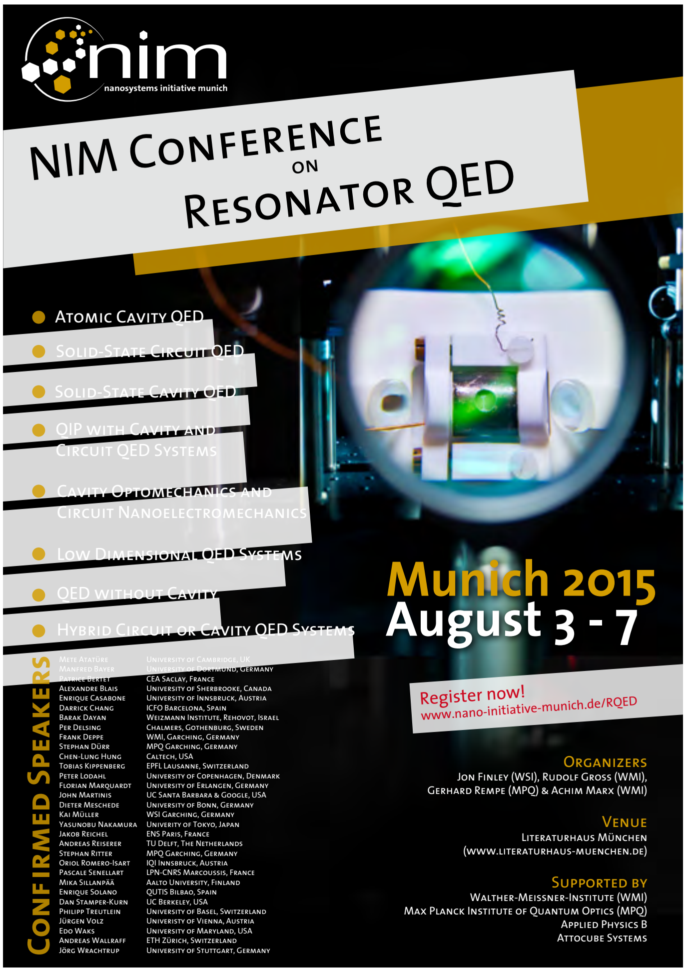

The NIM Conference on Resonator Quantum Electrodynamics (Resonator QED 2015) particularly aimed to bridge two communities in quantum physics – optical cavity QED and solid state circuit QED – to share, pursue and diffuse the benefits of collaborations in the science of elementary quanta. Both fields made spectacular progress in the past years, with a remarkable diversity of demonstrated physical effects. To list a few, milestones include the direct observation of the quantum jumps of microwave light, the deterministic generation and tomography of arbitrary quantum states of a resonator by superconducting quantum bits, the evidence of the Lamb shift in a solid-state system, the generation of nonlinear photonics with one atom, the realization of real-time feedback schemes on single atoms triggered by the detection of single photons, the nondestructive detection of an optical photon as well as the implementation of quantum gates between flying optical photons and stationary matter qubits. It is remarkable that circuit and cavity quantum electrodynamics share the same concepts, whereas they explore different regimes with essentially different techniques. Such complementarities gave a strong motivation to bring together the solid-state circuit and the atomic physics cavity groups to form a unified scientific community. Within Resonator QED 2015, the Cluster of Excellence NIM succeeded to foster interactions between the optical cavity QED and solid state circuit QED communities.

The program of Resonator QED 2015 was structured into eight half-day sessions covering the topics:

- Atomic Cavity QED
- Solid-State Circuit QED
- Solid-State Cavity QED
- QIP with Cavity and Circuit QED Systems
- Cavity Optomechanics and Circuit Nanoelectromechanics
- Low-Dimensional QED Systems
- QED without Cavity

- Hybrid Circuit or Cavity QED Systems

Each session was started with a tutorial. Besides these tutorials and the invited talks there were contributed talks selected from the contributed abstracts. In addition, there were two poster sessions. The best posters have been awarded by a poster prize sponsored by Applied Physics B.

As supporting program, there have been laboratory tours on Monday morning and Friday afternoon at the Max Planck Institute of Quantum Optics, the Walther-Meißner-Institute, and the Walter Schottky Institute.

Course 3 on "Physics and Electronics in Everyday Life" of the Ferienakademie 2014 (20 September – 02 October, 2015, Sarntal, Italy)

The course was hold by Rudolf Gross of WMI together with Prof. Dr. Gert Denninger, University of Stuttgart, and Prof. Dr. Vojislav Krstic, University of Erlangen-Nuremberg, within the *Ferienakademie*. The Ferienakademie is jointly organized by the Technical University of Munich, the University of Erlangen/Nuremberg, and the University of Stuttgart to motivate and foster highly talented students. It takes place annually at Sarntal in the Italian Alps.

Within course 3 of Ferienakademie the students prepare presentations on physical phenomena and problems which play an important role in our everyday-life but usually are poorly understood. Besides the seminars talks there are intensive discussions with the professors and members of other courses as well as experimental sessions. A relaxing atmosphere is provided by a varied supporting program (mountain hiking, excursions to Bozen, table tennis and chess tournament, Törgelen, etc.). Moreover, within the Ferienakademie the students have the opportunity to meet leaders from industry, politics and science. In 2015, these have been Siegfried Balleis (chairman of the Universitätsbund Erlangen/Nürnberg, former mayor of Erlangen), Bernhard Bauer (Google Germany) and Dr. Elmar Pritsch (CIO, Robert Bosch GmbH).

"Lange Nacht der Wissenschaften" (27 June 2015, Research Campus Garching, Germany)

The Walther-Meißner-Institute contributed to the Open House Event *"Lange Nacht der Wissenschaften"* taking place at the Research Campus Garching by an attractive program for anybody interested in science. On the one hand, the Open House Event is a considerable effort for all members of WMI since making preparations for this event is quite time consuming. On the other hand, this event is worth the effort since it allows us to communicate our research work to the interested public. The Open House Event 2015 was particularly successful with a new record number of visitors at WMI approaching 1000. In this way WMI not only could inform the broad public about the research activities of BAdW but also could fascinate a large number of kids and pupils about science and technology.

Between 6 pm and midnight, WMI offered hourly talks on the topics *On the Way to Quantum Computers* (Rudolf Gross) and *Superconductivity and Superfluidity* (Dietrich Einzel) which were completely overcrowded. Beyond the series of lectures the visitors could visit the laboratories for thin film deposition and single crystal growth to get an impression of state-of-the-art materials technology. In one of the low temperature laboratories they could get insight into the experimental study of superconducting qubits and quantum circuits, in particular on light-matter interaction and coherent quantum evolution.

Particularly fascinating for visitors are demonstration experiments on low temperature phenomena. Therefore, WMI has made a considerable effort to set up high quality demonstration experiments on the Meißner effect in superconductors (superconducting levitation) and the fountain effect in superfluid ^{4}He. For kids and pupils the superconducting racetrack of WMI and the large number of fascinating hands-on experiments with liquid nitrogen are always highly attractive. They can experience that low temperature physics is a lot of fun.

Cooperations

Other collaborations without direct project funding involve:

- Stanford University and the SLAC National Accelerator Laboratory, Stanford, USA (T.P. Devereaux, M. Greven, Z.-X. Shen, I. Fisher, B. Moritz)
- Universidad del País Vasco and Ikerbasque Foundation, Bilbao, Spain (E. Solano)
- Instituto de Física Fundamental, CSIC, Madrid, Spain (J.J. Garcia-Ripoll)
- Central Research Institute of the Electric Power Industry, Tokyo, Japan (Dr. S. Ono, Dr. Y. Ando)
- Green Innovation Research Laboratories, NEC Corporation, Japan (J.S. Tsai, K. Inomata, T. Yamamoto)
- University of Tokyo (Y. Nakamura)
- University of Vienna, Austria (M. Aspelmeyer)
- Heriot Watt University, Edinburgh, Scotland (M. Hartmann)
- University of Tohoku, Sendai, Japan (Gerrit E.W. Bauer, Eiji Saitoh)
- European Synchrotron Radiation Facility (ESRF), Grenoble (H. Müller, F. Wilhelm, K. Ollefs)
- Materials Science Research Centre, IIT Madras, India (M.S. Ramachandra Rao)
- Solid State Chemistry Unit, Indian Institute of Science, Bagalore, Indian (D.D. Sarma)
- ETH-Zurich, Switzerland (A. Wallraff, L. Degiorgi, R. Monnier, M. Lavagnini)
- Chalmers University of Technology Gothenburg, Sweden (P. Delsing, G. Wendin)
- University of Alabama, MINT Center, Tuscaloosa, USA (A. Gupta)
- Delft University of Technology, Kavli Institute of NanoScience, Delft, The Netherlands (T.M. Klapwijk, G.E.W. Bauer)
- B. Verkin Institute for Low Temperature Research and Engineering, Kharkov, Ukraine (V.G. Peschansky)
- Landau Institute for Theoretical Physics, Chernogolovka, Russia (P. Grigoriev)
- University of Oxford, Clarendon Laboratory, England (A. Karenowska)
- Russian Academy of Sciences, Chernogolovka, Russia (N. Kushch, A. Palnichenko)
- High Magnetic Field Laboratory, Dresden (E. Kampert, J. Wosnitza)
- High-Magnetic-Field Laboratory, Grenoble, France (I. Sheikin)
- High Magnetic Field Laboratory, Toulouse (C. Proust, D. Vignolles)
- National High Magnetic Field Laboratory, Tallahassee, USA (J. Brooks)
- IFW Dresden, Germany (B. Büchner, J. Fink, S.V. Borisenko, M. Knupfer)
- Max-Planck-Institut für Festkörperforschung, Stuttgart (B. Keimer, L. Boeri)
- University of Tübingen, Germany (R. Kleiner, D. Kölle)
- University of Würzburg, Germany (W. Hanke, F. Assaad, R. Thomale)
- University of Augsburg, Germany (P. Hänggi, A. Wixforth, A. Kampf, A. Loidl, J. Deisenhofer, V. Tsurkan)
- University of Leipzig, Germany (J. Haase)
- RWTH Aachen, Germany (G. Güntherodt, B. Beschoten)
- Ernst-Moritz-Arndt Universität Greifswald, Germany (Markus Münzenberg)
- Martin-Luther-Universität Halle, Germany (G. Woltersdorf)
- Universität Regensburg, Institut für Experimentelle und Angewandte Physik, Germany (Christian Back)
- Universität Bielefeld, Germany (G. Reiss, A. Thomas, T. Kuschel)

- University of British Columbia, Vancouver, Canada (D. Bonn, A. Damascelli)
- TU München, Physics Department, Germany (D. Grundler, Ch. Pfleiderer, F.C. Simmel, Jean Come Lanfranchi, P. Müller-Buschbaum, M. Abdi)
- TU München, Walter Schottky Institut, Germany (G. Abstreiter, M. Stutzmann, J. Finley, M. Brandt, A. Holleitner, U. Wurstbauer)
- TU München, Lehrstuhl für Technische Elektronik (M. Becherer)
- LMU München, Physics Department, Germany (J.P. Kotthaus, J. von Delft, E. Frey, J. Rädler, S. Ludwig)
- LMU München, Chemistry Department, Germany (H. Ebert, D. Ködderitzsch)
- Universidad de Zaragoza, Departamento de Fisica de la Materia Condensada, Spain (L. Morellon, J.M. de Teresa, D. Zueco)
- EPFL Lausanne, Switzerland (T. Kippenberg, H. Ronnov)
- University of New South Wales, Sydney, Australia (M. Simmons, A. Morello)
- Technische Universität Graz, Austria (E. Schachinger)
- Universität Konstanz (A. Leitenstorfer, E. Weig, J. Demsar, A. Pashkin)
- BMW Group, Munich, Germany (J. Schnagl, W. Stadlbauer, G. Steinhoff)
- Siemens AG, CT MM 2, Munich, Germany (R. Matz, W. Metzger)
- Attocube, Munich, Germany (K. Karrai, D. Andres, E. Hoffmann)
- THEVA Dünnschichttechnik, Ismaning, Germany (W. Prusseit)
- Johannes-Kepler-Universität Linz, Institut für Halbleiter- und Festkörperphysik, Austria (A. Ney)
- Jülich Centre for Neutron Science JCNS, Garching, Germany (S. Pütter)
- Université de Toulouse, Laboratoire de Physique Théorique, Toulouse, France (R. Ramazashvili)
- Lawrence Berkeley National Laboratory, Berkeley, USA (A. F. Kemper)
- University of Belgrade, Belgrade, Serbia (Z. Popovic, N. Lazarevic, D. Tanaskovic)
- University of Aveiro, Portugal (N. A. Sobolev)
- Macquarie University, MQ Research Centre for Quantum Science and Technology, Australia (J. Twamley)
- Instituto de Ciencia de Materiales de Sevilla, Spain (J. Poyato, J.L. Perez-Rodriguez)
- Hungarian Academy of Sciences, Research Institute for Solid State Physics and Optics, Budapest, Hungary (K. Kamaras, I. Tüttö, J. Balogh)
- University of Rome "La Sapienza", Rome, Italy (S. Caprara, C. Di Castro, M. Grilli)
- Hungarian Academy of Sciences, Budapest University of Technology and Economics, Budapest, Hungary (A. Virosztek, A. Zawadowski, G. Mihály)
- Goethe University, Frankfurt (S. Winter)
- National Institute of Standards and Technology, Boulder, USA (H. Nembach, J. Shaw, T.J. Silva)
- University of Manitoba, Winnipeg, Canada (C.-M. Hu)
- Kyoto University, Japan (M. Shiraishi)
- Technische Universität Braunschweig (D. Menzel, S. Süllow)
- Universidad Nacional de Colombia, Colombia (O. Moran)
- University of Birmingham, UK (E.M. Forgan)

Stays abroad

Extended visits of members of the Walther-Meißner-Institute at foreign research laboratories:

1. **Matthias Althammer**
   High Magnetic Field Laboratory, Grenoble, France
   20. - 30. 04. 2015 and 26. 07. - 05. 08. 2015
2. **Stephan Geprägs**
   European Synchrotron Radiation Facility (ESRF), Grenoble, France
   15. - 21. 04. 2015, 01. - 07. 07. 2015, 09. - 14. 09. 2015, and 27. 10. - 03. 11. 2015
3. **Sebastian Gönnenwein**
   Tohoku University, Sendai Japan
   08. - 21. 11. 2015
4. **Rudolf Gross**
   Indian Institute of Technology Madras, Chennai, India
   03. - 07. 11. 2015
5. **Rudolf Hackl**
   Institute of Physics, University of Belgrade, Serbia
   25. - 28. 11. 2015
6. **Matthias Opel, Kathrin Ganzhorn**
   European Synchrotron Radiation Facility (ESRF), Grenoble, France
   30. 06. - 07. 07. 2015 and 29. 10. - 03. 11. 2015
7. **Matthias Opel**
   Indian Institute of Science, Bangalore, India
   09. - 13. 11. 2015
8. **Matthias Opel**
   Indian Institute of Technology Madras, Chennai, India
   13. - 20. 11. 2015

Conference Talks and Seminar Lectures

Matthias Althammer

1. **Pure spin currents in ferromagnetic in insulator normal metal hybrids**
   Invited Talk, 22nd International Colloquium on Magnetic Films and Surfaces (ICMFS 2015), Krakow, Poland
   12. - 17. 07. 2015

Frank Deppe

1. **Spin-boson model with an engineered reservoir in circuit QED**
   Invited Talk, Max-Planck-Institut für Physik komplexer Systeme Dresden, Germany
   29. 06. - 03. 07. 2015
2. **Spin-boson model with an engineered reservoir in circuit QED**
   Invited Talk, NIM Conference on Resonator QED, Literaturhaus München, Germany
   03. - 08. 08. 2015
3. **Superconductivity and Superconducting Electronics**
   F. Deppe and R. Gross
   Invited Lecture Series, 35th Heidelberg Physics Graduate Days
   05. - 09. 10. 2015, Heidelberg, Germany.

Andreas Erb

1. **Single crystal growth of various oxide materials for basic research and applications**
   Invited Talk, Deutsche Kristallzüchtungstagung 2015, Frankfurt, Germany
   04. - 06. 03. 2015
2. **Single crystal growth of various oxide materials for basic research and applications**
   Institut für Kristallzüchtung, Berlin, Germany
   26. 06. 2015
3. **Single crystal growth of various oxide materials for basic research and applications**
   Kolloquium des Freiburger Materialforschungszentrums, Albert-Ludwigs-Universität Freiburg, Germany
   20. 11. 2015

Sebastian Gönnenwein

1. **Spin Currents in Ferromagnet/Normal Metal Heterostructures**
   Physik-Kolloquium der Universität Bielefeld, Bielefeld, Germany
   26. 01. 2015
2. **Spin Currents**
   Physical Chemistry Colloquium, Ludwig-Maximillian-Universität München, Germany
   15. 04. 2015
3. **Spin Current Transport**
   Seminar des Instituts für Festkörperphysik, Technische Universität Dresden, Germany
   24. 04. 2015
4. **Spin Currents and Spin Caloritronics**
   Physikalisches Kolloquium, Eberhard Karls Universität, Tübingen, Germany
   03. 06. 2015
5. **Spin Currents**
   Seminar des Instituts für Physik, Universität Augsburg, Germany
   29. 06. 2015
6. **Spin Currents in Ferromagnet/Normal Metal Heterostructures**
   Invited Talk, Canadian Association of Physicists (CAP) Congress, Edmonton, Canada
   17. 06. 2015
7. **Spin Current-Induced Magnetoresistance**
   Invited Talk, Gordon Research Conference "Spin Dynamics in Nanostructures", The Hong Kong University of Science and Technology, Hong Kong, China
   28. 07. 2015

Jan Goetz

1. **Characterization of superconducting transmission line resonators**
   Spring Meeting of the DPG, Berlin, Germany
   16. - 20. 03. 2015
2. **Circuit QED with a gradiometric tunable-gap flux qubit**
   Spring Meeting of the DPG, Berlin, Germany
   16. - 20. 03. 2015
3. **A physicistÂt's toy box: Quantum physics with microwave circuits at millikelvin temperatures**
   Institut für Hochfrequenztechnik Aachen, Germany
   20. 11. 2015

Rudolf Gross

1. **Solid State Circuits Go Quantum**
   R. Gross
   20. 04. 2015
   Physikalisches Kolloquium, Carl von Ossietzky Universität Oldenburg, Germany.
2. **Quantum Computation**
   R. Gross
   Invited Tutorial, 39. Edgar Lüscher-Seminar (Lehrerfortbildung)
   25. 04 2015, Zwiesel, Germany.
3. **Ultrastrong Coupling in Superconducting Circuit QED**
   R. Gross
   Invited Talk, 3rd International Conference on Quantum Technologies
   13. - 17. 07. 2015, Moscow, Russia.
4. **Superconducting Hybrid Quantum Systems**
   R. Gross
   16. 07. 2015
   V.V. Schmidt Lecture, The National University of Science and Technology MISiS, Moscow, Russia.
5. **Towards Solid-State Based Quantum Computation and Simulation**
   R. Gross
   Tutorial, Ferienakademie der TU München, Universität Erlangen-Nürnberg und der Universität Stuttgart
   20. 09. - 02. 10. 2015, Sarntal, Italy.
6. **Superconductivity and Superconducting Electronics**
   R. Gross and F. Deppe
   Invited Lecture Series, 35th Heidelberg Physics Graduate Days
   05. - 09. 10. 2015, Heidelberg, Germany.
7. **Solid-State Nanosystems: Low Temperature Physics Meets the Quantum- and Nanoworld**
   R. Gross
   03. 11. 2015
   Keynote Lecture, BTNT 2015 -âĂŞ 4^{th} Annual Conference of the Nanotechnology Industry in India, Chennai, India.
8. **Spin Currents in Magnetic Heterostructures**
   R. Gross
   05. 11. 2015
   Colloquium of the Indian Institute of Technology Madras, Chennai, India.

Rudolf Hackl

1. **Evidence for s- and d-wave pairing instabilities in Fe-based superconductors**
   Invited Talk, International Conference "Quantum in Complex Matter", Ischia, Italy
   15. 06. 2015
2. **Fluctuations in cuprates and Fe-based superconductors**
   Invited Talk, International Workshop "Two-dimensional chalcogenides", Dresden, Germany
   03. 09. 2015
3. **Fluctuations and phase transitions in iron-based compounds**
   Invited Talk, Workshop "From Hard Matter to Soft Matter and Back" on the occasion of the 60th

birthday of Prof. L. Forró, EPFL, Lausanne, Switzerland
04. 12. 2015

4. **Excitons in superconductors**
International Workshop "Novel Materials and Superconductors", Obertraun, Austria
12. 02. 2015
5. **Evidence for spin-fluctuation induced pairing in $Ba_{0.6}K_{0.4}Fe_2As_2$**
International Conference "Materials and Mechanisms of Superconductivity (M2S) 2015", Genève, Switzerland
27. 08. 2015
6. **Fluctuations and superconductivity in iron-based compounds**
Seminar Talk, Institute for Biomolecular Optics, LMU München, Germany
23. 04. 2015
7. **Fluctuations and phase transitions in iron-based compounds**
Colloquium on Condensed Matter Physics, Goethe-Universität, Frankfurt am Main, Germany
13. 11. 2015
8. **Conventional and unconventional superconductivity at high transition temperatures**
Seminar Talk, Institute for Solid State Physics, ETH Zurich, Switzerland
03. 12. 2015
9. **Fluctuations, phase transitions, and superconductivity in iron-based superconductors**
Colloquium on Condensed Matter Physics, Universität Konstanz, Germany
10. 12. 2015

Hans Hübl

1. **Nano-Opto-Mechanics at Microwave Frequencies**
Seminar Talk, Universität Wien, Austria
14. 01. 2015
2. **Spins, strings, and superconducting resonators: coupling harmonic oscillators in the solid state**
Seminar Talk, Technische Universität Kaiserslautern, Germany
28. 01. 2015
3. **Hybrid Systems - Coupling Spins, strings and superconducting resonators**
Kolloquium der Fakultät für Physik, Universität Bielefeld, Germany
15. 06. 2015
4. **Circuit Nano-Electromechanics**
Colloquium Talk, London Centre for Nanotechnology, University College London, UK
18. 11. 2015
5. **Hybrid Systems - Coupling Spins, strings and superconducting resonators**
Seminar Talk, NTT Tokyo, Japan
07. 08. 2015
6. **Spin Seebeck Effect in a Compensated Ferrimagnet**
APS March Meeting 2015, San Antonio, USA
02. - 06. 03. 2015
7. **Determination of effective mechanical properties of a double-layer beam by means of a nano-electromechanical transducer**
APS March Meeting 2015, San Antonio, USA
02. - 06. 03. 2015
8. **Microwave-Magnetic Hybrid Circuits**
Invited Talk, Gordon Conference "Spin Dynamics in Nanostructures", Hong Kong, China
25. - 31. 07. 2015

Mark Kartsovnik

1. **Superconductivity and charge-density-wave state in the layered organic conductors Îś-(BEDT-TTF)2MHg(SCN)4**
Invited Talk, International Conference on Quantum in Complex Matter "Superstripes 2015", Ischia, Italy
13. - 18. 06. 2015

2. **Interlayer charge transport and dimensional crossover in a layered organic conductor**
   International Symposium on Crystalline Organic Metals, ISCOM 2015, Bad Goegging, Germany
   06. - 11. 09. 2015

Achim Marx

1. **Ultrastrong Coupling in Two-Resonator Circuit QED**
   NIM Conference on resonator QED, Munich, Germany
   3. - 07. 08. 2015

Matthias Opel

1. **Origin of the Magnetoresistance (MR) in Pt on $Y_3Fe_5O_{12}$ (YIG)**
   Seminar of the Solid State Chemistry Unit, Indian Institute of Science, Bangalore, India
   12. 11. 2015
2. **Proximity Magnetism and Spin-Hall Anomalous Hall Effect in Pt on $Y_3Fe_5O_{12}$ (YIG)**
   Condensed Matter and Nanoscience Journal Club Seminar, Indian Institute of Technology Madras, Chennai, India
   18. 11. 2015

Kurt Uhlig

1. **Cryogen-free Dilution Refrigerators**
   Invited Talk, Fifty Years of Dilution Refrigeration, University of Manchester, England
   16. 09. 2015

Mathias Weiler

1. **Experimental test of the spin mixing conductance concept**
   Invited Talk, 580. WEH Seminar: Oxide Spintronics, Bad Honnef, Germany
   07. - 09. 01. 2015
2. **Quantifying the interfacial Dzyaloshinskii-Moriya interaction in metallic thin film bilayers**
   Invited Talk, 26. Edgar Lüscher Seminar, Klosters, Switzerland
   07. - 13. 02. 2015
3. **Phase-sensitive detection of the ac inverse spin Hall effect**
   Invited Talk, APS March Meeting, San Antonio, USA
   02. - 06. 03. 2015
4. **Quantifying the interfacial Dzyaloshinskii-Moriya interaction in metallic thin film bilayers**
   Invited Talk, Spinmechanics III, Munich, Germany
   22. - 26. 06. 2015
5. **Measuring the Dzyaloshinskii-Moriya interaction in thin films**
   Group Seminar "Korrelierte Elektronensysteme", Technische Universität Braunschweig, Germany
   15. 09. 2015
6. **Quantifying the interfacial Dzyaloshinskii-Moriya interaction in metallic thin film bilayers**
   Spring Meeting of the DPG, Berlin, Germany
   15. - 20. 03. 2015
7. **Spin pumping and spin torques**
   Festkörperkolloquium, Physik-Department, Technische Universität, München, Germany
   21. 05. 2015

Edwar Xie

1. **Two-resonator circuit quantum electrodynamics: ultrastrong interaction**
   APS March Meeting 2015, San Antonio, USA
   02. - 06. 03. 2015
2. **Tunable Coupling and Ultrastrong Interaction in Circuit Quantum Electrodynamics**
   Kryoelektronische Bauelemente Konferenz 2015, Burg Warberg, Germany
   27. - 29. 09. 2015

Honors and Awards

Several members of Walther-Meißner-Institute were receiving honors and awards in 2015.

Teaching Award "Goldene Kreide"

Sebastian Gönnenwein of Walther-Meißner-Institute received one of the prestigious "Golden Chalks" (*Goldene Kreide*) for the best lecture of the bachelor course (condensed matter physics I and II). The "Golden Chalks" are presented annually by the student body of the physics faculty for the best lectures in experimental and theoretical physics within the master course, the best lecture within the bachelor course, the best tutor exercise and the best "import" lecture given by a docent from another faculty. The "Golden Chalk" was handed over to Sebastian Gönnenwein on 16th July 2015 within the "Tag der Physik".

Presentation of the "Golden Chalks" by Florian Ettlinger (most left) from the student body of the physics faculty to (from left to right) Johannes Lang (best tutor exercise), Dr. Michael Kaniber (best lecture in experimental physics, master course), Dr. Sebastian Gönnenwein (best lecture in the bachelor course), Prof. Dr. Gregor Kemper (best "import" lecture). Not shown is Nicht im Bild Prof. Ulrich Gerland (best lecture in theoretical physics, master course). Picture: PH.TUM/Wenzel Schürmann.

DGKK Prize 2015

Andreas Erb of Walther-Meißner-Institute received the DGKK Prize 2015 for *"herausragende wissenschaftliche Leistungen auf dem Gebiet der erfolgreichen Züchtung von Einkristallen, insbesondere von komplizierten Oxidverbindungen höchster Perfektion, die er anderen Forschungsgruppen zur Verfügung stellte und die dort zu neuen fundamentalen Erkenntnissen führten."* The prize has been presented to Andreas Erb on 4th March 2015 at the Annual Conference of the Deutsche Gesellschaft für Kristallwachtum und Kristallzüchtung (DGKK) taking place at Frankfurt from 04 to 06 March 2015.

Presentation of the DGKK Prize 2015 to Andreas Erb (middle) by Dr.-Ing. Jochen Friedrich (left, Chairman of DGKK, Fraunhofer Institute for Integrated Systems and Device Technology IISB) and Dr. Wolfgang Löser (right, IFW Dresden) during the Annual Conference of the Deutsche Gesellschaft für Kristallwachtum und Kristallzüchtung (DGKK).

Silberne Verdienstmedaille of the Bavarian Academy of Sciences and Humanities

Rudolf Gross of WMI received the ***Silberne Verdienstmedaille*** of the Bavarian Academy of Sciences and Humanities (BAdW) in recognition of his outstanding contributions to the fostering of the scientific program and infrastructure of the Walther-Meißner-Institute.

The Bavarian Academy of Sciences and Humanities decorates the Silberne Verdienstmedaille to members and employees who render outstanding services to BAdW. Former prizewinners are Prof. Dr. Roland Bulirsch (TU Munich, 2011), Dr. Sylvia Krauß (Bavarian State Archives, 2010), Prof. Dr. Markus Schwoerer (University of Bayreuth, 2010), Prof. Dr. Ludwig Hammermayer (LMU Munich, 2008), Prof. Dr. Andreas Kraus (LMU Munich, 2008), Prof. Dr. Heinz-Gerd Hegering (LMU Munich, 2005), Prof. Dr. Friedrich L. Bauer (TU Munich, 2004), Prof. Dr. Dr. h.c. Dieter Medicus (LMU Munich, 2003) and Prof. Dr. Reinhard Lauth (LMU Munich, 2003).

The prize has been presented to Rudolf Gross on 26$^{\text{th}}$ June 2015 by the president of the Academy at the Munich Residence.

Leibniz Medal of IFW Dresden

Rudolf Gross of WMI received the ***Leibniz Medal*** of the Leibniz Institute for Solid State and Materials Research (IFW) Dresden in recognition of his great and longstanding contributions to IFW Dresden.

The IFW Dresden awards the Leibniz Medal to persons rendering outstanding services to the institute. Rudolf Gross has been member of the scientific advisory board of IFW Dresden from 2008 to 2015. During this period he tirelessly contributed to the prospering of IFW Dresden and the further development of its research strategy. The Leibniz Medal has been presented to Rudolf Gross on 6$^{\text{th}}$ October 2015 by the scientific director of IFW Dresden, Prof. Dr. Manfred Hennecke.

Appointments, Membership in Advisory Boards, etc.

1. **Frank Deppe** is associate member of the Cluster of Excellence *Nanosystems Initiative Munich (NIM)*.
2. **Andreas Erb** is spokesmen of the "Arbeitskreis Intermetallische und oxydische Systeme mit Spin- und Ladungskorrelationen" of the *Deutsche Gesellschaft für Kristallzüchtung und Kristallwachstum (DGKK)*.
3. **Sebastian Gönnenwein** is member and principal investigator of the Cluster of Excellence *Nanosystems Initiative Munich (NIM)*.
4. **Sebastian Gönnenwein** was co-organizer of the International Conference "Spin Mechanics 3", Munich, Germany.
5. **Rudolf Gross** is member of the Scientific Advisory Board of the Bayerisches Geoinstitut, Bayreuth, Germany.
6. **Rudolf Gross** is member of the committee for the allocation of Alexander von Humboldt Foundation Research Awards.
7. **Rudolf Gross** is member of the selection committee of the Stern-Gerlach-Medal of the German Physical Society.
8. **Rudolf Gross** is member of the Appointment and Tenure Board of Technical University of Munich.
9. **Rudolf Gross** is member of the Executive Board of the Cluster of Excellence *Nanosystems Initiative Munich (NIM)* and coordinator of the Research Area 1 on *Quantum Nanosystems*.
10. **Rudolf Gross** is member of the *Munich Quantum Center (MQC)*.
11. **Rudolf Gross** was spokesman of the Collaborative Research Center 631 on *Solid State Quantum Information Processing* of the German Research Foundation, July 2003 – June 2015.
12. **Rudolf Gross** was member of the Scientific Advisory Board of the Leibniz Institute for Solid-State and Materials Research, Dresden, until October 2015.
13. **Rudolf Gross** was co-organizer of the International Conference "Resonator QED 2015", Munich, Germany.
14. **Rudolf Gross** was co-organizer of the International Conference "Spin Mechanics 3", Munich, Germany.
15. **Rudolf Hackl** is deputy coordinator of the DFG Priority Program SPP 1458 on "High Temperature Superconductivity in the Iron Pnictides".
16. **Rudolf Hackl** is member of the evaluation board of the neutron source Heinz Maier-Leibnitz (FRM II).
17. **Hans Hübl** is member and principal investigator of the Cluster of Excellence *Nanosystems Initiative Munich (NIM)*.
18. **Mark Kartsovnik** is member of the Selection Committee of EMFL (European Magnetic Field Laboratories)
19. **Mark Kartsovnik** is member of the International Advisory Committee of the 10^{th} International Symposium on Crystalline Organic Metals Superconductors and Ferromagnets

(ISCOM 2015)

20. **Matthias Opel** is one of the four spokesmen of the scientific staff of the Bavarian Academy of Sciences and Humanities.
21. **Matthias Opel** is member of the International Advisory Committee of the STAC-9 (Science and Technology for Advanced Ceramics) Conference, Tsukuba, Japan
22. **Mathias Weiler** is member of the Editorial Review Board of IEEE Magnetics Letters.

Teaching

Lectures, Seminars, Courses and other Scientific Activities

Several members of the Walther-Meißner-Institute give lectures and seminars at the Technical University of Munich.

Lectures

Frank Deppe

WS 2014/2015	• Seminar: Superconducting Quantum Circuits (with R. Gross, A. Marx)
SS 2015	• Angewandte Supraleitung: Josephson Effekte, supraleitende Elektronik und supraleitende Quantenschaltkreise (Applied Superconductivity: Josephson Effects, Superconducting Electronics and Superconducting Quantum Circuits, with R. Gross)
	• Seminar: Superconducting Quantum Circuits (with R. Gross, A. Marx)
WS 2015/2016	• Seminar: Superconducting Quantum Circuits (with R. Gross, A. Marx)

Dietrich Einzel

WS 2014/2015	• Mathematische Methoden der Physik I (Mathematical Methods of Physics I)
	• Übungen zu Mathematische Methoden der Physik I (Mathematical Methods of Physics I, Problem Sessions)
	• WMI Seminar on Current Topics of Low Temperature Solid-State Physics (with R. Gross, S.B.T. Gönnenwein, R. Hackl, H. Hübl, A. Marx, M. Opel)
	• Seminar: Advances in Solid-State Physics (with R. Gross, S.T.B. Gönnenwein, H. Hübl, A. Marx, M. Opel)
SS 2015	• Mathematische Methoden der Physik II (Mathematical Methods of Physics II)
	• Übungen zu Mathematische Methoden der Physik II (Mathematical Methods of Physics II, Problem Sessions)
	• WMI Seminar on Current Topics of Low Temperature Solid-State Physics (with R. Gross, S.B.T. Gönnenwein, R. Hackl, H. Hübl, A. Marx, M. Opel)
	• Seminar: Advances in Solid-State Physics (with R. Gross, S.T.B. Gönnenwein, H. Hübl, M. Opel, A. Marx)
WS 2015/2016	• Mathematische Methoden der Physik I (Mathematical Methods of Physics I)
	• Übungen zu Mathematische Methoden der Physik I (Mathematical Methods of Physics I, Problem Sessions)
	• WMI Seminar on Current Topics of Low Temperature Solid-State Physics (with R. Gross, S.B.T. Gönnenwein, R. Hackl, H. Hübl, A. Marx, M. Opel)
	• Seminar: Advances in Solid-State Physics (with R. Gross, S.T.B. Gönnenwein, H. Hübl, A. Marx, M. Opel,)

Rudolf Gross

WS 2014/2015	• Supraleitung und Tieftemperaturphysik I (Superconductivity and Low Temperature Physics I)
	• Übungen zu Supraleitung und Tieftemperaturphysik I (Superconductivity and Low Temperature Physics I, Problem Sessions)
	• WMI Seminar on Current Topics of Low Temperature Solid-State Physics (with D. Einzel, S.T.B. Gönnenwein, R. Hackl, H. Hübl, A. Marx, M. Opel)
	• Seminar: Advances in Solid-State Physics (with D. Einzel, S.T.B. Gönnenwein, H. Hübl, A. Marx, M. Opel)
	• Seminar: Superconducting Quantum Circuits (with F. Deppe, A. Marx)
	• Festkörperkolloquium (Colloquium on Solid-State Physics, with D. Einzel)

SS 2015	• Supraleitung und Tieftemperaturphysik II (Superconductivity and Low Temperature Physics II) • Übungen zu Supraleitung und Tieftemperaturphysik II (Superconductivity and Low Temperature Physics II, Problem Sessions) • Angewandte Supraleitung: Josephson Effekte, supraleitende Elektronik und supraleitende Quantenschaltkreise (Applied Superconductivity: Josephson Effects, Superconducting Electronics and Superconducting Quantum Circuits, with F. Deppe) • Übungen zu Angewandte Supraleitung: Josephson Effekte, supraleitende Elektronik und supraleitende Quantenschaltkreise (Applied Superconductivity: Josephson Effects, Superconducting Electronics and Superconducting Quantum Circuits, Problem Sessions, with F. Deppe) • Seminar: Advances in Solid-State Physics (with D. Einzel, S.T.B. Gönnenwein, H. Hübl, A. Marx, M. Opel) • WMI Seminar on Current Topics of Low Temperature Solid-State Physics (with D. Einzel, S.T.B. Gönnenwein, R. Hackl, H. Hübl, A. Marx, M. Opel) • Seminar: Superconducting Quantum Circuits (with F. Deppe, A. Marx) • Festkörperkolloquium (Colloquium on Solid-State Physics, with D. Einzel) • Ferienakademie: Course 3 "Physics and Electronics in Everyday Life"
WS 2015/2016	• Physik der Kondensierten Materie I (Condensed Matter Physics I) • Übungen zu Physik der Kondensierten Materie I (Condensed Matter Physics I, Problem Sessions, with S. Geprägs) • WMI Seminar on Current Topics of Low Temperature Solid-State Physics (with D. Einzel, S.T.B. Gönnenwein, R. Hackl, H. Hübl, A. Marx, M. Opel) • Seminar: Advances in Solid-State Physics (with D. Einzel, S.T.B. Gönnenwein, H. Hübl, A. Marx, M. Opel) • Seminar: Superconducting Quantum Circuits (with F. Deppe, A. Marx) • Festkörperkolloquium (Colloquium on Solid-State Physics, with D. Einzel)

Sebastian T.B. Gönnenwein

WS 2014/2015	• Physik der Kondensierten Materie I (Condensed Matter Physics I) • Übungen zu Physik der Kondensierten Materie I (Condensed Matter Physics I, Problem Sessions, with S. Geprägs) • Seminar: Advances in Solid-State Physics (with D. Einzel, R. Gross, H. Hübl, A. Marx, M. Opel) • WMI Seminar on Current Topics of Low Temperature Solid State Physics (with D. Einzel, R. Gross, R. Hackl, H. Hübl, A. Marx, M. Opel) • Seminar: Spin Caloritronics and Spin Pumping (with M. Althammer, H. Hübl, M. Weiler) • Seminar: Current Topics in Magneto and Spin Electronics (with M. Brandt, H. Hübl)
SS 2015	• Physik der Kondensierten Materie II (Condensed Matter Physics II) • Übungen zu Physik der Kondensierten Materie II (Condensed Matter Physics I, Problem Sessions, with S. Geprägs) • Seminar: Advances in Solid-State Physics (with D. Einzel, R. Gross, H. Hübl, A. Marx, M. Opel) • Seminar: Spin Caloritronics and Spin Pumping (with M. Althammer, H. Hübl, M. Weiler) • WMI Seminar on Current Topics of Low Temperature Solid State Physics (with D. Einzel, R. Gross, R. Hackl, H. Hübl, A. Marx, M. Opel) • Seminar: Current Topics in Magneto and Spin Electronics (with M. Brandt, H. Hübl)
WS 2015/2016	• Seminar: Advances in Solid-State Physics (with D. Einzel, R. Gross, H. Hübl, A. Marx, M. Opel)

- WMI Seminar on Current Topics of Low Temperature Solid State Physics (with D. Einzel, R. Gross, R. Hackl, H. Hübl, A. Marx, M. Opel)
- Seminar: Spin Caloritronics and Spin Pumping (with M. Althammer, H. Hübl, M. Weiler)
- Seminar: Current Topics in Magneto and Spin Electronics (with M.S Brandt, H. Hübl, M. Weiler)

Rudi Hackl

WS 2014/2015
- Seminar: Advances in Solid-State Physics (with D. Einzel, R. Gross, S.T.B. Gönnenwein, A. Marx, M. Opel)

SS 2015
- Seminar: Advances in Solid-State Physics (with D. Einzel, R. Gross, S.T.B. Gönnenwein, A. Marx, M. Opel)

WS 2015/2016
- WMI Seminar on Current Topics of Low Temperature Solid-State Physics (with D. Einzel, R. Gross, S.B.T. Gönnenwein, H. Hübl, A. Marx, M. Opel)
- Seminar: Advances in Solid-State Physics (with D. Einzel, R. Gross, S.T.B. Gönnenwein, A. Marx, M. Opel)

Hans Hübl

WS 2014/2015
- Magnetismus (Magnetism)
- Übungen zu Magnetismus (Magnetism, Problem Sessions)
- Seminar: Spin Caloritronics and Spin Pumping (with M. Althammer, S. Gönnenwein, M. Weiler)
- Seminar: Advances in Solid-State Physics (with D. Einzel, R. Gross, S.T.B. Gönnenwein, A. Marx, M. Opel)
- WMI Seminar on Current Topics of Low Temperature Solid State Physics (with D. Einzel, R. Gross, S.T.B. Gönnenwein, R. Hackl, A. Marx, M. Opel)
- Seminar: Current Topics in Magneto and Spin Electronics (with S.T.B. Gönnenwein, M. S. Brandt)

SS 2015
- Spin Electronics
- Übungen zu Spin Electronics (Exercises to Spin Electronics)
- Seminar: Spin Caloritronics and Spin Pumping (with M. Althammer, S. Gönnenwein, M. Weiler)
- Seminar: Advances in Solid-State Physics (with D. Einzel, R. Gross, S.T.B. Gönnenwein, A. Marx, M. Opel)
- WMI Seminar on Current Topics of Low Temperature Solid State Physics (with D. Einzel, R. Gross, S.T.B. Gönnenwein, R. Hackl, A. Marx, M. Opel)
- Seminar: Current Topics in Magneto and Spin Electronics (with S.T.B. Gönnenwein, M. S. Brandt)

WS 2015/2016
- Supraleitung und Tieftemperaturphysik I (Superconductivity and Low Temperature Physics I)
- Übungen zu Supraleitung und Tieftemperaturphysik I (Superconductivity and Low Temperature Physics I, Problem Sessions)
- Seminar: Spin Caloritronics and Spin Pumping (with M. Althammer, S. Gönnenwein, M. Weiler)
- Seminar: Advances in Solid-State Physics (with D. Einzel, R. Gross, S.T.B. Gönnenwein, A. Marx, M. Opel)
- WMI Seminar on Current Topics of Low Temperature Solid State Physics (with D. Einzel, R. Gross, S.T.B. Gönnenwein, R. Hackl, A. Marx, M. Opel)
- Seminar: Current Topics in Magneto and Spin Electronics (with S.T.B. Gönnenwein, M. S. Brandt, M. Weiler)

Mathias Weiler

WS 2015/2016
- Magnetismus (Magnetism)

- Übungen zu Magnetismus (Magnetism, Problem Sessions)
- Seminar: Spin Caloritronics and Spin Pumping (with M. Althammer, S. Gönnenwein, H. Huebl)
- Seminar: Advances in Solid-State Physics (with D. Einzel, R. Gross, S.T.B. Gönnenwein, A. Marx, M. Opel)
- WMI Seminar on Current Topics of Low Temperature Solid State Physics (with D. Einzel, R. Gross, S.T.B. Gönnenwein, R. Hackl, A. Marx, M. Opel)
- Seminar: Current Topics in Magneto and Spin Electronics (with S.T.B. Gönnenwein, H. Hübl, M. S. Brandt)

The WMI Seminars

The Friday Seminar – Walther-Meißner-Seminar on Current Topics in Low Temperature Physics

WS 2014/2015:

1. **Exploring Spin Filter Materials for Oxide Spintronics**
   Prof. Dr. Martina Müller, Peter-Grünberg Institut, Forschungszentrum Jülich, Jülich, Germany
   12. 12. 2015
2. **Design and application of spin-wave majority gates**
   Stefan Klingler, Technische Universität Kaiserslautern, Germany
   12. 01. 2015
3. **Non-equilibrium spin and charge transport in atomic-size heterojunctions**
   Dr. Torsten Pietsch, Universität Konstanz, Germany
   16. 01. 2015
4. **Quantum simulation of the spin-boson model with circuits**
   Prof. J.J. Garcia Ripoll, CSIC, Instituto de Fisica Fundamental, Madrid, Spain
   26. 01. 2015
5. **Exploring low-energy phase diagrams of quantum critical materials: a microwave approach**
   Dipl.-Phys. Diana Geiger, Institut für Festkörperphysik Wien, Austria
   30. 01. 2015
6. **Single Molecular NMR**
   Dr. Friedemann Reinhard, Walter Schottky Institut, Garching, Germany
   20. 02. 2015

SS 2015:

7. **Spin Pumping in Antiferromagnets**
   Hans Skarsvag, Norwegian University of Science and Technology, Trondheim, Norway
   23. 04. 2015
8. **Spin-driven nematicity in $Ba(Fe_{(1-x)}Co_x)_2As_2$**
   Dr. Una Karahasanovic, Karlsruher Institut für Technologie, Karlsruhe, Germany
   08. 05. 2015
9. **Ultrafast, element-specific magnetization dynamics of multi-constituent magnetic materials by use of high-harmonic generation**
   Dr. Justin Shaw, National Institute of Standards and Technology, Boulder, Colorado, USA
   27. 05. 2015
10. **X-ray absorption spectroscopy under external stimuli**
    Dr. Katharina Ollefs, European Synchrotron Radiation Facility, Grenoble, France
    29. 05. 2015
11. **The Toric Code Hamiltonian in Superconducting Circuits**
    Prof. Dr. Michael Hartmann, Heriot-Watt University Edinburgh, United Kingdom
    19. 06. 2015
12. **Manitoba Trilogy of Spin Rectification vs Spin Pumping**
    Prof. Dr. Can-Ming Hu, University of Manitoba, Winnipeg, Canada
    17. 07. 2015
13. **Quantum Simulations with Superconducting Circuits**
    Dr. Lucas Lamata, University of the Basque Country, Bilbao, Spain
    17. 07. 2015
14. **AOA Fire Protection Systems**
    Dr. Jan-Boris Philipp, Apparatebau Gauting GmbH, Gilching, Germany
    24. 07. 2015
15. **Vom Physiker zum Patentanwalt und Manager**
    Dr. Mitja Schonecke, SKF GmbH, Schweinfurt, Germany
    24. 07. 2015

16. **Ab-initio simulations of structural and electronic properties of correlated materials under application of physical and chemical pressure**
    Dr. Milan Tomic, Johann Wolfgang Goethe-Universität, Frankfurt am Main, Germany
    04. 08. 2015
17. **Damping of perpendicular standing spin waves via VNA-FMR in sputtered Py/Ta films**
    Dr. Thomas J. Silva, National Institute of Standards and Technology Boulder, Colorado, USA
    07. 08. 2015
18. **Experimental verification of the reality of the quantum wave function**
    Dr. Stephanie Simmons, Simon Fraser University Burnaby, Canada
    17. 09. 2015

WS 2015/2016:

19. **Thin film B20 Chiral Magnets**
    Priv.-Doz.- Dr. Dirk Menzel, Technische Universität Braunschweig, Germany
    23. 10. 2015
20. **Unidirectional spin hall magnetoresistance in ferromagnet/normal metal bilayers**
    Dr. Can Onur Avci, ETH Zürich, Switzerland
    30. 10. 2015
21. **Silicon quantum processor with robust long-distance qubit couplings**
    Dr. Guilherme Tosi, University of New South Wales, Sydney, Australia
    27. 11. 2015
22. **Towards macroscopic quantum physics with levitated magneto-mechanics**
    Dr. Joshua Slater, Faculty of Physics, University of Vienna, Austria
    04. 12. 2015
23. **Detecting spin-currents generated by a ferrimagnetic insulator**
    Nynke Vliestra, University of Groningen, Groningen, The Netherlands
    18. 12. 2015

Topical Seminar on Advances in Solid State Physics – WS 2014/2015, SS 2015 and WS 2015/2016

WS 2014/2015:

1. **Preliminary discussion and assignment of topics**
   R. Gross, Walther-Meißner-Institut
   07. 10. 2014 and 14. 10. 2014
2. **Optical Detection of Radio Waves through a Nanomechanical Transducer**
   Daniel Schwienbacher, Technische Universität München
   28. 10. 2014
3. **Room-Temperature Antiferromagnetic Memory Resistor**
   Johannes Klicpera, Technische Universität München
   11. 11. 2014
4. **Spin Pumping and Spin-Transfer Torques in Antiferromagnets**
   Jörg Wohlketzetter, Technische Universität München
   18. 11. 2014
5. **Perowskite Oxides for Visible-Light-Absorbing Ferroelectric and Photovoltaic Materials**
   Zoltan Jehn, Technische Universität München
   02. 12. 2014
6. **Entangling Mechanical Motion with Microwave Fields**
   Bernhard Kalis, Technische Universität München
   16. 12. 2014
7. **An Electrically Pumped Polariton Laser**
   David Busse, Technische Universität München
   13. 01. 2015

8. **Quantum Limit of Heat Flow Across a Single Electronic Channel**
   Markus Manz, Technische Universität München
   20. 01. 2015
9. **Fermi Surface and Pseudogap Evolution in a Cuprate Superconductor**
   Maximilian Patzauer, Technische Universität München
   27. 01. 2015

SS 2015:

10. **Preliminary discussion and assignment of topics**
    R. Gross, Walther-Meißner-Institut
    14. 04. 2015 and 21. 04. 2015
11. **Magnon transistor for all-magnon data processing**
    Jakob Seidl, Technische Universität München
    12. 05. 2015
12. **Spin Transfer Torque Generated by a Topological Insulator**
    Junwen Zou, Technische Universität München
    02. 06. 2015
13. **Anisotropic magnetoresistance in an antiferromagnetic semiconductor**
    Johanna Fischer, Technische Universität München
    09. 06. 2015
14. **Charge Ordering in the Electron Doped Superconductor $Nd_{2-x}Ce_xCuO_4$**
    Sergej Fust, Technische Universität München
    09. 06. 2015
15. **Spin-Cherenkov effect and magnetic Mach cones**
    Josef Zimmermann, Technische Universität München
    16. 06. 2015
16. **Observation of Measurement-induced Entanglement and Quantum Trajectories of Remote Superconducting Qubits**
    Patrick Yard, Technische Universität München
    16. 06. 2015
17. **Passive radiative cooling below ambient air temperature under direct sunlight**
    Andreas Havreland, Technische Universität München
    23. 06. 2015
18. **Observation of quantized conductance in neutral matter**
    Mariana Hettich, Technische Universität München
    30. 06. 2015
19. **Observation of the Spin Peltier Effect for Magnetic Insulators**
    Paul Westphälinger, Technische Universität München
    07. 07. 2015
20. **Divergent Nematic Susceptibility in an Iron Arsenide**
    Ramez Hosseinian Ahangharnejhad, Technische Universität München
    07. 07. 2015
21. **Electronic properties of an organic superconductor in the vicinity of the Mott-insulating transition**
    Sebastian Oberbauer, Technische Universität München
    14. 07. 2015
22. **Rectification of Electronic Heat Current by a Hybrid Thermal Diode**
    Christian Besson, Technische Universität München
    14. 07. 2015

WS 2015/2016:

23. **Preliminary discussion and assignment of topics**
    R. Gross, Walther-Meißner-Institut

13. 10. 2015 and 20. 10. 2015

24. **Ferroelectric tunnel junctions for information storage and processing**
Rasmus Flaschmann, Technische Universität München
24. 11. 2015

25. **New perspectives for Rashba spin-orbit coupling**
Alexander Baklanov, Technische Universität München
08. 12. 2015

26. **Pressure-induced Mott Transition in an Organic Superconductor with a Finite Doping Level**
Sebastian Oberbauer, Technische Universität München
15. 12. 2015

27. **Optically induced coherent transport far above Tc in underdoped YBa2Cu3O6+?**
Jongho Kim, Technische Universität München
12. 01. 2016

28. **Realization of Microwave Quantum Circuits Using Hybrid Superconducting-Semiconducting Nanowire Josephson Elements**
Florian Kollmannsberger, Technische Universität München
19. 01. 2015

Topical Seminar: Spin Caloritronics and Spin Pumping – SS 2015 and WS 2015/2016

SS 2015:

1. **Preliminary discussion and assignment of topics**
Mathias Weiler, Walther-Meißner-Institut
16. 04. 2015 and 23. 04. 2015

2. **Spin Pumping in Antiferromagnets**
Hans Skarsvag, Norwegian University of Science and Technology, Trondheim, Norway
23. 04. 2015

3. **Spin-Hall Spin Torque Resonance in Yttrium Iron Garnet/Platinum thin film bilayers**
Michael Schreier, Walther-Meißner-Institut
30. 04. 2015

4. **Brillouin Light Scattering on Yttrium Iron Garnet thin films**
Mathias Weiler, Walther-Meißner-Institut
07. 05. 2015

5. **Seebeck Spin Tunneling**
Yuki Nojiri, Technische Universität München
21. 05. 2015

6. **Broadband ferromagnetic resonance spectroscopy**
Stefan Klingler, Walther-Meißner-Institut
28. 05. 2015

7. **Strong coupling and spin pumping**
Hannes Maier-Flaig, Walther-Meißner-Institut
11. 06. 2015

8. **Spin torque nano-oscillators**
Hiroto Sakimura, Technische Universität München
18. 06. 2015

9. **Time-resolved Spin Seebeck effect**
Franz Kramer, Walther-Meißner-Institut
02. 07. 2015

10. **(Inverse) spin Hall effect**
Göktug Yesilbas, Technische Universität München
09. 07. 2015

11. **Ferromagnetic resonance of compensated garnets at low temperature**

Philip Louis, Walther-Meißner-Institut
16. 07. 2015

WS 2015/2016:

12. **Preliminary discussion and assignment of topics**
Matthias Althammer, Sebastian Gönnenwein, Mathias Weiler, Walther-Meißner-Institut
15. 10. 2015 and 22. 10. 2015
13. **Long-distance transport of magnon spin information in a magnetic insulator at room temperature**
Tobias Wimmer, Walther-Meißner-Institut
19. 11. 2015
14. **Spin Hall Magnetoresistance**
Claudio de Rose, Walther-Meißner-Institut
26. 11. 2015
15. **Current induced magnetization switching in antiferromagnets**
Birte Cöster, Technische Universität München
10. 12. 2015

Topical Seminar on Superconducting Quantum Circuits – WS 2014/2015, SS 2015 and WS 2015/2016

WS 2014/2015:

1. **Preliminary discussion and assignment of topics**
F. Deppe, A. Marx, R. Gross, Walther-Meißner-Institut
07. 10. 2014 and 14. 10. 2014
2. **3D Cavities for circuit QED**
Gustav Andersson, Technische Universität München
21. 10. 2014
3. **Coupling of a transmon qubit to a CPW resonator**
Javier Puertas Martinez, Technische Universität München
04. 11. 2014
4. **Tracking photon jumps with repeated quantum non-demolition parity measurements**
Edwar Xie, Walther-Meißner-Institut, Garching
18. 11. 2014
5. **Defining and detecting quantum speedup**
Alexander Baust, Walther-Meißner-Institut, Garching
18. 11. 2014
6. **Fabrication stability of Josephson junctions and superconducting flux qubits**
Lujun Wang, Technische Universität München
02. 12. 2014
7. **8-Channel microwave receiver for quantum experiments**
Martin Betzenbichler, Technische Universität München
02. 12. 2014
8. **Quantum limited amplification and entanglement in coupled nonlinear resonators**
Martin Betzenbichler, Technische Universität München
16. 12. 2014
9. **Unconditional quantum teleportation between distant solid-state quantum bits**
Stefan Pogorzalek, Technische Universität München
16. 12. 2014
10. **Bidirectional and efficient conversion between microwave and optical light**
Jan Goetz, Walther-Meißner-Institut, Garching
20. 01. 2015

11. **Observation of a dissipation-induced classical to quantum transition**
Friedrich Wulschner, Walther-Meißner-Institut, Garching
20. 01. 2015

SS 2015:

12. **Preliminary discussion and assignment of topics**
F. Deppe, A. Marx, R. Gross, Walther-Meißner-Institut
14. 04. 2015 and 21. 04. 2015
13. **Time-domain characterization of the transmon qubit**
Miriam Müting, Technische Universität München
12. 05. 2015
14. **Gradiometric flux qubit with tunable magic point**
Jonas Lederer, Technische Universität München
02. 06. 2015
15. **Transmon qubit in a 3D cavity**
Daniel Arweiler, Technische Universität München
02. 06. 2016
16. **Observation of Topological Transitions in Interacting Quantum Circuits**
Deividas Sabonis, Technische Universität München
09. 06. 2015
17. **Displacement of squeezed vacuum states with Josephson parametric amplifiers**
Stefan Pogorzalek, Technische Universität München
23. 06. 2015
18. **Measurement and Control of Quasiparticle Dynamics in a Superconducting Qubit**
Paul Dichtl, Technische Universität München
07. 07. 2015

WS 2015/2016:

19. **Preliminary discussion and assignment of topics**
F. Deppe, A. Marx, R. Gross, Walther-Meißner-Institut
13. 10. 2015 and 20. 10. 2015
20. **Microwave-Controlled Generation of Shaped Single Photons in Circuit Quantum Electrodynamics**
Peter Eder, Walther-Meißner-Institut
03. 11. 2015
21. **Hybrid circuit cavity quantum electrodynamics with a micromechanical resonator**
Thomas Stolz, Technische Universität München
17. 11. 2015
22. **Tuneable on-demand single-photon source**
Jan Goetz, Walther-Meißner-Institut
01. 12. 2015
23. **A Quantum memory with near-millisecond coherence in circuit QED**
Lukas Hauertmann, Technische Universität München
15. 12. 2015
24. **Unconventionally coupled nano-electromechanics**
Daniel Schwienbacher, Walther-Meißner-Institut
26. 01. 2016

C: Solid State Colloquium

The WMI has organized the Solid-State Colloquium of the Faculty of Physics in WS 2014/2015, SS 2015, and WS 2015/2016. The detailed program can be found on the WMI webpage: http://www.wmi.badw-muenchen.de/teaching/Seminars/fkkoll.html.

Staff

Staff of the Walther-Meißner-Institute

Director
Prof. Dr. Rudolf Gross

Deputy Director
Priv.-Doz. Dr. habil. Sebastian Gönnenwein

Technical Director
Dr. Achim Marx

Administration/Secretary's Office
Ludwig Ossiander
Emel Dönertas

Scientific Staff
Dr. Matthias Althammer
Dr. Frank Deppe
Prof. Dr. Andreas Erb
Dr. Kirill Fedorov
Dr. Stephan Geprägs
Priv.-Doz. Dr. habil. Rudolf Hackl
Dr. Hans Hübl
Dr. Mark Kartsovnik
Dr. Matthias Opel
Dr. Mathias Weiler

Dipl.-Phys. Andreas Baum
Dipl.-Phys. Alexander Baust
Dipl.-Phys. Thomas Böhm
Dipl.-Phys. Nitin Chelwani
M. Sc. Alma Dorantes
Dipl.-Phys. Peter Eder
M. Sc. Michael Fischer
M. Sc. Kathrin Ganzhorn
Dipl.-Phys. Jan Goetz
M. Sc. Stefan Klingler
Dipl.-Phys. Michael Kunz
Dipl.-Phys. Hannes Maier-Flaig
Dipl.-Phys. Sibylle Meyer
Dipl.-Phys. Matthias Pernpeintner
M. Sc. Philip Schmidt
Dipl.-Phys. Michael Schreier
M. Sc. Stefan Weichselbaumer
Dipl.-Phys. Karl Friedrich Wulschner
M. Sc. Edward Xie
Dipl.-Phys. Christoph Zollitsch

Technical Staff
Peter Binkert
Thomas Brenninger, M.Sc.
Dieter Guratzsch
Astrid Habel
Karen Helm-Knapp
Dipl.-Ing. (FH) Josef Höss
Sebastian Kammerer
Julius Klaus

Robert Müller
Jan Naundorf
Georg Nitschke
Christian Reichlmeier
Alexander Rössl
Harald Schwaiger
Helmut Thies
Siegfried Wanninger

Assistants
Sybilla Plöderl
Maria Botta

Permanent Guests

Dr. Werner Biberacher
Prof. Dr. B.S. Chandrasekhar
Dr. Christian Probst
Prof. Dr. Dietrich Einzel
Dr. Kurt Uhlig

Guest Researchers

1. Dr. Werner Biberacher
   permanent guest
2. Prof. Dr. B.S. Chandrasekhar
   permanent guest
3. Prof. Dr. Dietrich Einzel
   permanent guest
4. Dr. Christian Probst
   permanent guest
5. Dr. Kurt Uhlig
   permanent guest
6. Dr. Mikel Sanz, Universidad del Pais Vasco, Bilbao, Spain
   08. 02. - 13. 02. 2015, 15. 06. - 23. 06. 2015, 07. 10. - 15. 10. 2015
7. Urtzi Las Heras, Universidad del Pais Vasco, Bilbao, Spain
   08. 02. - 13. 02. 2015, 15. 06. - 23. 06. 2015, 15. 09. - 23. 09. 2015
8. Akashdeep Kamra, Kavli Institute of Nanoscience, Delft University of Technology, Delft, The Netherlands
   23. 03. - 30. 03. 2015
9. Diana Geiger, Institut für Festkörperphysik, Technische Universität Wien, Austria
   26. 03. - 25. 04. 2015, 04. 05. - 09. 05. 2015, 10. 06. - 26. 06. 2015, 26. 10. - 08. 11. 2015, 21. 11. - 26. 11. 2015
10. Hans Skarsvag, Norwegian University of Science and Technology, Trondheim, Norway
    18. 04. - 25. 04. 2015
11. Michael Harder, University of Manitoba, Winnipeg, Canada
    30. 04. - 01. 08. 2015
12. Prof. Dr. Enrique Solano, Universidad del Pais Vasco, Bilbao, Spain
    08. 02. - 13. 02. 2015, 15. 06. - 16. 10. 2015
13. Laura Garcia-Alvarez, Universidad del Pais Vasco, Bilbao, Spain
    14. 06. - 19. 06. 2015, 07. 10. - 15. 10. 2015
14. Dr. Nedad Lazarevic, University of Belgrade, Belgrade, Serbia
    26. 06. - 13. 07. 2015, 02. 09. - 05. 09. 2015, 04. 12. - 23. 12. 2015
15. Marko Opacic, University of Belgrade, Belgrade, Serbia
    26. 06. - 03. 07. 2015
16. Dr. Lucas Lamata, Universidad del Pais Vasco, Bilbao, Spain
    01. 07. - 30. 07. 2015, 23. 09. - 30. 09. 2015
17. Julen S. Pedernales, Universidad del Pais Vasco, Bilbao, Spain
    13. 07. - 31. 07. 2015
18. Inigo Arrazola, Universidad del Pais Vasco, Bilbao, Spain
    23. 07. - 31. 07. 2015
19. Unai Alvarez-Rodriguez, Universidad del Pais Vasco, Bilbao, Spain
    26. 07. - 31. 07. 2015
20. Dr. Daniel Rossatto, Universidad del Pais Vasco, Bilbao, Spain
    02. 08. - 09. 08. 2015
21. Simone Felicetti, Universidad del Pais Vasco, Bilbao, Spain
    02. 08. - 08. 08. 2015
22. Dr. Enrique Rico, Universidad del Pais Vasco, Bilbao, Spain
    02. 08. - 08. 08. 2015, 30. 11. - 05. 12. 2015

23. Dr. Jesus Oswaldo Moran Campana, Universidad Nacional de Colombia Medellin, Medellin, Colombia
    01. 09. - 29. 11. 2015
24. Z. Popovic, University of Belgrade, Belgrade, Serbia
    02. 09. - 05. 09. 2015
25. Prof. Vladimir Zverev, Institute of Solid Physics, Chernogolovka, Russia
    11. 09. - 16. 09. 2015
26. Ryo Ohshima, Kyoto University, Kyoto, Japan
    05. 10. - 19. 10. 2015
27. Dr. A. Bardin, Institute of Problems of Chemical Physics, Chernogolovka, Russia
    12. 10. - 17. 10. 2015
28. Alisa ChernenÂťkaya, Johannes Gutenberg-Universität, Mainz, Germany
    14. 10. - 17. 10. 2015
29. Dr. Steve Winter, Goethe-Universität, Frankfurt, Germany
    26. 10. - 14. 11. 2015
30. Dr. Kevin Garello, Dr. Can Onur Avci, Johannes Mendil, ETH Zürich, Zuerich, Switzerland
    28. 10. - 30. 10. 2015
31. Dr. Harald Schuberth, Goethe-Universität, Frankfurt, Germany
    02. 11. - 07. 11. 2015
32. Dr. Natasha Kushch, Institute of Problems of Chemical Physics, Chernogolovka, Russia
    21. 10. - 15. 12. 2015
33. Dr. Guilherme Tosi, University of New South Wales, Sydney, Australia
    22. 11. - 16. 12. 2015
34. Dr. Joshua Slater, Universität Wien, Austria
    02. 12. - 14. 12. 2015
35. Joachim Hofer, Universität Wien, Austria
    02. 12. - 14. 12. 2015
36. Dr. Pavel Grigoriev, L.D. Landau Institute for Theoretical Physics, Chernogolovka, Russia
    16. 12. - 18. 12. 2015

Members of the WMI Scientific Advisory Board

In 2015 the Bavarian Academy of Sciences and Humanities (BAdW) has passed new statutes. In accordance with the new statutes valid from 1 October 2015, the former Commissions have been abolished to achieve a clear separation between the managing bodies of the Academy Institutes and Projects of BAdW responsible for the implementation of the research programs, and the corresponding supervisory bodies — the Institute and Project Advisory Boards — evaluating the quality of the scientific work. To this end, the former Commission for Low Temperature Research was replaced by the WMI Committee and the WMI Advisory Board.

The members of the WMI Advisory Board are appointed by the Section III "Naturwissenschaften, Mathematik, Technikwissenschaften" of BAdW for five years. They correspond to the former members of the Commission for Low Temperature Research listed above despite the director of WMI (Rudolf Gross) who is only a consultive member of the WMI Advisory Board. The WMI Advisory Board is headed by a chairman (Dieter Vollhardt) and deputy chairman (Gerhard Abstreiter). They are elected by the Section III "Naturwissenschaften, Mathematik, Technikwissenschaften" of BAdW for five years at the suggestion of the members of the WMI Advisory Board. The head of the Scientific Advisory Board must be member of BAdW.

The present members of the WMI Scientific Advisory Board are:

- **Vollhardt, Dieter**, chairman
  (Universität Augsburg)
- **Abstreiter, Gerhard**, deputy chairman
  (Technische Universität München)

- **Bloch, Immanuel**
  (Ludwig-Maximilians-Universität München and Max-Planck-Institut für Quantenoptik)
- **Bühler-Paschen, Silke**
  (Technische Universität Wien)
- **Finley, Jonathan**
  (Technische Universität München)
- **Gross, Rudolf**, consultive member
  (Technische Universität München)
- **Hänsch, Theodor**
  (Ludwig-Maximilians-Universität München and Max-Planck-Institut für Quantenoptik)
- **Schwoerer, Markus**
  (Universität Bayreuth)
- **Wallraff, Andreas**
  (Eidgenössische Technische Hochschule Zürich)
- **Weiss, Dieter**
  (Universität Regensburg)
- **Zinth, Wolfgang**
  (Ludwig-Maximilians-Universität München)

The director of WMI and the members of the WMI Committee are also appointed by the Section III "Naturwissenschaften, Mathematik, Technikwissenschaften" of BAdW for five years at the suggestion of the members of the WMI Advisory Board. The members of the WMI Committee are the director, the deputy director, the technical director and the elected representative of the scientific staff of WMI.

Contact:

Walther–Meißner–Institut
Bayerische Akademie der Wissenschaften
Walther–Meißner–Str. 8
D - 85748 Garching
GERMANY

Phone: +49 – (0)89 289 14201
Fax: +49 – (0)89 289 14206
E–mail: Sekretariat@wmi.badw.de

www.wmi.badw.de

Published by:

Walther–Meißner–Institut
Walther–Meißner–Str. 8, D - 85748 Garching
December 2015